Queen Mary
University of London

centre for digital music

Computational Methods for the Alignment and Score-Informed Transcription of Piano Music

By

Siying WANG

Submitted in partial fulfilment of the requirements
of the Degree of Doctor of Philosophy

London, UK

November 6, 2017

AUTHOR'S DECLARATION

I, Siying Wang, confirm that the research included within this thesis is my own work or that where it has been carried out in collaboration with, or supported by others, that this is duly acknowledged below and my contribution indicated. Previously published material is also acknowledged below.

I attest that I have exercised reasonable care to ensure that the work is original, and does not to the best of my knowledge break any UK law, infringe any third party's copyright or other Intellectual Property Right, or contain any confidential material.

I accept that the College has the right to use plagiarism detection software to check the electronic version of the thesis.

I confirm that this thesis has not been previously submitted for the award of a degree by this or any other university.

SIGNATURE: .... DATE: ....

Details of collaboration and publications: See Section 1.3.

ABSTRACT

This thesis is concerned with computational methods for alignment and score-informed transcription of piano music. Firstly, several methods are proposed to improve the alignment robustness and accuracy when various versions of one piece of music show complex differences with respect to acoustic conditions or musical interpretation. Secondly, score to performance alignment is applied to enable score-informed transcription.

Although music alignment methods have considerably improved in accuracy in recent years, the task remains challenging. The research in this thesis aims to improve the robustness for some cases where there are substantial differences between versions and state-of-the-art methods may fail in identifying a correct alignment. This thesis first exploits the availability of multiple versions of the piece to be aligned. By processing these jointly, the alignment process can be stabilised by exploiting additional examples of how a section might be interpreted or which acoustic conditions may arise. Two methods are proposed, progressive alignment and profile HMM, both adapted from the multiple biological sequence alignment task. Experiments demonstrate that these methods can indeed improve the alignment accuracy and robustness over comparable pairwise methods. Secondly, this thesis presents a score to performance alignment method that can improve the robustness in cases where some musical voices, such as the melody, are played asynchronously to others – a stylistic device used in musical expression. The asynchronies between the melody and the accompaniment are handled by treating the voices as separate timelines in a multi-dimensional variant of dynamic time warping (DTW). The method measurably improves the alignment accuracy for pieces with asynchronous voices and preserves the accuracy otherwise.

Once an accurate alignment between a score and an audio recording is available, the score information can be exploited as prior knowledge in automatic music transcription (AMT), for scenarios where score is available, such as music tutoring. Score-informed dictionary learning is used to learn the spectral pattern of each pitch that describes the energy distribution of the associated notes in the recording. More precisely, the dictionary learning process in non-negative matrix factorization (NMF) is constrained using the aligned score. This way, by adapting the dictionary to a given recording, the proposed method improves the accuracy over the state-of-the-art.

ACKNOWLEDGEMENTS

First and foremost, I would like to thank my two wonderful PhD supervisors - Sebastian Ewert and Simon Dixon. I have been feeling extremely lucky since the first day they agreed to supervise me. Back then, I was confused with my research topic and had strong self-doubt. I simply would not be able to accomplish the work in this thesis without their invaluable guidance and encouragement, support and faith in me. They shaped my understanding of good research and showed me the spirit of scientists. I especially want to thank Sebastian for always making the time to discuss with me, despite being very busy himself.

I want to express my gratitude to Professor Elaine Chew, for being my female role model. I was inspired by Elaine's attitude toward research and life in general and her efforts in gender equality.

The four years I spent in Queen Mary have always been enjoyable, thanks to my dear friends here. Especially Yading, Chunyang, Chris and Shan. I will never forget the laugh and tears we share together, the days and evenings we spent together working and chatting. I really appreciate that you are always there whenever I need, offering help and suggestions or simply listening. I would also like to thank Maria, Veronica, Mi, Tian, Beici, Simin, Katerina, Sid, Peter, Di, Mattias, Janis, Luwei, Matt, Eita for being great lab-mates and friends.

Thanks for Stella Sick and Werner Goebl for kindly providing the dataset.

Last but not least, my deepest thanks go to my family for their unwavering support and trust. Thanks to my parents for understanding and supporting me in pursuing my dream far from home. Thanks to Fran for your enduring trust, encouragement and caring for me, for keeping me physically and mentally healthy, sometimes simply by dragging me out from work to a walk, also for proofreading my thesis, discussing with me about my research from time to time and always providing good advices.

This work was funded by the China Scholarship Council.

TABLE OF CONTENTS

LIST OF TABLES

LIST OF FIGURES

List of Symbols

α	The forward matrix in the Baum Welch Training procedure;
β	The backward matrix in the Baum Welch Training procedure;
η	The weight of regulariser term on the spectral template matrix;
$\mathscr{F}$	A feature space;
γ	Its entry $\gamma_n(i)$ is defined as the probability of being in the state s_i at the frame n given the model λ and the observation sequence O
λ	A Hidden Markov Model (HMM);
$\mathscr{A}$	The index set of the attack templates for a pitch;
$\mathscr{B}$	The index set of the sustain templates for a pitch;
μ	The mean vector of the Gaussian observation distribution in an HMM;
Φ	The size of constraint region in 3D-DTW;
$\pi = (\pi_0, \pi_1, \ldots, \pi_L)$	The initial state distribution in an HMM;
ψ	A lookup table/matrix to store the best choice of each step in Dynamic Programming;
σ	The covariance matrix of the Gaussian observation distribution in an HMM;
Θ	The maximally allowed asynchrony in 3D-DTW;

ξ	Its entry $\xi_n(i,j)$ is defined as the probability of being in the state s_i at frame n and transiting to s_j at time $n+1$, given the model λ and the observation sequence O;
ζ	The weight of regulariser term on the activation matrix;
A	The activation matrix;
a_{ij}	The state transition probability;
$b_i(O_n)$	The observation probability;
C	A dissimilarity/similarity matrix;
c	A local dissimilarity/similarity measure on $\mathscr{F}$;
D	A total dissimilarity/similarity matrix;
F	The template data structure in a progressive alignment;
G	The gap symbol in a progressive alignment;
K	The number of versions of a piece used in a multiple alignment;
L	The number of states in an HMM;
N	The length of the observation sequence in an HMM;
$O=(O_1,O_2,\ldots,O_N)$	An observation sequence in an HMM;
P	The spectral template matrix;
p	An alignment;
$S=(s_1,s_2,\ldots,s_L)$	States in an HMM;
V	The magnitude spectrogram;
w	The weight to adjust the preference over the three step sizes in the alignment;
X,Y,Z	Feature sequences with their elements $x_n \in \mathscr{F}$, $y_m \in \mathscr{F}$ and $z_l \in \mathscr{F}$;

CHAPTER 1

INTRODUCTION

1.1 Motivation and Goals

The last few decades have seen a revolution in the way people interact with music, including how we make, store, share, learn and enjoy music. These developments have led to the explosive growth of digital music collections and music-related data. Music content providers (e.g. Spotify, iTunes, Pandora) rely on their existence, while national libraries and charitable organisations create and curate them in order to provide access to cultural heritage. For one piece of music, large collections often contain various recordings, videos, annotations and other metadata. In particular for Western classical music, there are often multiple versions associated with any given piece of music, including different editions of the sheet music, various types of symbolic representations (such as MIDI - Musical Instrument Digital Interface and MusicXML - Music Extensible Markup Language) and multiple recordings of musical performances (in the form of audio recordings or MIDI files).

To establish links between different versions of a piece of music, various music alignment methods have been proposed in recent years. The goal of music alignment is to map each temporal position in one version of a piece of music to the corresponding position in another version of the same piece. During the last decades, such methods have been of central importance for analysing, modelling and processing music signals. They have enabled a multitude of applications, including automatic score following and page turning (Arzt et al., 2014; Montecchio and Cont, 2011a), facilitated navigation in large collections (Müller et al., 2010), the identification of cover songs (Serrà et al., 2008), query-by-example retrieval (Casey et al., 2008) and the integration of prior knowledge in audio source separation (Ewert et al., 2014).

Various alignment methods have been proposed, including Dynamic Time Warping (DTW) (Hu et al., 2003), Hidden Markov and Semi-Markov Models (HMM) (Orio and Déchelle, 2001), Conditional Random Fields (CRF) (Joder et al., 2011), general graphical models (Raphael, 2004), and Particle Filter / Monte-Carlo Sampling (MCS) based methods (Montecchio and Cont, 2011a; Duan and Pardo, 2011). The performance of alignment methods has improved considerably over the years. As shown in previous studies, current methods yield a high accuracy in many cases (Joder et al., 2011; Ewert et al., 2009b; Dixon and Widmer, 2005). However, the task remains challenging. For cases with strong local differences between versions, even state-of-the-art methods may fail to identify the correct alignment. Such strong local differences often stem from two aspects. On the one hand, the acoustic conditions may vary regarding recording environment and instrumentation. On the other hand, musicians can interpret a piece in diverse ways with respect to the articulation, expressive timing, embellishments or the relative loudness of notes (balance).

The first goal of this thesis is to improve the alignment robustness against such strong local differences by developing novel alignment methods. Under this goal, the first idea is to make use of the information provided by multiple versions of a piece of music to stabilise the alignment process. Most state-of-art methods align two versions in a pairwise fashion, which may not be robust enough against substantial local differences. However, in many scenarios not only two but multiple versions of a given piece are available, especially for Western classical music. By processing multiple versions jointly, the alignment process can be provided with additional examples of how a section might be interpreted or which acoustic conditions may arise. This can help especially with sections where strong local differences are shown between any two versions.

The second idea to improve robustness and accuracy stems from a commonly used musical parameter: the asynchrony between voices. Current methods typically assume that notes occurring simultaneously in the score are played concurrently in a performance. However, musicians sometimes introduce asynchronies between simultaneous notes as a device of music expression. Such asynchronies may locally lead to a measurable drop in alignment accuracy because they are not taken into consideration by current methods. To handle such asynchronies, an idea presented in this thesis is to separate the melody and accompaniment voices in the score and compute a three-dimensional alignment between the two score timelines and the audio timeline. To lower the computational cost and improve the overall robustness, the standard two-dimensional alignment is used to constrain the computation in the proposed method.

A more accurate and robust alignment as provided by the two above methods is useful for various applications. One of them is to exploit the score information to analyse audio recordings of the same piece. The second goal of this thesis is thus to apply score to audio alignment to build a score-informed music transcription method. Automatic music transcription aims at obtaining a high-level symbolic representation of the notes played in a given audio recording. However, the performance of current methods is inadequate for many applications. The idea presented in this thesis is to provide score information, available in certain scenarios, as prior knowledge to the transcription system, in order to boost its accuracy. Such a method is particularly interesting for a specific application: music tutoring, in which the system provides feedback on when and how the student deviates from the given score. The alignment between the audio recording and the corresponding score indicates for each score note, an approximate time position in the audio. This information is used to construct a transcription method that is tailored to the given recording by a score-informed dictionary learning method.

Overall, this thesis aims to propose computational methods for both alignment and score-informed transcription. Although the methods are applicable to other genres of music, this thesis focuses on Western classical piano music.

1.2 Thesis Structure

The contribution of this thesis is two-fold. Firstly, it proposes novel alignment methods for two different scenarios, in Chapter 3 and Chapter 4 respectively. Secondly, it applies the alignment methods to build a score-informed music transcription system in Chapter 5. This section describes the structure of this thesis and provides a brief introduction to each chapter.

Chapter 1 is the introduction to the thesis. It explains its motivation and goals, followed by a description of thesis structure. Associated publications are listed at the end and their contributions to this thesis are specified.

Chapter 2 provides the background knowledge and core concepts which are used throughout the thesis. Some general related work is also mentioned there, while works specific to a certain chapter are discussed in the corresponding chapters. The chapter starts with a summary of different representations of music and related terminology, including the music score, the notion of performance and expression as well as MIDI notation. It then discusses two concepts used in alignment: feature representation and algorithms/methods. As feature design is not the focus of this thesis, it only mentions features commonly used in music alignment and describes the features used in Chapter 3 and Chapter 4. A discussion of alignment methods is given afterwards. The main description focuses on two categories of methods: Dynamic Programming and Probabilistic Modelling, which are both used in later chapters. Last but not least, the chapter provides an overview of score-informed Music Information Retrieval (MIR) research based on music alignment techniques, including score-informed source separation and score-informed music transcription to prepare the reader for Chapter 5.

Chapter 3 aims at increasing alignment robustness against strong local differences by exploiting the availability of multiple versions of the piece to be aligned. Inspired by the multiple sequence alignment problem in bio-informatics, this chapter proposes two joint alignment methods to process multiple performances. The two proposed methods are conceptually different but share some similarities from an algorithmic point of view. Experiments show that both of them can improve the alignment accuracy and robustness. Further, this chapter investigates their behaviours and compares them with respect to their computational efficiency and alignment accuracy.

Chapter 4 focuses on improving the alignment accuracy for cases with strong asynchronies between the melody and the accompaniment voice. It presents a novel score to performance alignment method that treats the two score voices in separate timelines and computes a joint three dimensional alignment using an extended version of Dynamic Time Warping (DTW) between them and the audio timeline using information obtained via classical DTW. Two types of constraints for the calculation of the cost matrix are proposed to lower the computational costs and to improve the overall alignment accuracy. Experiments show that the proposed method measurably improves the alignment accuracy for pieces with asynchronous voices and preserves the accuracy otherwise.

Chapter 5 presents a score-informed transcription system for identifying missing and extra notes from piano recordings. To improve the accuracy of automatic music transcription, the idea of this chapter is to exploit the music score as prior knowledge by applying score to audio alignment. A score-informed dictionary learning method is used to construct a transcription system that is tailored to the given audio recording. This chapter also analyses a case where the system fails, and designs several countermeasures to improve the performance. The influence of these extensions are investigated with further experiments.

Chapter 6 concludes the thesis and discusses possible directions for future work.

1.3 Associated Publications

Most of the work in this thesis has been published in international peer-reviewed conferences and journals, as listed below. How each paper relates to each chapter is specified accordingly.

1. (Wang et al., 2014) S. Wang, S. Ewert, and S. Dixon. *Robust Joint Alignment of Multiple Versions of A Piece of Music*, Proceedings of the International Society for Music Information Retrieval Conference (ISMIR), Taipei, Taiwan, 2014

   This paper proposes a novel method to align multiple versions of a piece of music in a joint manner, which stabilises the alignment process and leads to an increase in alignment robustness. It is the basis of (Wang et al., 2016).

2. (Wang et al., 2016) S. Wang, S. Ewert, and S. Dixon. *Robust and Efficient Joint Alignment of Multiple Musical Performances*, IEEE/ACM Transactions on Audio, Speech and Language Processing, 24(11), 2016

   This paper extends (Wang et al., 2014). It presents two joint alignment methods, progressive alignment and probabilistic profile, and discusses their fundamental differences and similarities on an algorithmic level. It also provides an in-depth analysis of both joint alignment methods and shows that both methods can improve the alignment robustness as well as the accuracy over comparable pairwise methods. It is the basis of Chapter 3.

3. (Wang et al., 2015) S. Wang, S. Ewert, and S. Dixon. *Compensating For Asynchronies Between Musical Voices In Score-Performance Alignment*, Proceedings of the IEEE International Conference on Acoustics, Speech, and Signal Processing (ICASSP), Brisbane, Australia, 2015 (Best Student Paper Award for the Audio and Acoustic Signal Processing track)

   This paper presents a score to audio alignment method that can handle asynchronies between the melody and accompaniment by treating the voices as separate timelines in a multi-dimensional variant of dynamic time warping (DTW). It is the basis for Chapter 4.

4. (Ewert et al., 2016) S. Ewert, S. Wang, M. Müller and M. Sandler. *Score-Informed Identification of Missing and Extra Notes in Piano Recordings*, Proceedings of the International Society for Music Information Retrieval Conference (ISMIR), New York, USA, 2016

   This paper proposes a score-informed transcription method for identifying missing and extra notes in piano recordings. The score information is used to constrain a dictionary learning process based on non-negative matrix factorisation (NMF), so that the learned dictionary is highly adapted to the given recording. This paper lays the ground work for Chapter 5.

5. (Wang et al., 2017) S. Wang, S. Ewert, and S. Dixon. *Identifying Missing and Extra Notes in Piano Recordings Using Score-Informed Dictionary Learning*, IEEE/ACM Transactions on Audio, Speech and Language Processing (Available online publication), 2017

   This paper extends (Ewert et al., 2016). It identifies several systematic weaknesses in the previous work and introduces three extensions as countermeasures to improve the performance of the proposed system. The influence of each extension is investigated, and experiments show that they indeed improve the accuracy for identifying extra notes. It is the basis for Chapter 5.

For publications 1-3 and 5, I developed the corresponding methods, conducted all the experiments and wrote the articles. Sebastian Ewert and Simon Dixon co-supervised my work, providing ideas and suggestions for the method and experimental design, as well as comments and corrections for the articles. For publication 4, Sebastian Ewert developed the method, conducted the experiments and wrote the paper. I helped with the experiments. Meinard Müller and Mark Sandler provided comments and corrections for the article.

CHAPTER 2

BACKGROUND

This chapter provides the background knowledge for this thesis. First, Section 2.1 will introduce some music terminology used throughout the thesis in this thesis. Next, Section 2.2 will describe audio features used in the music alignment task. A discussion of music alignment methods will be given in Section 2.3, followed by an overview of score-informed Music Information Retrieval (MIR) research based on music alignment techniques in Section 2.4.

2.1 Music Terminology

A piece of music, especially Western classical music, is often associated with multiple versions or representations, including sheet music of different editions, symbolic representations of various types such as MIDI (Musical Instrument Digital Interface) and MusicXML (Music Extensible Markup Language), or audio recordings of different performances. Each type of representation describes a different perspective on the piece and serves a different purpose. Composers use the score representation to provide detailed instructions on how to perform the music piece they created, while there is a certain degree of freedom for performers to interpret with different musical expression. In the following, the concept

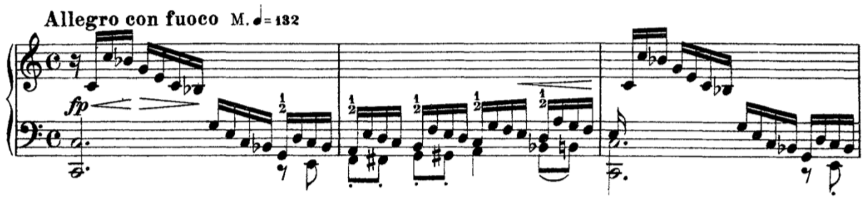

Figure 2.1: An example of music score: Liszt, Franz, Étude en douze exercices, S.136, No.1 (C major), bars 1-3

of musical score and performance will be introduced, followed by MIDI, a music notation format used in this thesis.

2.1.1 Musical Score

A musical score is regarded as the most fixed reference for the Western classical repertoire (Howat, 1995). Among various genres, Western classical music (which is the genre of interest in this thesis) has relatively little freedom in interpreting a piece and demands for a stricter adherence to the score, compared to genres such as jazz which grant a larger degree of improvisation (Cook, 2014; Miotto et al., 2010).

However, many details on the score are open to interpretation, especially the expressive markings. Examples include tempo markings such as *Vivace* (meaning lively and fast) and *Ritardando* (meaning gradually slowing down), dynamic markings such as ***p*** (meaning soft) and ***mf*** (meaning medium loud), articulation markings such as *staccato* (meaning shorten the note duration and separate from the following note) and *fermata* (meaning a pause on the current note), ornament markings such as trills and grace notes, pedal markings, or even descriptive words for expressive musical ideas such as *arpeggio* (meaning broken chord) and *con fuoco* (meaning with fire). Figure 2.1 shows the first three bars of Liszt's Étude en douze exercices, S.136, No.1 (C major) with various music symbols. These descriptive notations lead to many possible interpretations, subject to the playing time, the circumstances, the performer and many other factors. For example, Debussy explained for his descriptive or implicit pedalling notation (Nichols, 1992; Howat, 1995)

> *"Pedalling cannot be written down: it varies from one instrument to another, from one room, or one hall, to another"*

Additionally, the score itself may vary between different editions, due to the composer's copying and revising processes, corrections or additions from editors, or printing conventions (Howat, 1995).

2.1.2 Musical Performances and Expression

Many musicologists agree that the score is merely a "ghostly instantiation" of the musical work (Thomas and Smiraglia, 1998), while a performance of the piece is considered to be a more complete rendition because it turns the abstract content in the score to a concrete realisation in real time. Musical works are collaborations between composers and performers and they may accrue new meanings decades or even centuries after composition (Cook, 2014). Performers study the idiom of the composers through the score and reproduce the music with their very own expression. In this sense, the score is a guidance which cannot capture all the possible nuances of performances and every performance is a new creation of the musical work.

Within the constraints set by the structure of a composition, the performer can manipulate various expressive features to shape the musical work (Clarke, 1995), including tempo, timing, dynamics, timbre and articulation. For example, melody lead (which will be discussed in Chapter 4), is an expressive feature in which the performer emphasises the melody in multi-voice music by playing the melody louder and preceding other voices by around 30ms (Goebl, 2000).

Since an early investigation led by Seashore (1938), music performance research has been an active field for several decades (Fabian et al. (2014) have provided a comprehensive overview). Modern computational methods enable the large scale measurement and analysis of the nuances in musical expression, a process which previously was carried out manually and thus was limited to small-scale studies (Goebl et al., 2008). One approach to acquiring expression data is to use specifically equipped instruments, such as the Yamaha Disklavier system and Bösendorfer's SE and CEUS systems. They record the performance not as an audio recording, but in some symbolic formats which describe each note event, such as MIDI.

2.1.3 MIDI Notation

The MIDI (Musical Instrument Digital Interface) standard specifies a protocol for communication between electronic instruments (Chapman and Chapman, 2000). Instead of the sound waveform, MIDI carries the control data that encodes musical performance information (Roads, 1996), such as the start and stop time of a note, its pitch and its velocity[1] as well as clock messages for synchronisation purposes. The playback timbre and quality depends on the device that receives the MIDI message. Roads (1996) has provided a comprehensive introduction to the MIDI standard.

MIDI is widely used as a symbolic representation of a musical score. It stores the internal structure of the score in a sequence of MIDI messages. Although it cannot represent the graphical layout of the score and it is not able to store the expression markings, it is lightweight and universally compatible, and therefore most online digital score resources use the MIDI format. MIDI-format scores are used in the experiments in this thesis.

MIDI can also be used to record musical performances. MIDI compatible instruments such as synthesiser keyboards or digital pianos are used to capture clean expressive data from music performances in MIDI format, without the noise or reverberation which are unavoidable in the audio recordings. Furthermore, by offerering playback of MIDI files, the computer-monitored acoustic pianos such as the Yamaha Disklavier and Bösendorfer's SE and CEUS series combine the sound quality of the acoustic piano and the ability to record a performance in MIDI format. Such pianos are widely used in music performance study(Goebl et al., 2008; Gabrielsson, 2003; Cook, 2014; Goebl, 2000) and even in piano competitions[2]. In this thesis, MIDI representations of performances will be used as ground truth annotations of the pitch and timing of notes, as well as to be synthesised to audio for part of the evaluation.

2.2 Feature Representation in Music Alignment

As a fundamental problem in MIR, music alignment research has been active for several decades. The general principle used by most music alignment methods consists of

[1] For a MIDI instrument that has velocity sensing, velocity is usually related to the speed with which the instrument is being hit, thus the higher the velocity the louder the note. For example, for the Disklavier piano, the hammer velocity is recorded.

[2] `www.piano-e-competition.com`

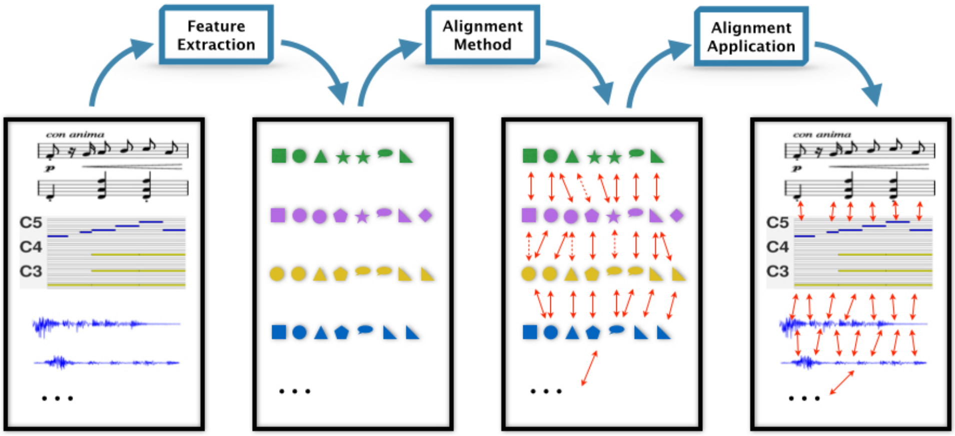

Figure 2.2: General framework of music alignment includes two steps: 1. Extract features from different versions of a piece of music with a common feature representation; 2. Align feature sequences in a suitable alignment method. Alignment can be applied in various scenarios (such as automatic score following (Arzt et al., 2014) and page turning (Montecchio and Cont, 2011a))

two main steps, illustrated in Figure 2.2. First, the files to be aligned including various types of score and audio representations, are converted into feature sequences. Then the feature sequences are compared to find an optimal mapping using some suitable alignment methods. Early approaches before the '90s (Dannenberg, 1984; Vercoe, 1984) were designed to align symbolic music representations such as MIDI. In recent years, the increase in computational power has enabled the processing of audio signals, and thus the last decades have seen efforts shifting towards robust feature representations and suitable alignment methods for aligning audio recordings.

For the feature representation, a major aim is to find an optimal, application-specific trade-off between the level of detail preserved in a feature and its robustness against noise and other musically irrelevant signal properties. In this context, low-level spectral representations have been used (Orio and Schwarz, 2001; Turetsky and Ellis, 2003; Cont, 2010) as well as musically motivated representations, especially pitch and chroma features (Dannenberg and Hu, 2003; Müller et al., 2005; Cont, 2006). More recently, it was found that accompanying such representations with features indicating onset positions can be used to improve the alignment accuracy (Ewert et al., 2009b; Joder et al., 2011). Other more recent developments are adaptive or employ learnt feature representations

(Cont, 2006; Niedermayer, 2009a; Joder et al., 2013; Raffel and Ellis, 2015).

In the following, two types of features will be introduce, which will be used throughout this thesis, chroma-based features and onset indicating features.

2.2.1 Chroma-based Feature

A fundamental phenomenon in music is "octave equivalence", i.e. the observation that pitches exactly one or more octaves apart are musically equivalent in many ways and are perceived as similar in "colour" by listeners. In the early 1960s, Shepard (1964) reported the circularity in pitch perception. He represented the frequency of each pitch with two dimensions, "height" and "tonality / tone chroma", which are essentially the "octave number" and "pitch class" in music theory. In a standard Western 12-tone system, each octave consists of 12 pitches and pitches one or more octaves apart have the same chroma value, from the set $\{C, C\#, D, D\#, E, F, F\#, G, G\#, A, A\#, B\}$ (here $C\#/D\flat$ etc are treated as equivalent).

Given the cyclic property of pitch perception, it is appropriate to use chroma based features in music processing. Fujishima (1999) proposed a Pitch Class Profile (PCP) feature, which maps spectrum bin indices to the corresponding chroma index, and which the authors used in a chord recognition system. In the same year, Wakefield (1999) presented a very similar idea, the Chromagram, which maps the frequency dimension of the spectrogram into 12 pitch classes. Since then, chroma based features have raised a considerable amount of research interest and the following decade saw considerable efforts in designing such features and improving their robustness. For example, Bartsch and Wakefield (2001) employed beat-synchronous frame segmentation for the chroma feature, in order to gain invariance to tempo changes. Gómez (2006) extended PCP to Harmonic Pitch Class Profiles (HPCP), by weighting the contributions of each harmonic for each pitch, to minimise the influence of tuning differences and inharmonicity. Müller and Ewert (2010) proposed CRP (Chroma DCT-Reduced log Pitch) as a feature robust against timbre variation which was achieved by discarding low-order cepstral coefficients which contain information closely related to timbre.

Chroma based features have been used in various MIR tasks, as they encode harmonic relationships (Bartsch and Wakefield, 2005) which are very important in analysing music signals. Applications include chord recognition (Peeters, 2006; Bello and Pickens, 2005; Cho et al., 2010; Fujishima, 1999; Harte and Sandler, 2005; Mauch and Dixon, 2010; Sheh and Ellis, 2003), music structural analysis (Bartsch and Wakefield, 2001, 2005; Chai, 2006; Dannenberg and Goto, 2008; Paulus et al., 2010), as well as music matching and alignment (Kurth and Müller, 2008; Müller et al., 2005; Hu et al., 2003; Joder et al., 2010; Müller, 2007).

2.2.1.1 Chroma Energy Normalised Statistics (CENS) feature

Chapters 3 and 5 employ the CENS (Chroma Energy Normalised Statistics) feature, proposed by Müller et al. (2005). It is obtained by calculating short-time statistics over the chroma energy distribution, to increase the robustness against variations in timbre, dynamics and articulation. Specifically, the audio is firstly converted to a sequence of chroma vectors. Each chroma vector is then normalised by the sum of its energy in all 12 chroma bands, in order to absorb variations in dynamics. Next, each chroma vector is quantised to several levels. After that, the sequence of quantised chroma vectors is convolved component-wise by a Hann window and then downsampled. To this end, each feature represents a weighted statistic of the energy distribution over the window size, to smooth out the local time deviations.

2.2.2 Decaying Locally adaptive Normalised Chroma Onset (DLNCO) Features

Besides the widely used chroma features, the experiments of this thesis use another type of feature: DLNCO (Decaying Locally adaptive Normalised Chroma Onset) feature. It was proposed by Ewert et al. (2009b) and experiments showed that the combination of chroma and DLNCO features largely improves alignment accuracy for music with clear note attacks such as piano music.

To obtain the DLNCO feature, firstly a local energy curve is computed for each MIDI pitch and the energy peaks are chosen as onset features. The pitch based onset features from the same pitch class are summed up into 12-dimensional chroma onset features. The analogy to chroma features is used to enhance the robustness against timbre variation while still preserving a notion of which note was played. Next, the features are normalised in a locally adaptive fashion to further improve the robustness against local dynamic variation. At the end, an additional temporal decay structure is employed, so that when DL-NCO feature sequences are compared using the Euclidean distance, a diagonal corridor of low cost will appear where the onset vectors are similar, therefore only significant events take effect on the cost matrix level.

2.3 Alignment Methods

After a suitable feature representation is chosen, different versions of a piece of music are converted to sequences of this common feature representation. The next step is to align the resulting feature sequences with a suitable method. Without losing the generality, the following considers the case of aligning two versions of a piece of music. Let $X := (x_1, x_2, \ldots, x_N)$ and $Y := (y_1, y_2, \ldots, y_M)$ be two feature sequences with $x_n, y_m \in \mathscr{F}$, where $\mathscr{F}$ denotes a suitable feature space. An alignment between X and Y is defined as a sequence $p = (p_1, \ldots, p_L)$ with $p_\ell = (n_\ell, m_\ell) \in [1:N] \times [1:M]$ for $\ell \in [1:L]$. satisfying $1 = n_1 \leq n_2 \leq \ldots \leq n_L = N$ and $1 = m_1 \leq m_2 \leq \ldots \leq m_L = M$ (boundary and monotonicity conditions), as well as $p_{\ell+1} - p_\ell \in \{(1,0),(0,1),(1,1)\}$ (step size condition). Each step p_ℓ matches elements x_n and y_m.

Various alignment methods have been proposed, including Dynamic Time Warping (DTW) (Müller, 2007), Hidden Markov Models (HMM) (Raphael, 1998), Conditional Random Fields (CRF) (Joder et al., 2011), general graphical models (Raphael, 2004), and Particle Filter / Monte-Carlo Sampling (MCS) based methods (Montecchio and Cont, 2011a; Duan and Pardo, 2011). The choice of methods varies with the application scenarios. For example, when aligning symbolic music such as MIDI, string matching based methods are often used (Dannenberg, 1984; Chen et al., 2014). In recent work, a convolutional neural network has been used in sheet music to audio alignment (Dorfer et al., 2016a). While numerous methods have been used for the music alignment task, many of them fall into two wide categories, *Dynamic Programming* and *Probabilistic Modelling*.

2.3.1 Dynamic Programming

Dynamic programming is an often used algorithmic approach to certain optimisation problems. The main idea is to break down a problem to into sub-problems and combine their solutions successively to obtain the final solution for the original problem. In the context where dynamic programming is applied, those sub-problems overlap with each other in some sense. Instead of recomputing the solution to reoccurring sub-problems, the algorithm stores the solution to a sub-problem in a look-up table and simply retrieves the corresponding solution next time the same sub-problem occurs.

We can apply Dynamic Programming methods to the alignment problem by viewing finding the best match between sequences as an optimisation problem. Its objective is to obtain an optimal alignment minimising the dissimilarity or maximising the similarity between features assigned to each other. Without loss of generality, we refer to similarity in this section. The similarity is calculated by a certain similarity measure, depending on the specific algorithm. The following paragraphs explain the idea behind using Dynamic Programming for alignment and some specific algorithms will be described in the next sections.

To align two feature sequences X and Y, let $c : \mathscr{F} \times \mathscr{F} \to \mathbb{R}$ denote a local similarity measure on $\mathscr{F}$. Define a resulting $(N \times M)$ similarity matrix C by $C(n,m) := c(x_n, y_m)$. The total similarity is the sum of the local similarity along the alignment path p. An alignment with maximal total similarity among all possible alignments is called an *optimal alignment*.

To determine such an optimal alignment, one recursively computes an $(N \times M)$-matrix D, where the matrix entry $D(n,m)$ is the total similarity of the optimal alignment between $(x_1,\ldots,x_n)$ and $(y_1,\ldots,y_m)$. The choice of each step is recorded in a matrix ψ which is later used to compute an optimal path via backtracking. More precisely, let

$$D(n,m) := \max \begin{cases} D(n-1,m-1) + w_1 C(n,m), \ \psi[n,m] = 0(\nwarrow); \\ D(n-1,m) + w_2 C(n,m), \ \psi[n,m] = 1(\leftarrow); \\ D(n,m-1) + w_3 C(n,m), \ \psi[n,m] = 2(\uparrow) \end{cases} \tag{2.1}$$

for $n, m > 1$. Furthermore, $D(n,1) := \sum_{k=1}^{n} w_2 C(k,1)$ for $n > 1$, $D(1,m) = \sum_{k=1}^{m} w_3 C(1,k)$ for $m > 1$, and $D(1,1) := C(1,1)$. The weights $(w_1, w_2, w_3) \in \mathbb{R}_+^3$ can be used to adjust the preference over the three step sizes.

Here, we break the optimal path problem into sub-problems of the best choice for each step, shown as Figure 2.3 (a). The matrix ψ is built up to store the solutions to each

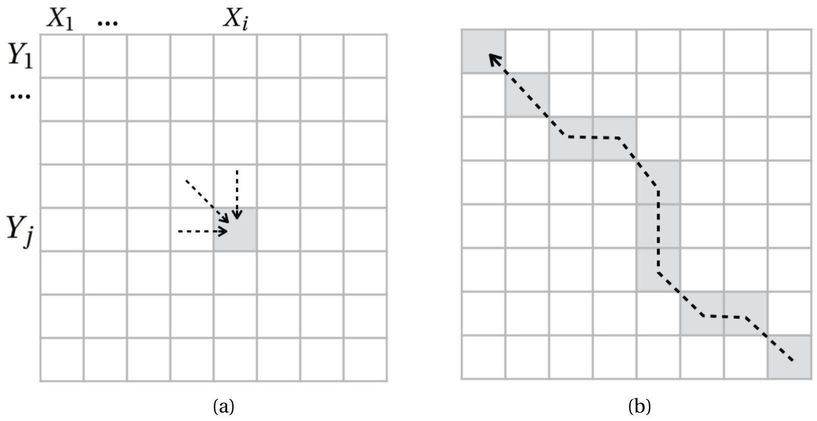

Figure 2.3: Solving dynamic programming problem with a look up table: (a) Build a look-up table to store solutions of sub-problems in a bottom-up fashion; (b) Trace back to get the optimal solution, see text for details.

sub-problem, in a bottom-up fashion. After filling each entry, an optimal alignment can be constructed by tracing back the choices of steps we made, as illustrated in Figure 2.3 (b).

Dynamic Programming was first introduced for music alignment by Dannenberg (1984), to align a symbolic performance with a score. Since then various DP based methods have been applied in MIR. Examples include the Smith-Waterman algorithm for cover song identification (Serrà and Gómez, 2008), Edit Distance in lyrics based music retrieval (Müller et al., 2007), and Longest Common Subsequence (LCS) in melody queries (Rho and Hwang, 2006). Dynamic Time Warping (DTW) is the most frequently used DP method for music alignment/score following (Orio and Schwarz, 2001; Dannenberg and Hu, 2003; Dixon and Widmer, 2005; Macrae and Dixon, 2010; Ewert et al., 2009b; Müller et al., 2006), where DTW is responsible for 50% of citations from 1995 to 2001 as reported by Macrae (2012). The following will provide an overview of several DP methods, starting with Longest Common Subsequence (LCS) and Dynamic Time Warping (DTW).

2.3.1.1 Longest Common Subsequence (LCS)

The Longest Common Subsequence (LCS) algorithm aims at finding the longest subsequence common to all sequences in a set. The elements of the subsequence must appear in all sequences in the same order but not necessarily consecutively. For example, $\{C, E, D\}$

is the longest common subsequence of $\{F, C, E, A, D\}$ and $\{A, C, B, E, D\}$.

Algorithm 1: Longest Common Subsequence (LCS) algorithm

```
Data: Sequences $X_N, Y_M$
Result: Length of LCS $D[n,m]$ and Table $\psi$
for $i = 1 : n$ do
    for $j = 1 : m$ do
        if $i == 1$ then
            $D[i,j] = 0; \psi[i,j] = 1(\leftarrow);$
        else if $j == 1$ then
            $D[i,j] = 0; \psi[i,j] = 2(\uparrow);$
        else if $x_{i-1} == y_{j-1}$ then
            $D[i,j] = L[i-1,j-1]+1; \psi[i,j] = 0(\nwarrow);$
        else if $D[i-1,j] >= D[i,j-1]$ then
            $D[i,j] = D[i-1,j]; \psi[i,j] = 2(\uparrow);$
        else
            $D[i,j] = D[i,j-1]; \psi[i,j] = 1(\leftarrow);$
        end
    end
end
```

The objective of LCS is to maximise the number of identical elements along the alignment paths, i.e. to maximise $D(N, M)$. In this case, the local dissimilarity/similarity measure is set to

$$\begin{cases} C[i,j] = 1, x_{i-1} == y_{j-1}; \\ C[i,j] = 0, x_{i-1} \neq y_{j-1} \end{cases} \tag{2.2}$$

In a music context, x_i and y_j could be pitches of the corresponding notes.

Intuitively, the algorithm exploits two properties: firstly, if the two sequences to compare end in the same element, then their LCS should end with that element, which can be removed from both sequences, i.e., for sequence $X_N := (x_1, x_2, \ldots, x_n)$ and $Y_M := (y_1, y_2, \ldots, y_m)$, if $x_n = y_m$, then $LCS(X_N, Y_M) = LCS(X_{N-1}, Y_{M-1}) \cup (x_n)$; Secondly, if $x_n \neq$

y_m, then $LCS(X_N, Y_M)$ is the longer one of $LCS(X_{N-1}, Y_M)$ and $LCS(X_N, Y_{M-1})$. Therefore we can break down the LCS problem into sub-problems and use dynamic programming to build the solution in a bottom-up fashion, as shown in Algorithm 1.

By tracing back the Table T obtained by Algorithm 1, the Longest Common Subsequence can be derived easily, see an example in in Table 2.1.

As a strict matching algorithm where the local similarity measure is binary, LCS is often applied to file comparison and biological sequence analysis tasks. In a music context, it is mainly used to align symbolic representations, such as score and performance data in MIDI format.

	y_j	F	C	E	A	D
x_i	0	← 0	← 0	← 0	← 0	← 0
A	↑ 0	↑ 0	↑ 0	↑ 0	↖ 1	← 1
C	↑ 0	↑ 0	↖ 1	← 1	↑ 1	↑ 1
B	↑ 0	↑ 0	↑ 1	↑ 1	↑ 1	↑ 1
E	↑ 0	↑ 0	↑ 1	↖ 2	← 2	← 2
D	↑ 0	↑ 0	↑ 1	↑ 2	↑ 2	↖ 3

Table 2.1: An example of LCS alignment

2.3.1.2 Needleman-Wunsch (NW)

The Needleman-Wunsch algorithm (NW) (Needleman and Wunsch, 1970) was one of the first dynamic programming algorithms to align biological sequences. Unlike LCS, it allows matching non-identical elements which are biologically meaningful to be matched together. Therefore the local similarity measure is not simply binary, instead, derived by the evolutionary relationship of the biological sequences. It also introduces the concept of "gap", which refers to the insertions and deletions in a sequence, which cannot be matched with any elements in another sequence. Gaps are usually penalised with a constant cost d. Therefore, the total similarity matrix in Equation 2.1 is rewritten as

$$D(n,m) := \max \begin{cases} D(n-1,m-1) + C(n,m), \psi[n,m] = 0(\nwarrow); \\ D(n-1,m) - d, \psi[n,m] = 1(\leftarrow); \\ D(n,m-1) - d, \psi[n,m] = 2(\uparrow) \end{cases} \tag{2.3}$$

In a music context, the Needleman-Wunsch algorithm is adapted in (Grachten et al., 2013) to align recordings with structural differences by adding a penalty to skipping in the alignment.

2.3.1.3 Dynamic Time Warping (DTW)

Dynamic time warping specialises in aligning temporal sequences. It has been well researched as a tool to compare different speech patterns in the speech recognition community since the 1970s (Itakura, 1975; Rabiner and Juang, 1993). Later in 2001, it was introduced for music alignment (Orio and Schwarz, 2001) and various extensions have been proposed over the years. This section will introduce the concept of DTW firstly and skim through some prominent extensions. For a comprehensive tutorial on DTW, see Chapter 4 of (Müller, 2007).

Basic algorithm

As the name suggests, Dynamic Time Warping compares sequences which are considered to be a non-linear "warp" of each other in the time dimension. The algorithm aims at finding a so called warping path that maps each time position in one version to the corresponding one in the other version. Therefore it can be used to measure the similarity of time series independently of non-linear variations in the time dimension. It has been applied in analysing various time series, including video, audio and graphics data.

In a music alignment context, the objective of DTW is to obtain an optimal alignment minimising the total dissimilarity along the path p. The feature space $\mathscr{F}$ typically denotes the space of normalised chroma features, the local cost measure c is usually a cosine (or Euclidean) distance with weights set to $(w_1, w_2, w_3) = (2,1,1)$ to remove a bias for the diagonal direction (Dannenberg and Raphael, 2006; Dixon and Widmer, 2005). An example

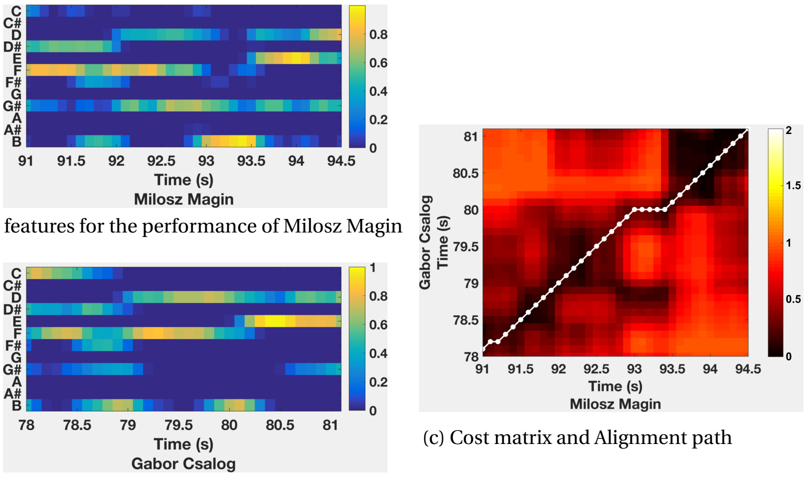

(a) CENS features for the performance of Milosz Magin

(b) CENS features for the performance of Gabor Csalog

(c) Cost matrix and Alignment path

Figure 2.4: An example of DTW alignment for two performance excerpts of Chopin Op. 24 No.2

of aligning two audio performance excerpts with DTW is shown in Figure 2.4, where the cosine distance $c(x_n, y_m) = 1 - \frac{\langle x_n, y_m \rangle}{\|x_n\| \|y_m\|}$ is used.

Same as NW, DTW also allows non-identical matches. It also allows the map from one to many, therefore there is no "gap" concept in DTW. That is because DTW is designed for time series and it assumes the main local difference comes from tempo, where one feature of one version could be time-stretched to several features in another version. NW is designed for biological sequences where the main local difference comes from mutation, therefore insertion and deletion are penalised.

Extensions to Lower the Running Time

Since the cumulative cost matrix D is of size $N * M$, the complexity of basic DTW algorithm is quadratic, i.e. is in $O(NM)$. Often, this is too high to be of practical use when aligning features with a high temporal resolution or recordings having a long duration. Several strategies have been proposed to make DTW-based methods more efficient. A straightforward way to reduce the search space is to use a constant global constraint region, such as the Sakoe-Chiba (Sakoe and Chiba, 1978) bound or the Itakura parallelogram (Itakura, 1975). They force the alignment path to be within a fixed distance from the main diagonal of the cumulative cost matrix. However, sometimes the optimal alignment may lie outside

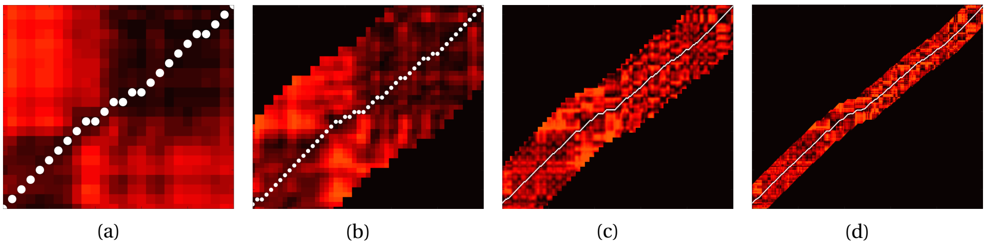

Figure 2.5: Multiscale DTW: The alignment path (in white dot) is computed in one level and projected to next level to construct the constraint (non-black region); The entries outside the constraint is not computed (black region); From (a) to (d), the feature resolution is increasing.

such global constraint. Later work proposed several strategies for more adaptive global or local constraints (Müller et al., 2006; Salvador and Chan, 2004; Prätzlich et al., 2016; Dixon and Widmer, 2005; Macrae and Dixon, 2010).

In particular, later chapters incorporate methods described in (Müller et al., 2006; Salvador and Chan, 2004), referred to as multiscale DTW (FastDTW). The general idea is to first compute a rough alignment at a low temporal resolution, which is then used to constrain the alignment process at higher resolutions, illustrated in Figure 2.5. This way, in the cost matrix C and accumulative cost matrix D, only entries around the projected path need to be computed. As shown in (Müller et al., 2006), this strategy is particularly useful for music due to the high temporal correlation between neighbouring feature vectors, i.e. the temporal feature resolution can be decreased without losing the information necessary to find the correct path on the coarser level. In practise, it typically leads to a drop in runtime by up to a factor of 30.

Extensions for Realtime Alignment

Many other techniques not only accelerate but enable a method to align sequences online or in real-time. For example, the method presented in (Dixon and Widmer, 2005) employs a greedy, locally optimal forward path estimation algorithm to constrain the alignment path, while (Macrae and Dixon, 2010) employs a windowed variant of DTW integrating ideas of the A^* algorithm (Hart et al., 1968) to dynamic programming.

Extensions to Account for Structural Differences

Some extensions of DTW aim at addressing structural differences, i.e. the situation when musicians unexpectedly choose to repeat or skip an entire section. The method proposed in (Arzt et al., 2008) caters for different choices musicians make in real-time by maintaining multiple alignment instances. For off-line cases, (Fremerey et al., 2010) extends the step size of DTW to include jumps between sections. (Müller and Appelt, 2008) analyses the cost matrix between two versions before alignment and extract partial matches from the alignment path.

2.3.1.4 Other Dynamic Programming Methods

There are some other dynamic programming based methods that have been applied to music alignment. For example, the Smith-Waterman algorithm (Smith and Waterman, 1981) is a common local alignment method for biological sequence analysis and it was used in (Ewert et al., 2009a) for partial alignment in the case of structural differences.

2.3.2 Probabilistic Modelling

It is natural to use dynamic programming if we think of finding the alignment path as an optimisation problem. However, we could also interpret the task as a latent state estimation problem by considering the *pattern* shared by all versions of a piece of music as the *latent*/*hidden* states, while their feature sequences are our observations emitted from the latent states. Following this train of thought, many probabilistic modelling methods have been applied to the music alignment task. The following sections will introduce a widely used and extended probabilistic modelling method, the Hidden Markov Model (HMM).

2.3.2.1 Hidden Markov Model (HMM)

This section will give a brief introduction to the standard Hidden Markov Model (HMM). For more details, see tutorials of HMM (Rabiner, 1989; Stamp, 2004) .

As the name suggests, an HMM models a system which is assumed to be a Markov process with *hidden* states. A Markov process is a stochastic process with the so called Markov property, which we will see in more detail below. In a signal processing context, a stochastic process is a system that evolves with time. The evolution in time is modelled by the transitions between states. The Markov property regulates that the transition probability from the current state to the next state only depends on the current state and not on the past states. In an HMM, the states are hidden and can be observed only by the random variables they emit according to certain probability distributions. To describe an HMM model, the following notation is used:

$L \leftarrow$ number of states;

$S = (s_1, s_2, \ldots, s_L) \leftarrow$ states in the model;

$N \leftarrow$ length of the observation sequence;

$O = (O_1, O_2, \ldots, O_N) \leftarrow$ observation sequence;

$a_{ij} \leftarrow$ state transition probability from s_i to s_j;

$\pi \leftarrow$ initial state distribution;

$b_i(O_n) \leftarrow$ observation probability

In a music alignment context, the observation O_n is usually a feature vector, emitted by state s_i with a certain probability distribution $b_i(O_n)$. The observation probability distribution could either be discrete or continuous and here a continuous normal distribution is discussed which is often used for time series,

$$b_i(O_n) = \mathcal{N}(O_n; \mu_i, \sigma_i^2) \tag{2.4}$$

Figure. 2.6 shows an example HMM with a fully connected (ergodic) topology, meaning every state can be reached from any state in a finite number of steps. There are other types of topologies, such as a left-right HMM which only allows transition from left to right, i.e. $a_{ij} = 0, j < i$. It is often used when the number of states is relatively large or avoid impractical or even infeasible parameter estimations.

An HMM can be applied to solve two problems in the music alignment task: decoding and training. Decoding an alignment is to find the state sequence $X := \{x_1, \cdots, x_N\}, x_i \subset S$, for $i = 1, \cdots, N$, which is most likely to generate the given observation sequence O. Training is to adjust the parameters of the model $\lambda = (a, b, \pi)$, so that it can best describe, or maximise the probability of generating the observation sequences. The following will introduce Viterbi decoding and Baum-Welch Traning for these two purposes.

Viterbi Decoding To find the best matched state sequence is an optimisation problem, which can be solved with Dynamic Programming in the same fashion as introduced before. Instead of minimising the total cost as in DTW, here the goal is to maximise the prob-

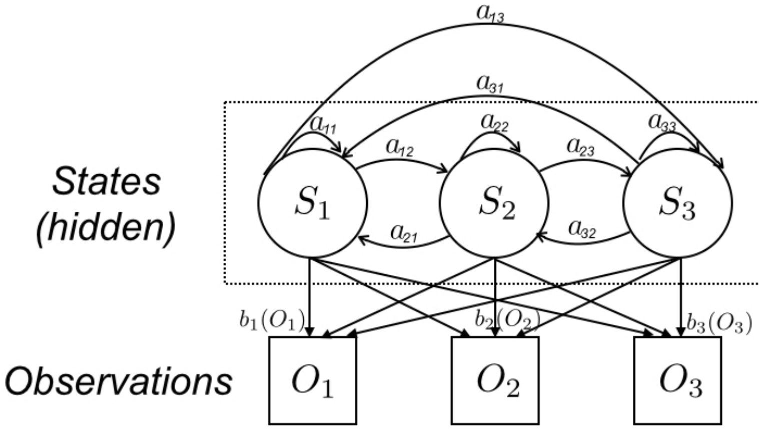

Figure 2.6: An example of HMM model

ability $P(X|O,\lambda)$ which is equivalent to maximising $P(X,O|\lambda)$. To do so, define $\delta_n(j) = \max P(x_1,x_2,\cdots,x_n = j,O_1,O_2,\cdots,O_n|\lambda)$, i.e. $\delta_n(j)$ is the highest probability given the observation until frame n. It can be calculated recursively as $\delta_n(j) = \max_i[\delta_{n-1}(i)a_{ij}]\cdot b_j(O_n)$ and the choice of each step is recorded in another matrix $\psi_n(j) = \arg\max_i \delta_{n-1}(i)a_{ij}$. At the end, the best matched state sequence can be obtained by tracing back ψ. This procedure is called Viterbi decoding (Rabiner, 1989).

Baum-Welch Training The Baum-Welch algorithm is often used in parameter estimation for HMMs. The main idea is to use the Expectation-Maximisation algorithm to find the Maximum Likelihood estimate of the model parameters. It iteratively performs three processes: the forward procedure, the backward procedure and the parameter re-estimation. The forward procedure computes a forward variable $\alpha_i(n)$, defined as the probability of the partial observation sequence until frame n and state S_i at frame n, given the model λ:

$$\alpha_i(n) = P(O_1,O_2\cdots O_n,x_n = s_i|\lambda) \tag{2.5}$$

After initialisation $\alpha_i(1) = \pi_i b_i(O_1), i = 1,2\cdots L$, one computes $\alpha_i(n)$ for $n = 2,3\cdots N$ and $i = 1,2\cdots L$ recursively:

$$\alpha_i(n) = [\sum_{j=1}^{L} \alpha_{n-1}(j)a_{ji}]b_i(O_n) \tag{2.6}$$

while terminates at $P(O|\lambda) = \sum_{i=1}^{L} \alpha_i(N)$. $P(O|\lambda)$ is the model likelihood that the Baum-Welch algorithm aims to maximise and it is used to define the termination criterion for the iterative parameter estimation.

The backward procedure computes a backward variable $\beta_i(n)$ in a similar way. $\beta_i(n)$ is the probability of the partial sequence from time $n+1$ to the end, given state S_i at time n and the model λ:

$$\beta_i(n) = P(O_n + 1, O_n + 2 \cdots O_N | x_n = s_i, \lambda) \tag{2.7}$$

After initialisation $\beta_i(N) = 1, i = 1, 2 \cdots L$, one computes $\beta_i(n)$ for $n = N-1, N-2 \cdots 1$ and $i = 1, 2 \cdots L$ recursively:

$$\beta_i(n) = \sum_{j=1}^{N} a_{ij} b_i(O_{t+1}) \beta_j(n+1) \tag{2.8}$$

To re-estimate the parameters, define $\xi_n(i,j)$ as the probability of being in the state s_i at time t and transiting to s_j at time $t+1$, given the model λ and the observation sequence O:

$$\xi_n(i,j) = P(x_n = s_i, x_{n+1} = s_j | \lambda, O), \tag{2.9}$$

which can be computed with the forward and backward variables:

$$\xi_n(i,j) = \frac{\alpha_i(n) a_{ij} b_j(O_{n+1}) \beta_j(n+1)}{P(O|\lambda)}, \tag{2.10}$$

Also define $\gamma_n(i)$ as the probability of being in the state s_i at the frame n given the model λ and the observation sequence O, which is the sum of $\xi_n(i,j)$ over j,

$$\gamma_n(i) = \sum_{j=1}^{L} \xi_n(i,j), \tag{2.11}$$

The re-estimation of A and π is computed as:

$$\tilde{\pi}_i = (\text{expected frequency of state } s_i \text{ at frame } n = 1) = \gamma_1(i) \tag{2.12}$$

$$\tilde{a}_{ij} = \frac{\text{expected number of transition from } s_i \text{ to } s_j}{\text{expected number of transition from state } s_i} = \frac{\sum_{n=1}^{N-1} \xi_n(i,j)}{\sum_{n=1}^{N-1} \gamma_n(i)} \tag{2.13}$$

When the normal distribution is used as the observation probability distribution, i.e. $b_i(O_n) = f(O_n|\mu_i, \sigma_i^2)$, the re-estimation of B is computed as:

$$\tilde{\mu}_i = \frac{\sum_{n=1}^{N} \gamma_n(i) \cdot O_n}{\sum_{n=1}^{N} \gamma_n(i)} \tag{2.14}$$

$$\tilde{\sigma}_i^2 = \frac{\sum_{n=1}^{N} \gamma_n(i) \cdot (O_n - \mu_i)^2}{\sum_{n=1}^{N} \gamma_n(i)} \tag{2.15}$$

For a more complicated probability density function, one could use a M-component Gaussian mixture model,

$$b_i(O) = \sum_{m=1}^{M} c_{im} \mathcal{N}(O; \mu_{im}, \sigma_{im}^2), \tag{2.16}$$

where c_{im} is the mixture coefficient for mth mixture in state i, for more detail see (Rabiner, 1989). In summary, the Baum-Welch training follows:

- Initialisation: $\lambda = (A, B, \pi)$;
- Recurrence:
  - Calculate $\alpha_i(n)$ and $\beta_i(n)$ with the forward-backward procedure;
  - Calculate $\xi_n(i, j)$ and $\gamma_n(i)$;
  - Re-estimate the model $\tilde{\lambda} = (\tilde{A}, \tilde{B}, \tilde{\pi})$;
- Termination condition: the model likelihood $P(O|\lambda)$ stops increasing or is larger than some predefined threshold or the maximum number of iterations is exceeded.

Viterbi Training As an alternative to the Baum-Welch algorithm, one can also use Viterbi training (Durbin et al., 1999) to train the HMM. It replaces the forward-backward procedure with Viterbi decoding to get the most likely state sequence and uses it to re-estimate the model parameters in every iteration. This way, instead of a soft value encoding the probability of being in a certain state at a certain time frame, the Viterbi decoding makes a hard choice and sets the probability of the state-time pair to 1 if it is on the most probable path, and to 0 otherwise. Compared to Baum-Welch, it does not aim to maximise the model likelihood and therefore the estimated parameters may not be as good as the ones obtained from the Baum-Welch algorithm. However, since the continuous model likelihood is not computed, Viterbi training tends to converges much faster than Baum-Welch training.

Numerical Issues Note that the above computation will easily run into numerical issues. For example, for the forward variable, since the transition probability is usually smaller than 1, after multiplication for $i = 1, 2 \cdots, L$ and $n = 1, 2 \cdots, N$, the value of $\alpha_i(n)$ exponentially approaches zeros. If the absolute value is even smaller than the computer can actually represent, the true value will be replaced by zero. The solution to this underflow error is to scale variables. For each n, define a scaling coefficient c_n,

$$c_n = \frac{1}{\sum_{i=1}^{L} \alpha_i(n)} \tag{2.17}$$

The forward and backward variables are scaled as $\tilde{\alpha}_i(n) = c_n \cdot \alpha_i(n)$ and $\tilde{\beta}_i(n) = c_n \cdot \beta_i(n)$. Furthermore, the logarithm of $P(O|\lambda)$ is computed as $\log[P(O|\lambda)] = -\sum_{n=1}^{N} \log c_n$. The parameter re=estimation keeps the same after replacing the $\alpha_i(n)$ and $\beta_i(n)$ with $\tilde{\alpha}_i(n)$ and $\tilde{\beta}_i(n)$ respectively. For details of the derivation, see (Rabiner, 1989; Stamp, 2004).

Adaptation to Music Tasks As a statistical modelling method for sequence analysis, the HMM has been widely applied in various fields such as finance and biological sequence analysis as well as speech recognition. It was introduced in the context of music alignment in (Raphael, 1998) and has been widely studied and extended in MIR since then (Orio and Déchelle, 2001; Cont, 2006; Miotto et al., 2010; Cont, 2010).

The HMM and its variations have been particularly popular in score-to-audio alignment tasks, as here each state intuitively corresponds to a note or a constellation of concurrent notes as specified by the score (Raphael, 1998; Orio and Déchelle, 2001; Cont et al., 2005), while other assumptions about the music can be captured in higher-level HMM structures. For examples, high-level states might encode the current tempo (Raphael, 2004), or each note-state can be subdivided into attack-decay-release sub-states (or similar temporal evolutions). Such high level structures lead to hierarchical HMMs and semi-Markov graphical models, or generalisations thereof such as Dynamic Bayesian Networks (DBNs) (Cont, 2010; Maezawa et al., 2014). It should be noted that many of these more advanced models can still be represented as a standard HMM.

HMM based music alignment usually can work in real-time. The model is trained offline and alignment is performed using online decoding methods (Raphael, 1998; Orio and Déchelle, 2001; Pardo and Birmingham, 2005). On the contrary, the method proposed in (Cont, 2010) avoids the need for offline training by using an anticipatory forward propagation algorithm for real-time inference. To account for structural differences, possible repeats and jumps according to the score could be encoded into the model through modification to the transition function (Pardo and Birmingham, 2005). However, the method proposed in (Pardo and Birmingham, 2005) is only for symbolic music alignment.

2.3.2.2 Other Probabilistic Modelling Methods

There are many other probabilistic modelling methods employed by the MIR community for music alignment. Even before the HMM was introduced, Grubb and Dannenberg (1997) proposed a stochastic method which models the score position with a continuous probability density function, avoiding the problem of discrete states in contrast to a standard HMM.

Recently, conditional random fields (CRFs) have been used for music synchronisation (Joder et al., 2011). As an advantage, CRFs loosen several limitations of HMM-based methods in contrast to more general DP methods, e.g. DTW. In particular, their use of so-called feature-functions generalises the notion of observation probability and thus enables measuring distances between features in a more general way than HMMs allow.

Conceptually quite different from the above are state-space methods, where states such as position or tempo are elements of a continuous space. Transitions between states are modelled using transition functions that, applied to the current state, yield the next one (Duan and Pardo, 2011). Depending on specific properties of the sources of noise in the model, one typically uses parameter estimation methods based on the Kalman filter, particle filter or more general Monte-Carlo sampling methods (Montecchio and Cont, 2011a).

2.3.3 Similarity between Dynamic Time Warping and Hidden Markov Model

Among various alignment methods, the most often used and extended ones are DTW and HMM. They belongs to the above mentioned two categories respectively, with one being described as an optimisation and the other as a probabilistic inference problem.

However, there are many similarities between them from an algorithmic point of view. In particular, under certain conditions, DTW is equivalent to a negative log-likelihood implementation of an HMM using multivariate Gaussian distributions for the observations. This is the case if a Euclidean distance is used to compare features and additive is used instead of multiplicative weights are used for different step sizes. With these limitations, the application of a logarithm transforms the HMM-likelihood from a product of probabilities to a sum of log-probabilities, which for the case of a Gaussian takes the form of a Euclidean distance. One can show that the result is equivalent to DTW by interpreting the features of one DTW sequence as HMM states, using the features as the mean of the corresponding Gaussians and adding some non-emitting states to model certain step sizes – see (Rabiner, 1989; Cox, 1990) for some discussion. Furthermore, both the calculation of an optimal alignment path in DTW and the decoding of the most probable path are instances of dynamic programming.

2.3.4 Other Techniques used in Music Alignment

Non-negative Matrix Factorisation (NMF) is applied in (Niedermayer, 2009b) as a post-processing step in score to audio alignment to refine the mapped note onset positions. NMF will be introduced in detail in Chapter 5. Recently, neural networks have been used in a few works (Dorfer et al., 2016a,b) to map short music audio snippets to the corresponding image location of a scanned sheet score.

2.4 Exploiting Score Information using Alignment Techniques in MIR

In music information retrieval (MIR) research, musical knowledge is often exploited to improve the performance of a system. The score, as a natural source of music information, has been used for a variety of tasks. This section will provide an overview of MIR research which exploits score information based on alignment techniques.

2.4.1 Score-informed Expressive Parameter Extraction

A large body of work employs score to audio alignment techniques as a foundation for extracting expressive parameters from recorded music performances. Here, score to audio alignment is used to identify the rough time boundaries (onsets and/or offsets) for each score note in a given audio recording, which then provides guidance for analysing the audio performance.

For example, Scheirer (1995) proposed a method which employs the score to extract onset and offset timing as well as dynamics for each score note from audio recordings of musical performances. In this method, the tempo estimator is updated based on a linear regression model of matched pairs of past score notes and detected onsets. Based on the estimated tempo, a search window is chosen to extract onset, offset as well as dynamics

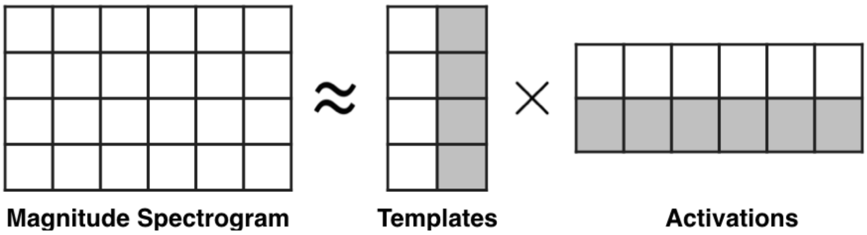

Figure 2.7: Non-Negative Matrix Factorisation (NMF)

for each score note by spectral analysis. Earis (2007) used a similar idea to extract onset time and dynamics from expressive performances, in which the manually aligned score constrains the search window of the onset detection. This idea is also exploited in (Niedermayer and Widmer, 2010), where NMF is used to refine the note onset position after automatically aligning the given audio recording to the corresponding score. To estimate note intensities in a music recording, Ewert and Müller (2011) proposed a parametrised spectrogram model, which is initialised using the aligned score for each note event. The model parameters are estimated iteratively to minimise a distance between the audio and model spectrogram. Most recently, a framework is proposed (Abeßer et al., 2017) for analysing the tuning, intonation, pitch modulation and dynamics in Jazz recordings. It is based on a score-informed solo and accompaniment separation. The use of score information can help achieve a high quality source separation for music and it has attracted much research interest in recent years. The following section will discuss it in more detail.

2.4.2 Score-informed Source Separation

Separating individual music sources from a mixture audio signal is a challenging task. Usually music is distributed in a stereo format, that is to say, when there are several instruments playing simultaneously, the signals from more than one instrument will be mixed in the same channel (by recording with a single microphone or mixing down several channels afterwards). To boost the performance of the separation, many works use score information to help identify and locate sound events in the corresponding audio recording.

For example, a commonly used source separation method is Non-Negative Matrix Factorisation (NMF), which decomposes an input spectrogram into the product of two non-negative matrices, one containing spectral template vectors and the other encoding the activity of each template over time, demonstrated in Figure 2.7. For more details on NMF, see (Lee and Seung, 2000). Essentially, NMF is an unsupervised learning process which is expected to learn a dictionary consisting of the spectral patterns for individual components in the input signal. (An individual component could be one pitch played by one instrument.) However, the objective function of NMF is to minimise the distance between the input spectrogram and the one reconstructed by multiplying the spectral template matrix and the activation matrix. Therefore it may not produce a useful decomposition even if the distance reaches a minimum in the learning process. However, from a machine learning perspective, NMF belongs to the group of generative models, which often employ interpretable parameters and thus enable a direct way to incorporate prior knowledge and adapt the method to specific acoustic conditions (Ozerov et al., 2012; Ewert and Sandler, 2016). One rich source of prior information to guide the NMF learning process is the score. After aligning the score to the given audio recording, one knows for each time position in the recording, which instruments and which notes are expected to sound. The pitch and timbre information can be used to constrain the spectral patterns for each component, while the timing information (note boundaries) allows constraining the corresponding activities for each component. For a comprehensive overview, see (Ewert et al., 2014).

Score-informed source separation techniques have been applied to note-based audio editing (Driedger et al., 2013), remixing and upmixing of stereo music (Woodruff et al., 2006), instrument-wise equalisation (Itoyama et al., 2008) and singing voice separation (Chan et al., 2015). The idea of score-informed dictionary learning can be adapted to automatic music transcription (AMT). For example, for piano transcription, the components of the expected dictionary could be the 88 piano pitches. The concept of score informed transcription will be briefly introduced next.

2.4.3 Score-informed Transcription

The goal of automatic music transcription (AMT) is to obtain a high-level symbolic representation of a given audio recording. As a fundamental problem in music processing, a wide range of approaches has been proposed over the years, see (Klapuri and Davy, 2006; Christensen and Jakobsson, 2009; Benetos et al., 2013) for more comprehensive overviews. For example, Yeh et al. (2010) proposed a joint pitch estimation method by progressively combining F0 candidates into pitch or note objects. Further, various probabilistic models have been employed for AMT, such as a method using maximum a posteriori (MAP) estimation (Emiya et al., 2010) or methods based on non-parametric Bayesian models (Yoshii and Goto, 2012). Modelled as a classification or regression task, transcription has also been addressed by several discriminatively trained methods, using support vector machines (Poliner and Ellis, 2007), convolutional neural networks (Marolt, 2004; Kelz et al., 2016), deep belief networks (Nam et al., 2011) or recurrent neural networks (Böck and Schedl, 2012; Sigtia et al., 2015).

Among the various approaches, most state-of-the-art AMT methods are based on spectrogram factorisation techniques, such as Non-negative Matrix Factorisation (NMF) or its probabilistic formulation, Probabilistic Latent Component Analysis (PLCA) – see (Virtanen et al., 2015) for an overview. NMF was introduced into AMT by Smaragdis and Brown (2003) and many variants have been proposed in recent years. One type of variants regularise the learning procedure by adding constraints to spectral templates so as to enforce a harmonic structure (Vincent et al., 2010; Bertin et al., 2010), or constraints for the activity matrix to enhance temporal continuity and sparsity properties (Virtanen, 2007). Other variants such as non-negative matrix deconvolution (NMD) (Smaragdis, 2004) employ, instead of individual spectral template vectors as used in NMF, entire spectro-temporal blocks as templates, each modelling a part of an entire segment in a time-frequency representation. Since these blocks have a fixed size, NMD has mainly been used for drum sound separation and transcription (Roebel et al., 2015). Shift-invariant PLCA enhances NMF's capability to represent changes in fundamental frequency by effectively coupling the parameter estimation for those templates associated with a specific musical pitch (Benetos and Dixon, 2012). Finally, Markov constraints can be used to express that non-stationary sounds can often be modelled a sequence of specific spectral templates, where the order is modelled using a graphical model (Ozerov et al., 2009; Benetos and Dixon, 2013; Ewert et al., 2015); as discussed in (Ewert and Sandler, 2016), this approach is particularly useful for modelling a few concurrent speakers but leads to various numerical issues when applied to highly polyphonic sounds such as piano recordings.

However, despite being researched for several decades, current AMT methods are still inadequate for many applications and seem to have reached a plateau in performance.

To boost the accuracy, some works exploit the availability of additional information, such as annotations made by users for the recording under analysis (Kirchhoff et al., 2012), or single note recordings giving more details about the instrument in use and the recording conditions (Klapuri and Davy, 2006; Ewert and Sandler, 2016). Another particular type of prior knowledge is a musical score. Given the goal of AMT, score information may look like the output rather than the prior knowledge. However, some applications, such as music tutoring or performance analysis, aim to identify differences between the performance and the given score. In these cases, score information is often available and can readily be exploited to improve the AMT system.

Score-informed transcription is a relatively new concept. Benetos et al. (2012) proposed such an AMT system to reduce the number of falsely detected notes by transcribing both the performance recording and a synthesised recording of the score. The system then discards the notes detected in both recordings which are not actually on the score. It can be considered as a post-processing step to correct the results of a standard AMT method. In contrast, Chapter 5 presents a method that integrates the score information directly into the dictionary learning process so that the obtained spectral patterns are tuned to the specific recording. The idea is inspired by score-informed source separation, introduced in the previous section. Since the dictionary is highly adapted to the given audio recording, it eliminates the requirement of single note recordings, in contrast to (Benetos et al., 2012).

2.5 Discussion

This chapter reviewed the literature on music alignment and score-informed MIR research which applies the alignment techniques. For one piece of music, there are often various versions, including different forms of musical score and multiple recordings of musical performances. Music alignment provides a way to establish links between these different versions. Specifically, the goal of music alignment is to map each temporal position in one version to the corresponding positions in other versions of the same piece. Feature representations used in music alignment and the related work on alignment methods were discussed.

Thanks to the considerable amount of research efforts over the years, various alignment methods have been proposed and current methods have achieved high accuracy in many cases. However, musicians can interpret a piece in diverse ways, which leads to complex differences on a musical level between individual performances. Additionally, the wide range of possible acoustic conditions adds another layer of complexity to the music alignment task. If such differences are substantial, even state-of-the-art methods may fail in identifying a correct alignment. This thesis aims to improve the robustness for some of these cases by developing novel sequence models and alignment methods that can make use of specific information available in music synchronisation scenarios. Chapter 3 and Chapter 4 will propose two strategies of improving the alignment robustness in different scenarios.

By applying music alignment techniques, the score information can be exploited to assist various MIR tasks, including expressive parameter extraction, source separation and automatic music transcription. For automatic music transcription (AMT), the accuracy of current methods are inadequate for many applications. To boost the accuracy of AMT, Chapter 5 will apply the alignment techniques to exploit the score information in the dictionary learning process.

CHAPTER 3

ROBUST JOINT ALIGNMENT OF MULTIPLE PERFORMANCES

3.1 Introduction

Chapter 2 reviewed various methods for aligning different versions of a piece of music. The goal of most of these methods is to map each temporal position in one version of a piece of music to the corresponding position in another version. Such pairwise alignment methods achieve high accuracy in many cases (Joder et al., 2011; Ewert et al., 2009b; Dixon and Widmer, 2005). However, even the state-of-art still often fails to identify a correct alignment if versions differ substantially with respect to acoustic conditions or musical interpretation. To increase the robustness for these cases, this chapter exploits the availability of multiple versions of the piece to be aligned. By processing these jointly, the alignment process can be stabilised with additional examples of how a musician can realise a section of a piece or which acoustic conditions might prevail in a recording.

The chapter is arranged as follows. First, the motivation of this work is discussed in Section 3.2. As the proposed methods are inspired by the multiple sequence alignment methods as used in biology, related work and some necessary background is given in Section 3.3. Two proposed joint alignment methods are described in Section 3.4, based on

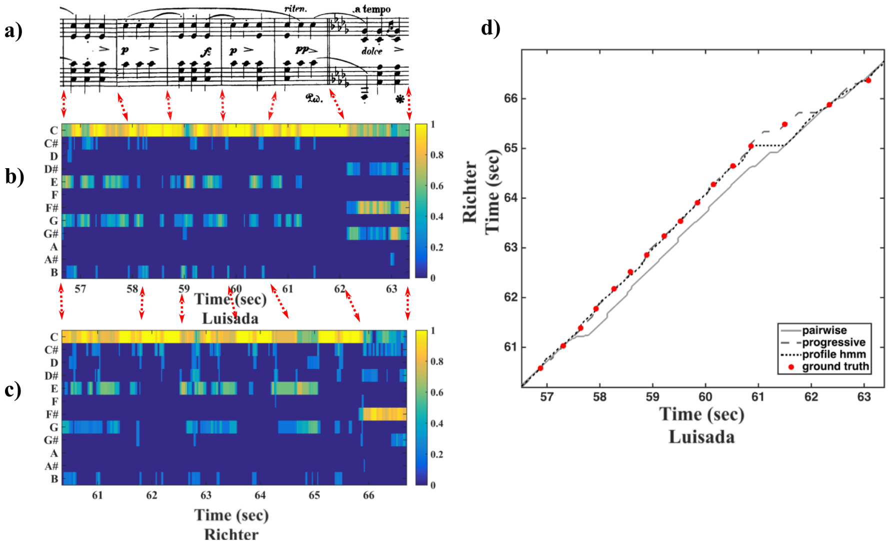

Figure 3.1: Alignment of two interpretations of Chopin Op. 24 No. 2, measures 52-57: **(a)** Score for the six measures. **(b)** / **(c)** CENS features (a variant of chroma features proposed in (Müller et al., 2005)) for interpretations by Luisada and Richter, respectively. **(d)** Alignment results for the pairwise (solid), proposed progressive alignment (dashed) and profile HMM (dotted); ground truth are given as corresponding beat positions from the two versions (red).

progressive alignment and profile HMM respectively. Their differences and similarities are discussed in Section 3.5. An in-depth analysis of the behaviour of both joint alignment methods is provided in Section 3.6. A conclusion is given in Section 3.7.

3.2 Motivation

As shown in Chapter 2, the objective of pairwise alignment is to find an alignment path along which the two versions match best or more precisely, to minimise the total dissimilarity between features from both versions, subject to some path constraints . However, a musician can interpret a piece in diverse ways, which can lead to substantial local differences between versions in terms of articulation and note lengths, ornamental notes (grace notes, trills), or the relative loudness of notes (balance). Additionally, there could also be complex differences in the acoustic environment, instrumentation and recording conditions. Those differences can reduce the alignment accuracy of state-of-the-art methods drastically.

Figure 3.1 shows a real-world example of a pair-wise method failing to compute a correct alignment between two recordings of Chopin's Op. 24 No. 2. Chroma features for both recordings shown in Figure 3.1b and c reveal acoustical (more noise in the C$^\sharp$ and D chroma bands in Figure 3.1c) and musical differences (more pronounced staccato on the E and G notes in Figure 3.1b). Since the piece shows a repetitive pattern on the chroma level, such differences cause a pairwise method (Ewert et al., 2009b) to compute an incorrect alignment between the two versions. The results are shown in Figure 3.1d as a grey alignment path, which encodes corresponding positions between the two recordings as computed by the method – note how the path deviates from the correct positions between 57.5–61.5 seconds (in the timeline of Luisada's version).

To improve the alignment accuracy for such difficult cases, this chapter exploits the fact that in many cases not only two but multiple versions of a piece are available. This is the case, for example, in comparative performance analysis (Widmer et al., 2003; Sapp, 2007; Müller et al., 2009) and expressivity studies (Liem and Hanjalic, 2011), in music production where corresponding audio takes need to be aligned (Montecchio and Cont, 2011b), when coordinating user-generated videos of a concert (Başaran et al., 2015) or generating ground-truth for large scale distance learning (Raffel and Ellis, 2015). If multiple versions are indeed available, the idea is to align them in a joint way, which facilitates the synchronisation process as every additional version presents another example of how a musician can realise a section of a piece or which acoustic conditions might prevail in a recording.

Instead of only aligning two versions with strong local differences, including other available versions can help stabilising the alignment process. As a first indication, this is illustrated in Figure 3.1d: the results computed using the proposed joint alignment methods are shown as two additional paths (dashed and dotted), in which the overall robustness and alignment accuracy is increased considerably.

3.3 Background on Multiple Sequence Alignment

The straightforward idea to align multiple versions is to extend dynamic programming techniques (reviewed in Chapter 2) to multiple dimensions so that several sequences can be aligned jointly. Instead of constructing a two-dimensional look-up table as in Figure 2.3, a multi-dimensional table can be built to store solutions to all sub-problems. This has been demonstrated in the context of gesture recognition (Holt et al., 2007) and multi-modal speech recognition (Wöllmer et al., 2009). However, it is easy to spot that the computational complexity of this strategy will increase exponentially with the number of sequences. Assuming that each sequence to be aligned is roughly of length N, the time and memory requirement to align K versions is $O(N^K)$. Path pruning techniques can be used to mitigate such problems for small values of K as shown in the next chapter of this thesis. But in general for large K, it can be very difficult to lower the computational costs enough to become practically feasible and find accurate alignments at the same time.

On the other hand, a joint synchronisation of music recordings can be considered as an instance of the *multiple sequence alignment problem*, a task well-studied in bioinformatics (Durbin et al., 1999; Gusfield, 1997). For example, the MAFFT (Katoh and Standley, 2013) and CLUSTAL (Sievers et al., 2011) families of algorithms have been in development for almost three decades. While a lot of the functionality in such packages is highly specific to the alignment of biological sequences such as DNA or protein sequences, some central ideas can be adapted for the music alignment task, taking music specific properties into account.

Most of the multiple sequence alignment algorithms fall into two classes, *progressive alignment (PA) methods* and *probabilistic profile (PP) methods*. PA methods begin with a pairwise alignment of the most similar sequences, and progressively include more sequences typically ordered in a suitable way according to their alignment difficulty. More precisely, the alignment process follows a previously built "guide tree", which orders the sequences by an efficient clustering method based on the pairwise alignment score for each pair. PP methods , one the other hand, are typically based on Hidden Markov Models (HMM), where the *hidden* states represent the ancestral sequence of the sequences to be aligned. Every time a new sequence is processed, the model is updated and it influences the alignment of all sequences. On the contrary, in PA methods, the alignments of prior sequences are fixed and will remain the same even if new information arrives. The heuristics of PA methods often lead to a considerably higher computational efficiency compared to the PP methods. However, as reported by Pais et al. (2014), PP methods were found to yield a higher alignment accuracy in some bioinformatics tasks.

Music recordings, however, have properties quite different from biological sequences. First, this work does not consider structural differences between performances (e.g. a section being left out in one version), which is in stark contrast to biological sequences where such fundamental differences are common. Second, music recordings change more slowly over time leading to a high temporal correlation between neighbouring sequence elements, which again is quite different from protein sequences. Due to these differences, it is interesting to test whether the two types of methods can benefit the alignment accuracy in a musical context and how they differ in behaviour in such a scenario. This work adapts these two types of multiple sequence alignment methods to the music context and their detailed description is given in the next section.

With respect to musical applications, aligning multiple performances of a piece of music is a relatively novel concept in music processing and has only been exploited by a few approaches. A generative note duration model is proposed by (Maezawa et al., 2015) that couples parameters associated with tempo curves from different performances. Arzt and Widmer (2015) use multiple performances to improve the accuracy in an on-line score-following application by computing several pairwise alignments in parallel. Further, Bergomi (2015) aligns multiple symbolic sequences for harmonic and motivic analysis.

In some sense, the idea of using multiple versions to improve the performance of music alignment is similar to the co-segmentation problem in computer vision, where the segmentation accuracy can often be improved by supplying the algorithm with additional images that share certain foreground characteristics with a given image and segmenting them jointly (Rother et al., 2006). In addition, Müller and Röder (2006) proposed a method to identify the related motion capture data in some database, by learning a motion template from existing motion data sequences. A motion template is an average of alignments between each existing motion sequence with a reference motion sequence. In a way, the template captures the essence of all the existing data sequences. It can help improve the accuracy of identification and the robustness against the large variations among the motion sequences. The main difference between it and the idea of this Chapter is that, the proposed methods in this Chapter do not require choosing a reference sequence beforehand which may lead to some loss of robustness. Instead, as described below, a data structure that represents the consensus of all the available sequences is built gradually as sequences are processed.

3.4 Methods for Joint Music Alignment

Essentially, both PA and PP methods build up a data structure successively representing an average sequence or *central consensus* against which all given sequences can be aligned. In biological sequence analysis, the consensus sequence can be viewed as the common ancestor from which all sequences are descended. In a musical context, constructing this consensus form can incorporate information from every single recording such that the overall alignment becomes easier (as the influence of outlier information can be reduced) and therefore becomes more accurate and robust. In the following, two conceptually different methods are presented for computing such a central consensus in a music synchronisation scenario. Their differences include how the central consensus is represented (keeping all information in contrast to averaging some) and how it is built up (early versus late updates). Both of these affect the resulting alignment accuracy and computational performance, as discussed in more detail below.

3.4.1 Progressive Alignment

The first method can be regarded as a member of the family of progressive alignment (PA) algorithms in the context of bioinformatics (Katoh and Standley, 2013) and it takes the form of a general dynamic programming approach. The idea is, instead of simultaneously aligning all feature sequences, to successively add the sequences to a data structure referred to as the *template*. The template comprises a set of feature sequences that are aligned to each other. More precisely, after computing an alignment between a new sequence and the template at each step, the sequence is added using the alignment information to stretch both the template and the sequence. The stretching step causes all the feature sequences in the template to have the same length, which enables efficient access to aligned sequence elements. This is repeated until all sequences are contained in the template, which allows for deriving pairwise alignments between any two sequences.

To describe the alignment procedure in more detail, assume that there are K different versions of a piece and that their feature sequences are denoted by $X^k = (x_1^k, \ldots, x_{N_k}^k)$ with

$k \in [1:K]$ and $x_n^k \in \mathscr{F}$, where $\mathscr{F}$ denotes a suitable feature space. Further, the template data structure is refereed to as F and initialised to X^1. As part of the alignment process, the remaining feature sequences $X^2, \ldots, X^K$ are aligned successively to F, updating F after each step. To this end, let X^k denote the sequence to be aligned and $F = (f_1, \ldots, f_M)$ the current template of length M. Each $f_m \in (\mathscr{F} \cup \{G\})^{k-1}$ contains $k-1$ elements which are either feature vectors or *gap symbols* G, where individual components are denoted by $f_m^1, \ldots, f_m^{k-1} \in \mathscr{F} \cup \{G\}$. The idea behind the gap symbol will be discussed below. Further, to simplify the notation later, the sequence $(f_1^r, \ldots, f_M^r)$ is denoted by F^r for $r \in 1, \ldots, k-1$.

An alignment between F and X^k is defined as a sequence $p = (p_1, \ldots, p_L)$ with $p_\ell = (m_\ell, n_\ell) \in [1:M] \times [1:N_k]$ for $\ell \in [1:L]$ satisfying $1 = m_1 \leq m_2 \leq \ldots \leq m_L = M$ and $1 = n_1 \leq n_2 \leq \ldots \leq n_L = N_k$ (boundary and monotonicity conditions), as well as $p_{\ell+1} - p_\ell \in \{(1,1), (1,0), (0,1)\}$ (step size condition). To compute an alignment p between F and X^k, a cost matrix $C^r \in \mathbb{R}^{M \times N_k}$ comparing each pair of elements in F^r and X^k is computed by:

$$C^r(m,n) = \begin{cases} c(f_m^r, x_n^k), & f_m^r \neq G, \\ \mathscr{C}_G, & f_m^r = G, \end{cases} \tag{3.1}$$

where $c : \mathscr{F} \times \mathscr{F} \to \mathbb{R}$ is a suitable dissimilarity measure between feature vectors and $\mathscr{C}_G > 0$ is a constant referred to as the *gap penalty*. By combining these individual cost matrices C^r to a *merged cost matrix* $C \in \mathbb{R}^{M \times N_k}$, a dissimilarity measure is obtained between every sequence element in F and X^k. A simple yet effective combination is averaging:

$$C(m,n) = \frac{1}{k-1} \sum_{r=1}^{k-1} C^r(m,n). \tag{3.2}$$

This process is illustrated with an example of aligning five synthetic recordings in Figure 3.2, where a template (Figure 3.2a) containing four sequences of chroma-based vectors (with yellow entries indicating gap symbols) is aligned to a fifth sequence (Figure 3.2b). The resulting four cost matrices C^1 to C^4 are shown in Figure 3.2c-f, using $\mathscr{C}_G = 3$ and a cosine distance $c(f,x) = 2 - \frac{\langle f,x \rangle}{\|f\|\|x\|}$ [1]. The resulting merged cost matrix C is shown in Figure 3.2g.

By combining the information provided by each individual cost matrix, the influence of strong local differences on the alignment, that often only occur between specific pairs of

[1] Here a constant 1 is added to the cosine distance, in order to make the distance of chroma-based features comparable with the Euclidean distance of DLNCO features, mentioned in 3.5.1.3.

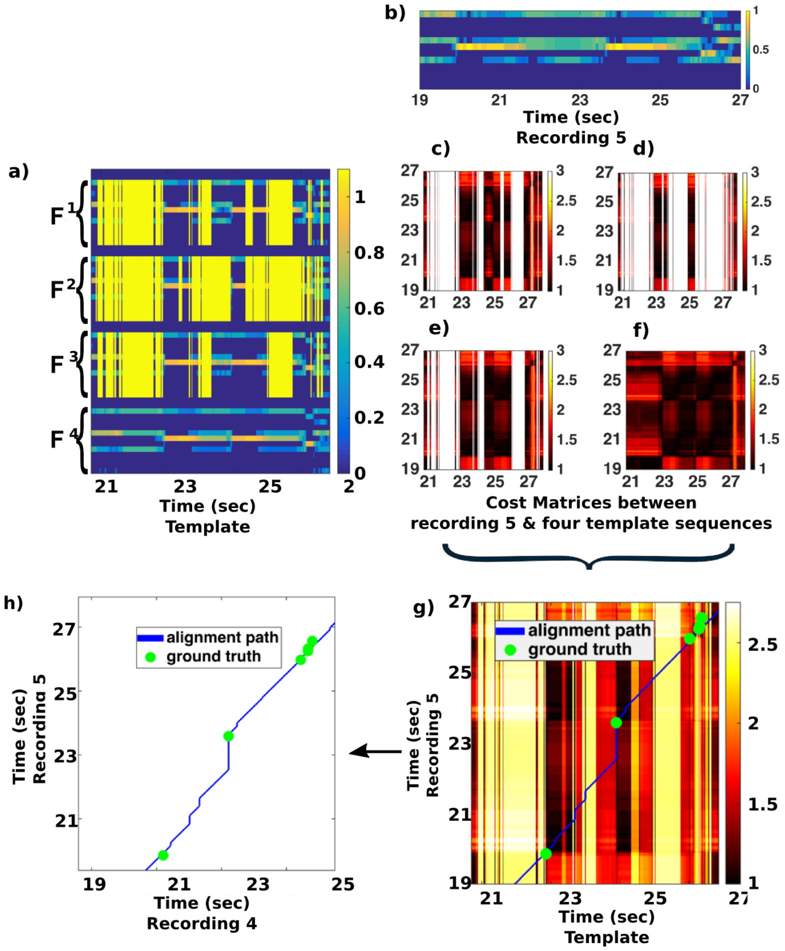

Figure 3.2: Aligning the fifth recording with the template of the first four recordings: the feature sequence of the fifth recording (b) is compared with each feature sequence in the template (a: yellow blocks indicate the gaps) to obtain four cost matrices (c,d,e,f); these cost matrices are combined into a single cost matrix to compute the alignment (g: the ground truth onset position for the alignment between the fourth and the fifth recording is stretched according to the gap inserted version of the fourth feature sequence, in order to be fitted onto the cost matrix between the template and the fifth recording). The resulting alignment path between the fourth and fifth recordings is shown in (h).

versions, can be attenuated. Note that we also tried other combination strategies, including weighting schemes, taking the minimum over the individual cost matrices or more general order statistics including the median and other percentiles. We also tested using logistic regression to learn a dissimilarity measure based on the individual cost matrices to optimise for overall alignment accuracy. However, using the same experimental setup as described in Section 3.5.1, replacing only the combination strategies, none of these strategies yielded consistently better results than the averaging described above.

Once a merged cost matrix is computed, one can apply dynamic programming similar to DTW or Viterbi decoding to derive an alignment p between F and X^k, as shown previously in Chapter 2, Section 2.3.1.3. To integrate X^k into F, p is used to stretch F and X^k to the same length, such that corresponding features are aligned and become part of the same element of F. There are several ways to define this stretch and a first idea is to simply set

$$\widetilde{f}_\ell = (f^1_{m_\ell}, \dots, f^{k-1}_{m_\ell}, x^k_{n_\ell}), \tag{3.3}$$

where $\widetilde{F} = (\widetilde{f}_1, \dots, \widetilde{f}_L)$ denotes the updated template and $p = \big((m_1, n_1), \dots, (m_L, n_L)\big)$. This simple solution, however, introduces a temporal uncertainty: if the step size $(1,0)$ or $(0,1)$ is used in p, an element in F or X^k is aligned to more than one element in the other sequence, respectively. As a consequence of this simple update rule, some elements of F or X^k would occur several times in $\widetilde{F}$. It would lead to a temporal uncertainty, as features of the next sequence can equally well be aligned against the original or a copied feature in a template sequence.

Given these issues, the idea here is to introduce a rule that replaces copies of elements with a gap symbol. First, define the terms

$$E_1^p(m) := \operatorname*{argmin}_{\{(m,\widetilde{n}) \in p\}} C(m, \widetilde{n}), E_2^p(n) := \operatorname*{argmin}_{\{(\widetilde{m},n) \in p\}} C(\widetilde{m}, n). \tag{3.4}$$

E_1 and E_2 are used to find the pair of elements that has the lowest cost, if an element in one sequence is aligned to several in the other sequence. Thus the update rule is defined as follows:

$$\widetilde{f}_\ell = \begin{cases} (f^1_{m_\ell}, \dots, f^{k-1}_{m_\ell}, x^k_{n_\ell}), & \text{if } (m_\ell, n_\ell) = E_1^p(m_\ell) = E_2^p(n_\ell) \\ (f^1_{m_\ell}, \dots, f^{k-1}_{m_\ell}, G), & \text{if } (m_\ell, n_\ell) \neq E_2^p(n_\ell) \\ (G, \dots, G, x^k_{n_\ell}), & \text{if } (m_\ell, n_\ell) \neq E_1^p(m_\ell) \end{cases} \tag{3.5}$$

Intuitively, for the case that p aligns an element m of one sequence to multiple elements of the second sequence, this update rule uses C to select the best of these multiple elements to align with m, and then the remaining elements are aligned to new gap symbols, illustrated with an example in Figure 3.3. This contrasts with the first idea where the multiple elements would be aligned to copies of m.

Here the progressive alignment is viewed as an extension of DTW rather than NW despite the usage of gap symbols. This is because unlike NW, the progressive alignment

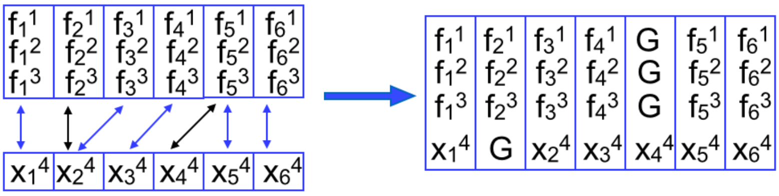
f_1^1 f_2^1 f_3^1 f_4^1 f_5^1 f_6^1
f_1^2 f_2^2 f_3^2 f_4^2 f_5^2 f_6^2
f_1^3 f_2^3 f_3^3 f_4^3 f_5^3 f_6^3
x_1^4 x_2^4 x_3^4 x_4^4 x_5^4 x_6^4
f_1^1 f_2^1 f_3^1 f_4^1 G f_5^1 f_6^1
f_1^2 f_2^2 f_3^2 f_4^2 G f_5^2 f_6^2
f_1^3 f_2^3 f_3^3 f_4^3 G f_5^3 f_6^3
x_1^4 G x_2^4 x_3^4 x_4^4 x_5^4 x_6^4

Figure 3.3: An example of replacing copies of elements with gap symbols after aligning a new sequence X to the template F, where $C(3,2) < C(2,2)$ and $C(5,5) < C(5,4)$.

procedure does not open gaps when computing an alignment. Instead, gaps are opened when integrating the newly aligned sequence X^k into F according to the computed alignment path at each step. This way, the algorithm will not penalise the tempo difference when computing an alignment. Rather, the gap is used when updating F, in order to avoid temporal uncertainty in aligning the remaining sequences.

The importance of the gap symbol will be investigated in Section 3.6.2. Also, the order in which feature sequences are aligned is crucial to the PA method and will be discussed in Section 3.6.3.

3.4.2 Probabilistic Profile

Another central class of multiple sequence alignment methods are probabilistic profile (PP) methods. For these methods, the central consensus data structure takes the form of a Hidden Markov Model (HMM), in a specific configuration. Such a *Profile HMM* is adapted to the music synchronisation scenario in the following; see also (Durbin et al., 1999) for similar concepts used in bio-informatics.

The topology of the proposed profile HMM is illustrated in Figure 3.4. Overall, the model contains three different types of states: *Match* states (M), *Insert* states (I) and *Delete* states (D). Intuitively, the series of match states will encode the core of a consensus sequence representing the commonalities among different recordings, while the insert and delete states are used to model the temporal diversity. To find appropriate parameters for the various probability distributions involved, each given sequence is interpreted as a noisy observation of the consensus sequence with insertions and deletions, and thus can be used to train the model using a Baum-Welch procedure. Interpreted in this way, it should be noted that the match states do not necessarily correspond to musical events like

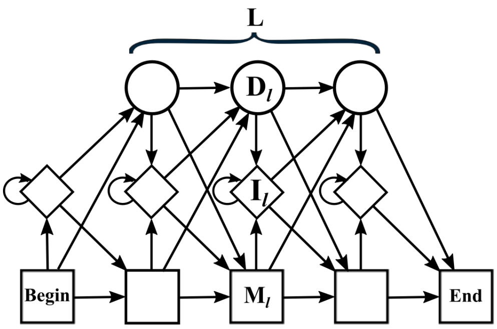

Figure 3.4: Topology of a Profile HMM (Durbin et al., 1999), showing rows of delete states (top), insert states (middle) and match states (bottom)

specific chords or note constellations as specified by a score. Our goal is to train the model using the given sequences, such that the final model captures a statistical description of the consensus as well as the diversity among multiple versions, which provide a higher robustness against large local discrepancies when the alignment for each pair is inferred from the model.

To describe the model in more detail, the same notation as above is employed, i.e. K different versions of a piece are assumed to be given with corresponding feature sequences denoted by $X^k = (x_1^k, \ldots, x_{N_k}^k)$ for $k \in [1:K]$, where each $x_n^k \in \mathscr{F}$. Some general concepts are similar to the standard HMM, which was described in Chapter 2. To define the structure of the profile HMM, the first step is to choose the length L of model: The number of M and D states is L, respectively, while there are $L+1$ I-states, compare Figure 3.4. Note that L is the length of the model, not the length of a decoded sequence. Although L could simply be a constant (as often used in bio-informatics), experiments described in the following sections show that the best results are obtained by adapting L to the length of the given feature sequences. More precisely, it is set to $L = \text{median}(N_1, \ldots, N_K)$, which fixes the overall topology, shown in Figure 3.4. Compared to other alternatives including the minimum, maximum and twice the maximum, the median led to a higher overall alignment accuracy in the experiments.

From a generative point of view, we start from a non-emitting Begin state. This way, the first features of sequences are not forced to align together. From there we can enter the first match state, the first insert state or the first delete state. If we enter the first match state, we can draw a feature vector according to the corresponding observation probability and proceed to the next state since match states do not have self-transitions. Insert states have self transitions and thus can generate an arbitrary number of feature vectors according to their observation probabilities – useful for modelling observation sequences that locally have a lower tempo compared to the consensus sequence. Delete states are non-emitting states and, since transitions between them are allowed, can be used to skip an arbitrary number of match states – useful for modelling observation sequences with a higher local tempo. Note that by allowing direct jumps from a match state to subsequent, non-neighbouring match states, one could also model deletions in a different way. The separate delete states, however, are introduced to avoid the problem of specifying a maximal length for such jumps and deletions. The possible transitions are shown in Figure 3.4.

To represent the observation probabilities of the match and insert states, multivariate Gaussian distributions are employed with means μ_ℓ^M, μ_ℓ^I and covariance matrices $\sigma_\ell^M, \sigma_\ell^I$. A benefit of using a Gaussian distribution is that the parameters have a straightforward interpretation. In particular, the means are elements of the feature space $\mathscr{F}$ and thus the sequence $\mu_1^M, \dots, \mu_L^M$ can be interpreted as encoding the consensus feature sequence, while the insert state means $\mu_1^I, \dots, \mu_L^I$ encode the diversities of the local context. Note that the number of parameters for each state would equal the square of the dimension of the feature space if full covariance matrices were used (Rabiner, 1989). This would greatly complicate the parameter estimation and typically there would not be enough feature sequences to training the model reliably. Therefore here diagonal matrices are employed for the covariance. Also, it is reasonable to assume that the dimensions of the feature vector are roughly decorrelated in the given data, and if not this could be performed as a pre-processing step. Further, instead of generating the observation model artificially from the score as is often done in the audio-score alignment task (Cont, 2010), here the consensus feature sequence is learnt from the feature sequences of all performances. Regarding the transition probabilities, only a low number of parameters need estimating due to the sparsely connected structure of the profile HMM: three for each state (compare Figure 3.4). Instead of fixing them to specific values, experiments to be discussed in the following show that estimating them from data improves the overall alignment accuracy. In particular, learnt from data, the transition probabilities encode how likely the sequences are to deviate from the consensus sequence locally, thus provide additional guidance during the alignment process.

Parameters of the model are estimated using a multiple sequence variant of the Baum-Welch algorithm (Rabiner, 1989). The algorithm is similar to the Profile HMM used in the biological sequence analysis (Durbin et al., 1999), for completeness of the discussion, it is specified as below.

Firstly, the forward algorithm is adjusted according to the topology of the model. Unlike the basic algorithm, here we have three forward variables, $\alpha_{M_l}(n)$, $\alpha_{I_l}(n)$, $\alpha_{D_l}(n)$, corresponding to three types of states, where $\alpha_{M_l}(n)$ represents the probability of the partial observation sequence until state M_l at the feature frame n, given the model λ ($\alpha_{I_l}(n)$ and $\alpha_{D_l}(n)$ are defined similarly). Let the first non-emitting Begin state be M_0. The forward variable is initialised as $\alpha_{M_0}(0) = 1$. The recursion steps to compute forward variables at feature frames $n = 1, 2 \cdots N_k$ are:

$$\alpha_{M_l}(n) = b_{M_l}(x_n)[\alpha_{M_{l-1}}(n-1)a_{M_{l-1}M_l} + \alpha_{I_{l-1}}(n-1)a_{I_{l-1}M_l} + \alpha_{D_{l-1}}(n-1)a_{D_{l-1}M_l}] \tag{3.6}$$

$$\alpha_{I_l}(n) = b_{I_l}(x_n)[\alpha_{M_l}(n-1)a_{M_l I_l} + \alpha_{I_l}(n-1)a_{I_l I_l} + \alpha_{D_l}(n-1)a_{D_l I_l}] \tag{3.7}$$

$$\alpha_{D_l}(n) = \alpha_{M_{l-1}}(n)a_{M_{l-1}D_l} + \alpha_{I_{l-1}}(n)a_{I_{l-1}D_l} + \alpha_{D_{l-1}}(n)a_{D_{l-1}D_l} \tag{3.8}$$

where b represents the emission probability and a represents the transition probability. The forward variable of the first insertion state is defined as $\alpha_{I_0}(n) = b_{I_0}(x_n)a_{M_0 I_0}$, while the forward variable of the first delete state is defined as $\alpha_{D_1}(n) = a_{M_0 D_1}$. The above recursion steps terminate at the End state, defined as M_{L+1}, where $P(X|\lambda) = \alpha_{M_{L+1}}(N+1) = \alpha_{M_L}(N)a_{M_L M_{L+1}} + \alpha_{I_L}(N)a_{I_L M_{L+1}} + \alpha_{D_L}(N)a_{D_L M_{L+1}}$.

Similarly, the backward algorithm is initialised as $\beta_{M_{L+1}}(N+1) = 1$ and the recursion steps at the feature frames $N, N-1 \cdots, 0$ are:

$$\beta_{M_l}(n) = b_{M_{l+1}}(x_{n+1})\beta_{M_{l+1}}(n+1)a_{M_l M_{l+1}} + b_{I_l}(x_{n+1})\beta_{I_l}(n+1)a_{M_l I_l} + \beta_{D_{l+1}}(n)a_{M_l D_{l+1}} \tag{3.9}$$

$$\beta_{I_l}(n) = b_{M_{l+1}}(x_{n+1})\beta_{M_{l+1}}(n+1)a_{I_l M_{l+1}} + b_{I_l}(x_{n+1})\beta_{I_l}(n+1)a_{I_l I_l} + \beta_{D_{l+1}}(n)a_{I_l D_{l+1}} \tag{3.10}$$

$$\beta_{D_l}(n) = b_{M_{l+1}}(x_{n+1})\beta_{M_{l+1}}(n+1)a_{D_l M_{l+1}} + b_{I_l}(x_{n+1})\beta_{I_l}(n+1)a_{D_l I_l} + \beta_{D_{l+1}}(n)a_{D_l D_{l+1}} \tag{3.11}$$

To avoid the numerical issues mentioned in 2.3.2.1, the actual implementation computes the above equations in the log domain. The forward and backward variables are computed for each sequence. As mentioned in 2.3.2.1, the Baum-Welch training procedure uses the Expectation-Maximisation algorithm. That is to say, the expectations are calculated for each sequence and the maximisation step is performed on the accumulated expectations of all sequences. The steps to re-estimate the model parameters are specified as the following: Let the expected number of transition from state $S_l : M_l, I_l, D_l$ to state M_{l+1},I_l and D_{l+1} for all sequences be $\mathscr{E}_{S_l M_{l+1}}$, $\mathscr{E}_{S_l I_l}$ and $\mathscr{E}_{S_l D_{l+1}}$ respectively, computed as:

$$\mathscr{E}_{S_l M_{l+1}} = \sum_k^K \frac{1}{P(X^k|\lambda)} \sum_n^{N_k} b_{M_{l+1}}(x_{n+1}^k) \alpha_{S_l}^k(n) \beta_{M_{l+1}}^k(n+1) a_{S_l M_{l+1}} \tag{3.12}$$

$$\mathscr{E}_{S_l I_l} = \sum_k^K \frac{1}{P(X^k|\lambda)} \sum_n^{N_k} b_{I_l}(x_{n+1}^k) \alpha_{S_l}^k(n) \beta_{I_l}^k(n+1) a_{S_l I_l} \tag{3.13}$$

$$\mathscr{E}_{S_l D_{l+1}} = \sum_k^K \frac{1}{P(X^k|\lambda)} \sum_n^{N_k} \alpha_{S_l}^k(n) \beta_{D_{l+1}}^k(n) a_{S_l D_{l+1}} \tag{3.14}$$

The transition probabilities are then computed as:

$$a_{S_l M_{l+1}} = \frac{\mathscr{E}_{S_l M_{l+1}}}{\mathscr{E}_{S_l M_{l+1}} + \mathscr{E}_{S_l I_l} + \mathscr{E}_{S_l D_{l+1}}} \tag{3.15}$$

$$a_{S_l I_l} = \frac{\mathscr{E}_{S_l I_l}}{\mathscr{E}_{S_l M_{l+1}} + \mathscr{E}_{S_l I_l} + \mathscr{E}_{S_l D_{l+1}}} \tag{3.16}$$

$$a_{S_l D_{l+1}} = \frac{\mathscr{E}_{S_l D_{l+1}}}{\mathscr{E}_{S_l M_{l+1}} + \mathscr{E}_{S_l I_l} + \mathscr{E}_{S_l D_{l+1}}} \tag{3.17}$$

To re-estimate the means and covariance matrices of the observation probabilities, the probability of being in the state S_l at the feature frame n given the model λ and the observation sequence X^k is represented by,

$$\gamma_{S_l}^k(n) = \frac{\alpha_{S_l}^k(n) \beta_{S_l}^k(i)}{P(X^k|\lambda)} \tag{3.18}$$

The means are computed as:

$$\mu_l^M = \frac{\sum_{k=1}^K \sum_{n=0}^{N_k} \gamma_{M_l}^k(n) x_n^k}{\sum_{k=1}^K \sum_{n=0}^{N_k} \gamma_{M_l}^k(n)} \tag{3.19}$$

$$\mu_l^I = \frac{\sum_{k=1}^K \sum_{n=0}^{N_k} \gamma_{I_l}^k(n) x_n^k}{\sum_{k=1}^K \sum_{n=0}^{N_k} \gamma_{I_l}^k(n)} \tag{3.20}$$

The covariances are computed as:

$$\sigma_l^M = \frac{\sum_k^K \sum_n^{N_k} \gamma_{M_l}^k(n)(x_n^k - \mu_l^M)^2}{\sum_k^K \sum_n^{N_k} \gamma_{M_l}^k(n)} \tag{3.21}$$

$$\sigma_l^I = \frac{\sum_k^K \sum_n^{N_k} \gamma_{I_l}^k(n)(x_n^k - \mu_l^I)^2}{\sum_k^K \sum_n^{N_k} \gamma_{I_l}^k(n)} \tag{3.22}$$

The multiple sequence variant of the Baum-Welch algorithm is summarised in Algorithm 2:

Algorithm 2: A Multiple Sequence Variant of the Baum-Welch Algorithm

```
Data: Sequences $X^1, X^2, \cdots X^K$
Result: New model parameters
Initialise the model parameters
repeat
    for each sequence $X^k$, $k = 1, 2 \cdots K$ do
        Calculate the forward variable $\alpha_{S_l}^k(n)$ with Equations 3.6-3.8
        Calculate the backward variable $\beta_{S_l}^k(n)$ with Equations 3.9-3.11
        Calculate $\gamma_{S_l}^k(n)$ with Equation 3.18
    end
    Re-estimate the model parameters with Equations 3.12-3.22
until the likelihood of the model $\prod_k^K P(X^k|\lambda)$ stops increasing or is larger than the
threshold or the maximum number of iterations is exceeded;
```

Since in a music synchronisation scenario the number of available sequences is typically several orders of magnitude smaller than in bioinformatics, the initialisation strategy is crucial to avoid running into poor local maxima of the likelihood function. The highest alignment accuracies are obtained using the following initialisation strategy: the match and insert means are initialised using the feature vectors of a sequence whose length is equal to the above chosen L. Excluding that sequence from the training procedure enables the model to properly account for the other sequences without overfitting the initialising sequence. Other strategies to obtain a proper initialisation led to lower alignment accuracies, including random initialisations as well as resampling all sequences to the same length (corresponding to a linear stretch), followed by averaging. The covariance matrices

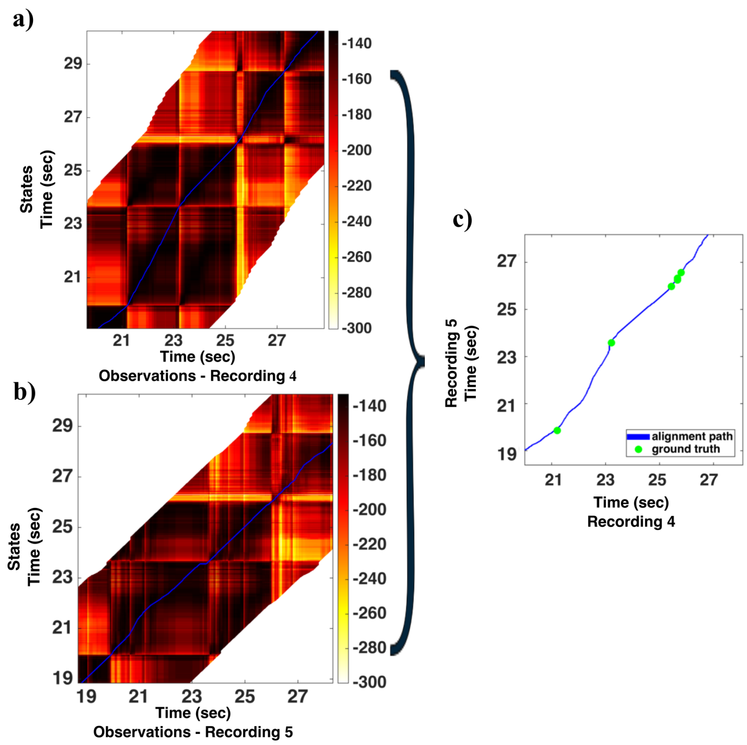

Figure 3.5: Emission probability matrices for match states with alignment path (blue) between states and observations of (a) the fourth recording and (b) the fifth recording. The values on colour bar are in log scale. Note that the extremely low probabilities (white area) on the top left and the bottom right corner result from the path constraint described in Section 3.4.3; (c) The resulting alignment path between the fourth and fifth recordings.

were uniformly initialised to a fixed, relatively high value as a measure to overcome overfitting. Additionally, to avoid the collapsing-Gaussian problem, the estimated variances are constrained to a reasonable minimum (Durbin et al., 1999). The transition probabilities were initialised uniformly, with the exception of match-match and delete-insert transitions: the former are encouraged and the latter discouraged.

After training the profile HMM, alignments between the model and each sequence can be obtained using the Viterbi algorithm. Pairwise alignments between any two sequences can be derived using the model as a central intermediary. This last step is illustrated with an example of aligning the same recordings also used in Figure 3.2. Figure 3.5a and b shows the observation probabilities (log-scaled) for two sequences against a number of match states based on the trained profile HMM. The optimal state sequence found via Viterbi decoding for each sequence is illustrated as an alignment path in blue (alignments against non-match states are not directly visible in the figure and the path is interpolated accordingly). Each element in the computed path aligns a given feature vector in the first sequence to states in the profile HMM, which then can be aligned to feature vectors in the second sequence using the other alignment. The resulting pairwise alignment between the given feature sequences is illustrated in Figure 3.5c.

3.4.3 Accelerating Alignments Using Multi-Scale Dynamic Programming

To obtain alignments of high accuracy, it is necessary to use features with a high temporal resolution. The resulting increase in length of the feature sequences compared to lower resolutions, however, also leads to a considerable increase of the computational cost for the alignment methods described above. In particular, assuming that all sequences are roughly of length N, the time and memory requirements of the dynamic programming technique presented in Section 3.4.1 as well as of the Baum-Welch (in each iteration) and Viterbi algorithms used in Section 3.4.2 are quadratic in N. Therefore, for large N, the alignment problem can easily become computationally impractical or even infeasible.

To increase the computational efficiency, the multi-scale alignment strategy proposed in the context of DTW (Müller et al., 2006; Salvador and Chan, 2004) is adapted for both joint alignment methods, since progressive alignment and the Baum-Welch/Viterbi algorithms share common algorithmic roots. For a description of this strategy, see Section 2.3.1.3. Similarly to Müller et al. (2006) and Ewert et al. (2009b), a total of four different feature resolutions are used here, with the lower three ones obtained from the highest using low-pass filtering (smoothing) and down-sampling. The resulting temporal resolutions are 1 sec, 0.5 sec, 0.1 sec and 0.02 sec. After computing an alignment (or a Baum-Welch iteration) on a coarser level, the path is projected to the next finer resolution and constrains alignments to run in a neighbourhood of the projected path, illustrated in Figure 2.5. This is illustrated in Figure 3.5a and b for the profile HMM: an alignment path computed on a coarse level was projected to the final feature resolution, where it is used to constrain which entries in the observation probability matrix are computed. Entries outside the constraint region are formally given an extremely low probability (white entries). Similar constraint regions are also applied during the computation of the observation and posterior probability matrices used in the Baum-Welch algorithm. The experiments show similar speed-ups as reported by Müller et al. (2006), i.e. the resulting methods were typically faster by a factor of 40-100 depending on the length of the recordings used – without a decrease in alignment accuracy.

3.5 Comparing Pairwise, Progressive and Profile-HMM Based Alignment

The two methods described in Section 3.4 differ considerably on a formal level, with one being described as an optimisation and the other as a probabilistic inference problem. However, since they are extensions to DTW and HMM respectively, they share many similarities on the algorithmic level, as discussed previously in Section 2.3.3.

Given these algorithmic similarities, it is interesting to note where the central conceptual differences between our two approaches are and how they could affect the alignment results. A first difference is *adaptability in size*. The progressive method retains every feature sequence it encounters, gradually adapting the size of the template as needed. The profile HMM has a fixed size and topology once the parameter L is set during the initialisation. A second difference is *early vs late merging*. Here, the progressive method merges information from features only at the distance level (computing the cost matrix C), which could be called late-merging. In contrast, the profile HMM learns a consensus in the form of a sequence of means for the match states: for a given match state, the mean is computed during the maximisation step in Baum-Welch as a weighted sum of feature vectors (where the weights correspond to the posterior probabilities computed using the forward-backward procedure). Therefore, the averaging of information is already done at the feature level, which could be called early-merging. A third difference is the *distance measure*. In a progressive method one is free to choose or design a distance measure to compare feature vectors. For example, as we will see in Section 3.5.1, the cosine distance is used for CENS features and the Euclidean distance for DLNCO features. Note that DLNCO features were designed to be used with the Euclidean distance, see Section 2.2.2. In a profile HMM, distances correspond to observation probabilities and as such one typically has to choose from specific families of distributions (like the Gaussian family). However, the parameters of these distributions (e.g. the covariance matrices) can be learnt and adapted, which conceptually can be regarded as local feature distances adapted to the sequence. A fourth difference is the *greediness of updates.* To process a single sequence, the progressive method computes an alignment with the current template and updates the template before the next sequence is processed. The profile HMM employs the forward-backward procedure as part of Baum-Welch to compute the posterior, which conceptually can be interpreted as computing a soft alignment between each given feature sequence and the states in the profile HMM. Interpreted this way, in each iteration of Baum-Welch the profile HMM first computes an alignment for every single sequence before it updates its parameters. In this respect, the progressive method is more greedy than the profile HMM.

Overall, it is difficult to argue whether, for example, the increase in flexibility resulting from adaptability in size could give our progressive method an advantage over our profile HMM, or whether the greedy updates of the progressive method not only lower the computational costs but also reduce its alignment accuracy (as the profile HMM updates might be more robust due to taking all feature sequences into account). Therefore, this section describes a series of experiments to assess the alignment quality of both methods under real-world conditions. To maximise the comparability, the same features are used for both methods and the parameter configuration is set to maximise the alignment accuracy, as described below. Furthermore, to identify whether the methods indeed have benefits over standard synchronisation methods, they are compared with the results of two widely-used pairwise methods (Ewert et al., 2009b; Dixon and Widmer, 2005). While the method presented by Dixon and Widmer (2005) uses a different set of features (a low level spectral representation of the audio data, generated from a windowed FFT of the signal), the method of Ewert et al. (2009b) is directly comparable to our methods as the same types of features are used. In the algorithmic aspect, the offline implementation of Dixon and Widmer (2005) is used, which can be regarded as a standard DTW algorithm with the path-adaptive constraint. Ewert et al. (2009b) uses the multiscale DTW (FastDTW) algorithm (Müller et al., 2006), which constrains a standard DTW algorithm with the multiscale strategy mentioned in Section 2.3.1.3 and Section 3.4.3.

Table 3.1: Chopin Mazurkas and their identifiers used in the experiments. The last two columns indicate the number of performances available for the respective piece and the number of evaluated unique pairs.

ID	Piece	No. Rec.	No. Pairs
M17-4	Opus 17 No. 4	62	1891
M24-2	Opus 24 No. 2	62	1891
M30-2	Opus 30 No. 2	34	561
M63-3	Opus 63 No. 3	81	3240
M68-3	Opus 68 No. 3	49	1176

3.5.1 Dataset and Settings

3.5.1.1 Dataset

The dataset for evaluation consists of 288 recordings covering five of Chopin's Mazurkas, with 30-80 individual performances per piece, see Table 3.1. It is suitable for several reasons. First, interpretations of Mazurkas are often quite expressive, leading to considerable differences in terms of timing, dynamics, balance, articulation and playing style. Second, the recordings were made in a time span ranging from 1931 to 2002 across a wide range of venues, often resulting in extensive differences regarding the noise level, reverberation and room acoustics, acoustical properties of the instrument in use, recording equipment and audio quality as well as stylistic choices typical for a specific time period. Overall, these differences present substantial challenges to an automatic alignment method.

Further, in this dataset corresponding positions across different performances were manually annotated at the beat level as part of the Mazurka project[2], which enables a straightforward evaluation of automatic alignment methods as described next. Since handling structural differences is out of the scope of this work, performances with structural differences (such as additional repetitions of a part of a piece) are excluded from the experiments.

3.5.1.2 Evaluation Measure

In order to evaluate the alignment accuracy, for each manually annotated beat position in the one version, an alignment path is used to locate the corresponding position in the other version. The absolute differences between the manually annotated beat positions and those obtained from the alignment are computed and averaged for all beats. The

[2] http://www.mazurka.org.uk

average (in milli-seconds) is employed as the evaluation measure, which is referred to as the *average beat deviation (ABD)* in the following. It is measured for each Mazurka and each pair of recordings in our experiments. Note that the number of pairs for one Mazurka is a binomial coefficient, for example, for M17-4 our setup contains 62 recordings, which results in $\binom{62}{2} = 1891$ unique pairs and corresponding ABD values, see Table 3.1. Further, to increase the interpretability of the evaluation results, the results for a baseline method that simply linearly stretches the shorter to the longer recording to obtain an alignment, is also provided in Table 3.2.

3.5.1.3 Features and Parameters

The Pairwise method II (Ewert et al., 2009b) and two joint alignment methods all employ the same features, a combination of CENS (Müller et al., 2005), which is a type of chroma feature with uniform energy distribution, and DLNCO features (Ewert et al., 2009b), which estimate onset positions separately for each chroma, as discussed previously in Section 2.2. A 20ms temporal resolution is used for both features. Both the pairwise method and progressive alignment use the cosine distance for CENS and the Euclidean distance for DLNCO, as proposed by Ewert et al. (2009b). Further, the weights $(w_1, w_2, w_3) = (2, 1.5, 1.5)$ are set for both methods. The progressive alignment method uses a gap penalty $\mathscr{C}_G = 3.6$ and sorts the feature sequences to be aligned according to their length from short to long. (The influence of these parameters will be investigated in more detail in Section 3.6.) The Pairwise I method, described by Dixon and Widmer (2005) employs spectrogram-based features and the Euclidean distance to compare them. The following experiments use its default settings.

3.5.2 Comparison Between the Pairwise and Joint Alignments

Before individual components of the proposed methods are investigated in more detail, this section gives a general comparison of the alignment accuracy of the pairwise and joint alignment methods. The distribution of the average beat deviation (ABD) values for all pairs is summarised for each of the five Mazurkas separately in Table 3.2 as well as

Table 3.2: Alignment error(mean and standard deviation of average beat deviation in milliseconds) for four types of alignment methods and a random baseline.

	Pairwise I **(Dixon and Widmer, 2005)**		**Pairwise II** **(Ewert et al., 2009b)**		**Profile HMM**		**Progressive Alignment**		**Baseline**	
ID	mean	std	mean	std	mean	std	mean	std	mean	std
M17-4	116	638	68	19	62	12	59	12	3997	1908
M24-2	79	35	39	20	33	9	31	6	2726	2485
M30-2	69	121	30	8	32	7	30	5	2403	1401
M63-3	181	1332	46	32	39	11	40	11	2874	1846
M68-3	212	1444	58	23	51	19	46	13	1947	1177

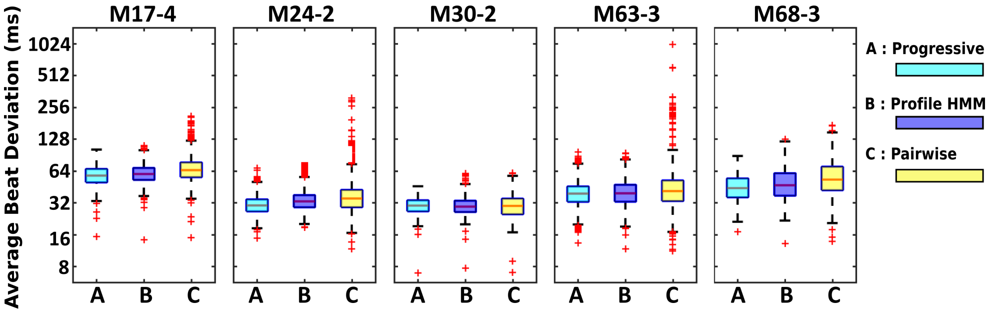

Figure 3.6: Comparison of the pairwise alignment method(Ewert et al., 2009b) with the proposed progressive alignment method and profile HMM method. The boxplots illustrate the distribution of the average beat deviation values for each Mazurka separately on a logarithmic scale.

in the boxplots[3] shown in Fig. 3.6. As a reference, Table 3.2 also includes the results of two pairwise methods, referred to as Pairwise I (Dixon and Widmer, 2005) and Pairwise II (Ewert et al., 2009b), and the baseline method, which uses a linear stretch as discussed in Section 3.5.1.2. Note that the std in Table 3.2 refers to the sample standard deviation rather than the standard deviation of the mean.

As shown in Table 3.2, all alignment methods are better than the baseline and both joint alignment method as well as the Pairwise II method are better than Pairwise I method. Furthermore, both joint alignment methods reduce the mean ABD compared to the Pairwise II method, for most pieces. For example, the mean ABD for M68-3 drops from 58ms using pairwise alignment, to 51ms with the profile HMM alignment (decrease by 12%), and even lower to 46ms with the progressive alignment (decrease by 21%). On average, the mean ABD drops by 12% using the profile HMM and by 15% using progressive

[3] Standard boxplots are used here: the box gives the $25th$ and $75th$ percentiles (p_{25} and p_{75}), where the centre bar indicates the median. The whiskers extend to the smallest data point greater than p_{25} - $1.5(p_{75}$ - $p_{25})$ and the largest data point less than $p_{75} + 1.5(p_{75}$ - $p_{25})$, and the outliers are plotted as red crosses.

alignment. However, a more considerable improvement resulting from the joint alignment methods is a higher robustness. As can be seen from Fig. 3.6, the inter-quartile range is smaller for all five pieces using either of the two joint alignment methods, and the number of large-value outliers is drastically reduced. This improvement can also be measured by the decrease of the standard deviation (std), which for M68-3 is 17% using the profile HMM (drops from 23ms to 19ms) and 43% using progressive alignment (from 23ms to 13ms). This decrease is even greater for other Mazurkas (M24-2 and M63-3). On average, the standard deviation of ABD is reduced by 51% using the profile HMM and 58% using progressive alignment.

Overall, the two joint alignment methods are more stable compared to pairwise alignment, as both of them provide a higher robustness against large alignment errors, which also leads to an increase in alignment accuracy. As an exception, the improvement on M30-2 is limited, as the mean ABD using the progressive alignment is the same as using pairwise alignment (30ms), while the profile HMM is a bit worse (32ms), and the std drops only slightly (from 8ms to 7ms using profile HMM and to 5ms using progressive alignment). However, the experimental results indicate that this piece is relatively easy to align, since the mean ABD using pairwise alignment is 30ms (which is already low compared to the feature resolution level of 20ms) and the outliers are few and not as extreme as in other pieces. In this case, there is less room for the joint alignment methods to improve. This result matches the main effect observed from the joint alignment, which is a gain in robustness against strongly incorrect alignments.

To test this hypothesis further, another experiment was conducted to show which error level is improved the most by the proposed methods. To this end, Fig. 3.7 shows a histogram of the deviation for all individual beat pairs using all alignment pairs without averaging (corresponding to around 2.5 million evaluated beat pairs). It shows that both joint alignment methods reduce the number of alignment errors clearly in the range of 100ms - 1000ms beat deviation, compared to the Pairwise II alignment method.

The superior robustness of the proposed joint alignment methods over pairwise methods is also illustrated with an example aligning performances of Op. 24 No. 2 by Luisada and Richter. Figure 3.1 shows an excerpt of the alignment which is problematic for Pairwise II method. As shown in the corresponding score, the six measures are mainly com-

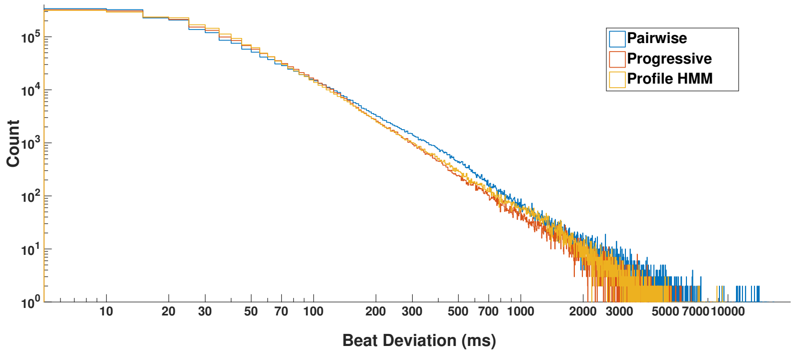

Figure 3.7: Histograms of beat deviation using the Pairwise II alignment method (Ewert et al., 2009b), the progressive alignment and profile HMM method.

posed of repeated notes or chords with expressive markings. In addition to differences in balance (the relative loudness), as can be seen from the CENS features, the two performers also play differently with regard to the timing. Furthermore, the two recordings contain different degrees of noise. In the presence of the above differences, the pairwise method fails to identify the correct alignment, see the solid path in Fig. 3.1, compared to the annotated beat positions (red dots). The other two alignments, which are shown as dashed and dotted paths in Fig. 3.1, result from our two joint alignment methods. In computing them, five other recordings are included and their information helps to stabilise the alignment. As a consequence, these two paths coincide almost always with the ground truth annotations.

3.5.3 Comparison of the Two Joint Alignment Methods

As shown in Table 3.2 and Fig. 3.6, the two joint alignment methods have a similar alignment accuracy and robustness, with the profile HMM having a slightly higher mean and std ABD for some pieces. To asses the relevance of these small differences, we would like to conduct a significance testing to compare ABD values for all alignment pairs using the PA and PP methods. Although the ABD values are not mutually independent, traditional NHST (null hypothesis significance testing) might provide an idea of whether observed differences are relevant. To this end, we perform a t-test as the ABD values seem to follow a quasi-Gaussian distribution[4]. It indicates that there is a statistically significant dif-

[4] Both parametric and non-parametric tests require independence of samples which is not met in this case. The fact that a q-q (Quantile-Quantile) plot suggests a quasi-Gaussian distribution encourages us to use a simple t-test.

ference between the ABD values using the PA method ($M = 42, SD = 14$) and PP method ($M = 44, SD = 16$); $t(8758) = 20.4$, $p = 1e{-}90$. However, despite the significance, the difference between the two is relatively small in this experiment, which is also reflected by Cohen's measure for effect size: $d_s = 0.1$, indicating that the statistical significance is mainly reached due to the fairly large sample size. Therefore, the next section will describe a series of experiments on both joint alignment methods, to better understand their behaviour in other scenarios, to give an in-depth analysis of the influence of their parameters and to show possible extensions to further improve their performance.

3.6 Further Investigations of the Joint Alignment Method

This section describes six groups of additional experiments to further understand the behaviour of our joint alignment methods. The investigation starts with the effect the number of available performances has on the proposed methods. Next, the influence of the gap concept and the gap penalty parameter on the progressive alignment method is studied, followed by an analysis of the influence of the order in which recordings are aligned. After that, as an alternative model training method to the Baum-Welch process, Viterbi training is implemented in order to further accelerate the profile HMM. A reverse idea is to include an iterative extension to the progressive alignment method, to study whether it can be used to exchange computation time for an increase in alignment robustness. Finally, the evaluation results for new pieces with highly precise ground truth are provided to further test how our methods behave under clean recording conditions (compared to the highly varied acoustic scenarios available in the Mazurka dataset).

3.6.1 Subset Experiments

The previous experiments used large numbers (30 to 80) of performances of each piece to perform joint alignments. However, there is not always such a large number of different versions available for the same piece. Therefore, this experiment investigates how many recordings are required to observe an improvement in robustness using the joint alignment methods compared to a pairwise method.

Experiments are performed with subsets of different sizes ranging from 3 to 10 recordings. For each size, 10 sets were randomly chosen from all the recordings of a given piece.

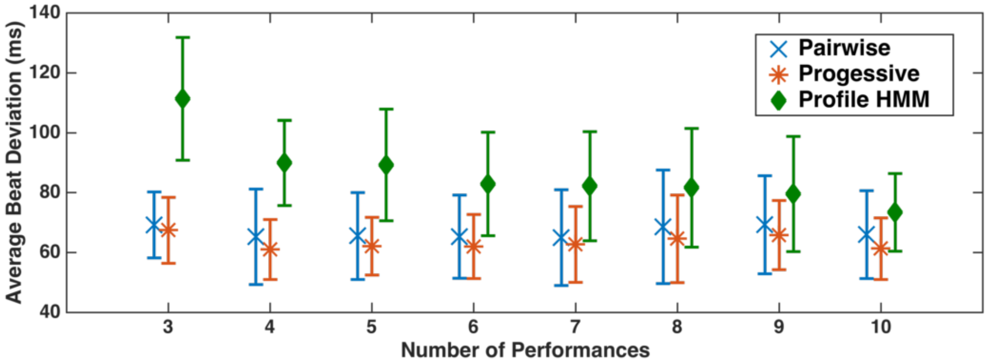

Figure 3.8: Comparison between the Pairwise II alignment method (Ewert et al., 2009b) and two joint alignment methods for subset experiments.

Numerical results for the Pairwise II alignment method (Ewert et al., 2009b) are compared with both PA and PP methods in Fig. 3.8. As shown, the progressive alignment method decreases the mean and std ABD for subsets of all sizes steadily, compared to the pairwise method. The difference when there are only three recordings available is relatively small but still measurable, and it becomes more pronounced when more recordings are included in the alignment procedure. The results indicate that progressive alignment can improve the alignment accuracy and robustness even with a small set of recordings, i.e. it is not necessary to have a large number of versions in order to benefit from the proposed method.

On the other hand, the Profile HMM method is worse in terms of mean and std ABD than both pairwise and progressive alignment methods when only a few recordings are available. The main reason here is that the profile HMM employs training data to adjust the internal sequence representation to the given data, and with so little training data this capability simply cannot yet unfold its advantages. Its performance improves with larger subsets, as more data is available for model training. This behaviour could indicate that the increase in alignment accuracy for profile HMM based methods as reported in some bio-informatics publications might only be achievable if a similar number of training sequences is available. Since there are often several thousand sequences available in bio-informatics (Thompson et al., 2005), the situation is quite different to music processing where such a high number cannot be expected.

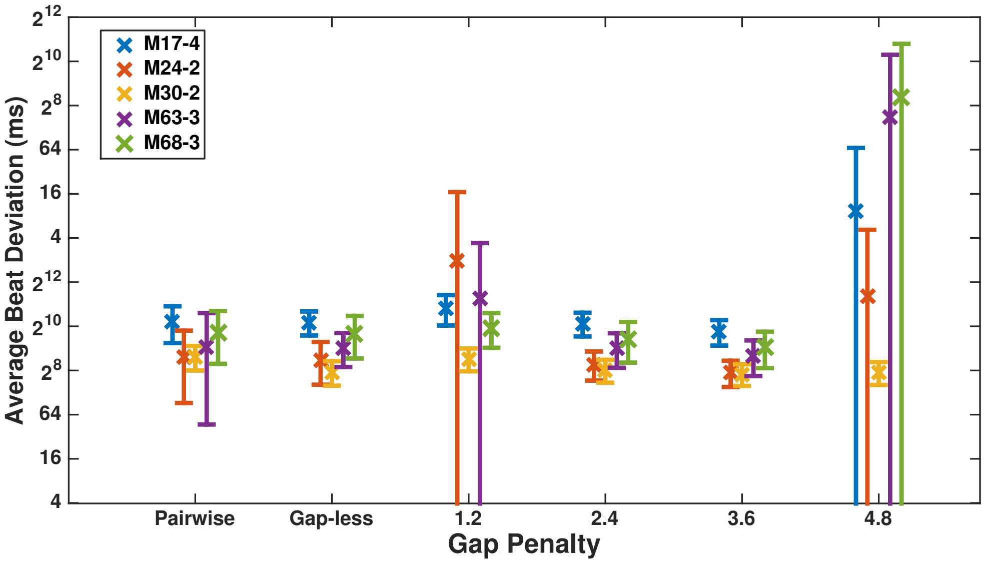

Figure 3.9: Average beat deviation (ABD) values for the five Mazurka pieces with progressive alignment using a gap-less variant and different values of gap penalty, compared with the Pairwise II alignment method(Ewert et al., 2009b). The cross markers represent the mean ABD and the error bars show the standard deviation.

3.6.2 Gap Penalty

To avoid a possible temporal uncertainty caused by copying features, the progressive alignment method inserts a special gap symbol when updating the template (Section 3.4.1). The following studies the influence of these gaps on the alignment accuracy by experimenting with different values of the gap penalty parameter and a gap-less variant.

For the gap-less variant, a simple strategy is employed, described in Section 3.4.1 where we set $\tilde{q}_\ell = (q^1_{n_\ell}, \dots, q^{k-1}_{n_\ell}, x^k_{m_\ell})$. As can be seen from Figure 3.9, compared with the baseline pairwise method, this gap-less variant leads to small improvements, mostly with respect to robustness as indicated by the decrease in dispersion. However, these improvements are more pronounced using the proposed progressive method with a gap penalty value of 3.6. Further, the gap-less variant does not reduce the mean ABD compared to the pairwise alignment. This behaviour could indicate that copying the features to stretch the newly aligned sequence, as done in the gap-less variant, indeed leads to a temporal uncertainty in the features causing the loss of alignment accuracy compared to the gap-variant.

However, Figure 3.9 also indicates that the value of the gap penalty needs to be sufficiently large, at least larger than the maximum value of the local cost measure (which is 3.0

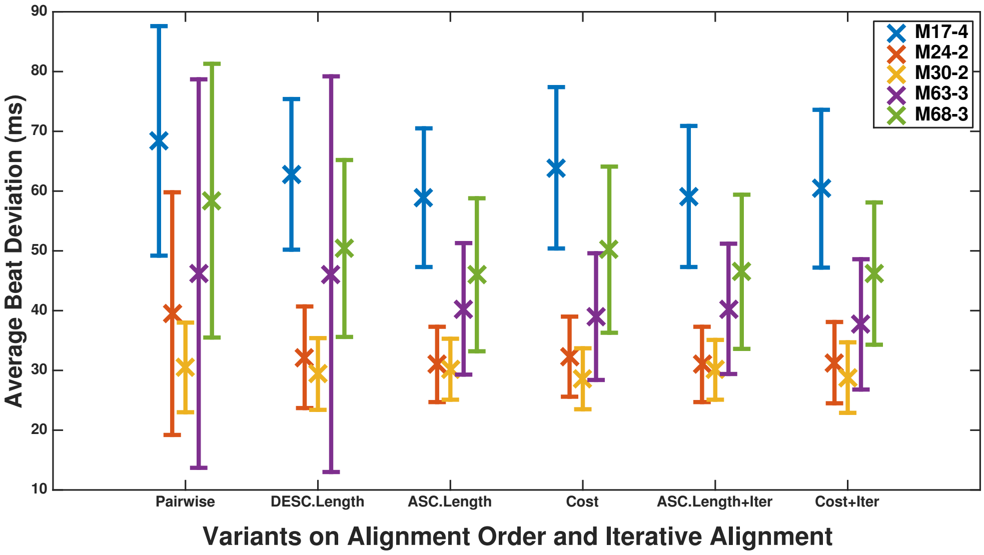

Figure 3.10: Average beat deviation (ABD) values for the five Mazurka pieces with progressive alignment using different alignment orders and the iterative extension, compared with the Pairwise II alignment method (Ewert et al., 2009b).

in our case), to ensure every gap is sufficiently penalised. On the other hand, if the value is too large, features in the new sequence $x^k_{m_\ell}$ are not likely to get aligned to the q_l if it contains a gap which can lead to a loss of accuracy as well. 3.6 is found in the experiments as a suitable value for the gap penalty during the development of the method using only M17-4. As seen in Figure 3.9, this value yields the best results for the remaining Mazurkas as well. Furthermore, it works well with additional pieces in Section 3.6.6.

3.6.3 Alignment Order

As described in Section 3.4.1, the template Z in our progressive method is built up gradually by successively aligning the feature sequences $X^1, \ldots, X^K$. The order in which they are aligned should be chosen with care for two reasons. Firstly, feature sequences at the beginning have less information from other versions to stabilise the alignment. Secondly, errors made at an early stage may propagate to the following alignments. Therefore, four different ordering strategies are compared in the next experiments. The first strategy is ordering versions randomly. The next two are length-based ordering strategies, where versions are sorted by their duration in ascending or descending order. The last strategy tries to find an order for the sequences such that each sequence being aligned is the easiest to be aligned among all remaining sequences, in some sense. More precisely, first an alignment is computed for each pair of recordings and a corresponding total cost using the Pairwise II alignment method (Ewert et al., 2009b). Each cost is normalised by dividing it by the length of the corresponding alignment path. The pair with the smallest normalised cost defines the first two feature sequences to be aligned, i.e. X^1 and X^2. Next, X^3 is set to the feature sequence where the sum of its normalised costs to X^1 and X^2 is the smallest among all remaining sequences. Following this strategy, the next version is always chosen as the one having the lowest sum of normalised costs between itself and each of the previously placed versions. This procedure is repeated until all recordings are sorted. Note that this strategy is considerably more computationally expensive than the first three. Intuitively, it is similar to the idea of a "guide tree" in biological sequence alignment, which is built before the sequence alignment to guide the alignment processing from the most similar pair to the most distantly related, as mentioned in Section 3.3.

Results are shown in Fig. 3.10, where the random order strategy is excluded as the resulting error was relatively high and would have occluded the nuances in the other strategies. As indicated by the results, the alignment order is indeed important in progressive alignment. The progressive alignment with a descending length-based order shows improvements in both accuracy and robustness over the pairwise method for most pieces. The ascending length-based order leads to an even better result. The possible reason could be that the template monotonically grows in length with each sequence being aligned: with a descending length based order, the difference in length between the template and the sequence to be aligned will become large when aligning the last several sequences, much larger than for the ascending length-based order where the template length grows slowly with the sequences being aligned. That may lead to a slight drop in alignment accuracy when aligning shorter sequences at the end as the DTW weights in use have a slight bias in favour of the main diagonal direction, i.e. $(w_1 < w_2 + w_3)$ (Section 3.5.1). Both the ascending length-based and the cost-based order strategy decrease the mean ABD and the standard deviation without any significant differences between them. However, the considerable difference in computational costs between these two strategies makes the ascending length-based order preferable.

3.6.4 Viterbi Training

Since the progressive alignment and the profile HMM have comparable alignment accuracies on larger datasets (Section 3.5), their computational complexities are compared in the following to see whether other factors contribute to choosing one approach over the other when many versions of a piece are available. To this end, let K be the number of recordings, each having about N features. To align the k-th recording to the template, the progressive alignment method computes $k-1$ cost matrices each with a time and memory requirement of $O(N^2)$ (the acceleration technique described in Section 3.4.3 with a fixed number of feature resolutions does not change the complexity level for this step). Since this step is repeated for K times, $\frac{K(K-1)}{2}$ cost matrices have to be computed and so the method is in $O(K^2N^2)$ (just as standard pairwise methods). A single Baum-Welch iteration of the profile HMM computes K forward matrices and K backward matrices of size $3N^2$ (since there are three states per feature in the profile HMM). If the number of Baum-Welch iterations is set to a fixed value independent of the number of available recordings, the overall complexity is in $O(KN^2)$. Therefore, for a high number of recordings, the profile HMM will eventually be the preferable approach, as the complexity is lower and with a high number of recordings the difference in alignment accuracy between the PA and PP method vanishes as well. In practice, with 10 Baum-Welch iterations, the runtime for the profile HMM will be lower for more than ≈ 120 recordings, as in this case K becomes higher than the ratio of constant factors influencing the absolute runtime of the profile HMM to that of progressive alignment (assuming similar runtime costs for the observation probabilities and the local cost measure).

Choosing the number of iterations, however, depends on the convergence behaviour of the method. Fig. 3.11 shows the average beat deviation for each piece after each Baum-Welch iteration. As can be seen, the method typically converges rather quickly, with only little change after the first five to ten iterations (which motivated us to limit the number of iterations to 10 in the initial experiment).

A further technique often used in large scale procedures in speech processing to accelerate the training is *Viterbi Training* (Durbin et al., 1999), as mentioned in Section 2.3.2.1. The forward-backward procedure is replaced with a simple Viterbi decoding therefore a single iteration with Viterbi training is about twice as fast as one iteration of Baum-Welch.

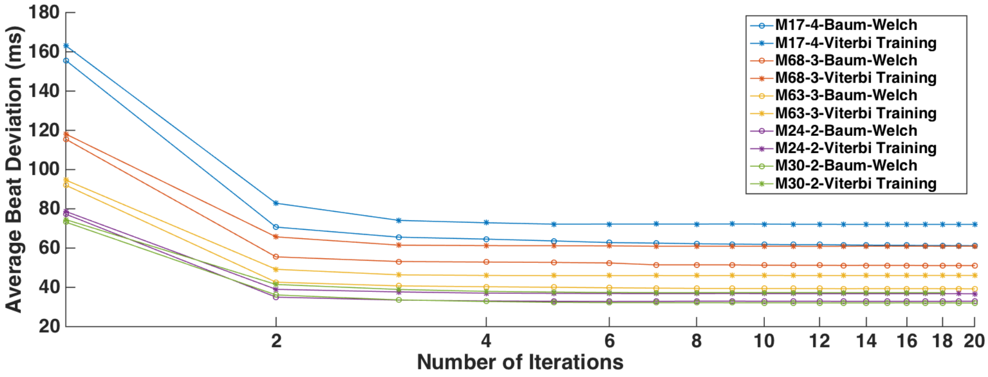

Figure 3.11: The convergence of average beat deviation with increasing number of iterations for two model learning methods for the profile HMM.

In addition, Viterbi training often converges faster than Baum-Welch in terms of the number of iterations, at the cost of being more prone to local minima of the likelihood function.

Fig. 3.11 shows the convergence results using Viterbi Training in the proposed Profile HMM method. It can be seen that the number of iterations necessary to reach convergence using Viterbi Training is about the same as using Bauch-Welch. Further, there is a slight but consistent loss of alignment accuracy, as expected, resulting from the use of Viterbi training. Therefore, Viterbi Training could be most useful as an alternative to Baum-Welch to accelerate the model training if the number of available recordings is very high, however, at the cost of a slight drop in alignment accuracy.

3.6.5 Iterative Alignment

As mentioned in Section 3.5, progressive alignment is greedier regarding the updating process. Intuitively, this greediness may lead to an accuracy drop, as reported in some bio-informatics tasks. In particular, the first alignments need to be more reliable as they have less information available and, at the same time, will influence the alignment with all remaining sequences. To circumvent this potential problem, this section introduces an iterative extension to the progressive alignment to further refine the template. The basic idea is to remove individual versions from the template and re-align them to the remaining template. Specifically, one version is taken out at a time, starting from the first one, and the alignment is performed between this version and the template of the remaining versions. The resulting template after re-alignment is evaluated by a score value, defined

Table 3.3: Comparing the Pairwise II alignment method (Ewert et al., 2009b)), Profile HMM and Progressive Alignment methods in terms of average note onset deviation (in milliseconds)

	Pairwise II		**Progessive**		**Profile HMM**	
Piece	mean	std	mean	std	mean	std
KV331	21	4	21	4	20	4
D783	27	7	24	4	27	8
Etude	26	6	24	3	24	3
Ballade	30	8	29	5	31	8

as the sum of the alignment costs between all pairs in this template (which can easily be extracted from the template). If the alignment score increases, the process restores the previous template. The re-alignments are continued until no further improvement can be achieved.

The iterative refinement process is tested with both ascending length based order and cost based order. As shown in Fig. 3.10, the iterative process leads to slightly worse result with ascending length based order for some pieces. The possible reason is that the iterative process has the disadvantage of descending length, i.e., the short pieces have to be re-aligned to a long template. The performance of cost based order is improved by the iterative process, to the similar level as ascending length based order without iterative process. Overall, the experiments show that progressive alignment is able to deliver alignments of both high accuracy and robustness with a single pass using a suitable alignment order.

3.6.6 Further evaluation

Although the Mazurka data is highly varied in terms of acoustic conditions and expressive local tempo variations (Section 3.5.1), the pieces are all of the same style and by one composer. Therefore, additional experiments were conducted with a set of four excerpts compiled by Goebl (1999a) from: Mozart Piano Sonata No. 11 in A major, KV331 first movement, Schubert German Dance D.783, No. 15, Chopin Etude in E major, Op. 10, No.3, and Chopin Ballade in F major, Op. 38. Each excerpt has 22 performances by skilled pianists recorded on a Bösendorfer computer-monitored piano. Compared to the Mazurka dataset, there are several major differences. First, all recordings were made using the same instrument under the same recording conditions and at the same time, such that the acoustic conditions do not differ within the dataset. Second, the recording quality is very high and contains only little reverberation. Third, compared to the Mazurka pieces with manually annotated beat positions, this dataset contains precise onset annotations for each note. To account for the higher quality annotations, the evaluation measure is changed from average beat deviation (ABD) to average note onset deviation in this section.

By providing cleaner acoustic conditions, this dataset can be used to test whether our methods also improve the alignment accuracy in less difficult scenarios, or whether a pairwise method can translate the clean conditions into higher accuracies than our proposed methods. The results for the Pairwise II alignment method (Ewert et al., 2009b) and the two joint alignment methods are shown in Table 3.3, where we used the same settings as described in Section 3.5.1.3. First, we can see that the results reflect the recording quality in this dataset, with relatively low alignment errors for all three methods. Further, we can see that also using this dataset our joint alignment methods slightly improve the mean of the alignment error, with the progressive alignment slightly ahead of the profile HMM. More importantly, we observe a similar behaviour regarding the robustness of the alignments as before, with a considerably lower standard deviation for the joint methods: compared to the pairwise method, progressive alignment again lowers the standard deviation by between 38% and 50% – despite the higher audio quality. These results demonstrate that our method indeed can be used to remove many outlier alignments, where the pairwise method fails to compute an accurate alignment.

3.7 Conclusion

This chapter introduced two methods for the joint alignment of multiple performances of a piece of music: a progressive alignment (PA) and a probabilistic profile (PP) method. As demonstrated by experiments using recordings of Chopin Mazurkas, both methods can be used to improve the alignment accuracy and robustness over state-of-the-art pairwise methods. An increase in accuracy using a method from the PP family over a member of the PA family as reported in bioinformatics could not be observed in our music synchronisation scenario. Moreover, although the theoretical complexity of the PP method is lower, due to the constants involved and the typical sizes of datasets, it is unlikely that the PP method would yield computational savings in practice. Additional experiments were conducted to investigate the behaviour of the proposed joint alignment methods by testing the influence of various parameters and to analyse the performance of various extensions aiming to increase the alignment accuracy and computational efficiency. In particular, experiments with smaller datasets showed that the PA method can outperform state-of-the-art pairwise methods even if only a small set of recordings is available.

CHAPTER 4

COMPENSATING FOR ASYNCHRONIES BETWEEN MUSICAL VOICES IN SCORE-PERFORMANCE ALIGNMENT

4.1 Introduction

The work in the last chapter improves the alignment robustness for cases where versions of the same piece of music have substantial differences locally, with respect to acoustic conditions or musical interpretations. This chapter continues this line of work and focuses on a special but important type of musical expression: asynchronies between musical voices in the context of score-to-performance alignment.

The goal of score-performance alignment is to align a given musical score to an audio recording of a performance of the same piece. Current methods assume that notes occurring simultaneously in the score are played concurrently in a performance. Musical voices such as the melody, however, are often played asynchronously to other voices, which can lead to significant local alignment errors. To handle asynchronies between the melody and the accompaniment, this chapter presents a novel method that treats the voices as separate timelines in a multi-dimensional variant of dynamic time warping (DTW). Experiments show that the proposed method measurably improves the alignment accuracy for pieces with asynchronous voices and preserves the accuracy otherwise.

This chapter is organised as follows. First, the motivation of this work is given in Section 4.2. Next, technical details of the proposed method are described in Section 4.3. Section 4.4 reports on the experimental results. Finally, conclusions and discussions of future work are given in Section 4.5.

4.2 Motivation

In general, given a symbolic score representation (MIDI, MusicXML) and an audio recording of one performance of a piece of music, the task of score to performance alignment aims at linking each note event in the score to its corresponding position in the recording. As mentioned in previous chapters, one main challenge stems from the diversity of possible musical interpretations. Musicians shape a piece of music using various musical parameters, including the playing style, expressive timing, or embellishments, leading to complex differences between the score and the performance.

To increase overall robustness, many alignment methods make simplifying assumptions and disregard various musical parameters. For example, state-of-the-art methods typically assume that notes occurring simultaneously in the score are also played concurrently during a performance (Joder et al., 2011; Ewert et al., 2009b; Dixon and Widmer, 2005). However, introducing asynchronies between simultaneous notes is considered an important part of musical expression. For example, emphasising a musical voice such as the melody by playing it earlier compared to other voices is a form of expression typically referred to as melody lead (Goebl, 2001). While such asynchronies usually do not have a strong effect on the alignment on a coarse level, the alignment accuracy on a finer, local level can drop measurably as the asynchrony is not modelled by current methods.

Figure 4.1 shows an example of differences between score and performance due to such asychronies. For the first bar of Chopin Op. 28 No. 15, the figure provides the score on the upper left side as well as a piano roll representation of two MIDI files on the right side. The top MIDI file is the score MIDI, where the simultaneous score notes are strictly aligned in time. The bottom MIDI file shows a performance of the piece. The latter was taken from the dataset used in the experiments described in Section 4.4 and was recorded

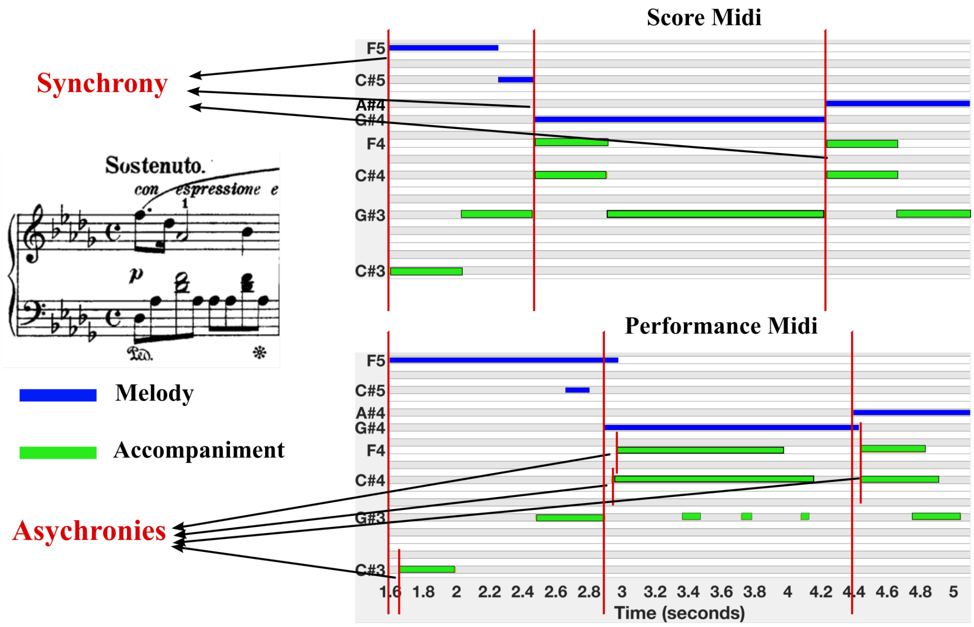

Figure 4.1: An example of asynchronies between the melody and the accompaniment in one performance of Chopin Op. 28 No. 15, 1st bar, while the corresponding notes are simultaneous on the score.

on a Yamaha Disklavier. As can be seen, in the performance, the melody is played ahead of the accompaniment voices by several tens of milliseconds.

To cope with possible asynchronies between the melody and the accompaniment, the main idea of this work is to separate the score into two voices (or more generally into two disjunct partitions) and to compute a joint three-dimensional alignment between the two score timelines and the audio timeline. While, in this basic form, the additional degree of freedom in the alignment can lead to measurable improvements in alignment accuracy on a fine level, it can also cause a loss of accuracy on a coarser, global level. Therefore, to exploit the overall robustness of existing alignment methods, this work employs a state-of-the-art method to compute a coarser alignment in a first step, which is then used to constrain and guide the alignment in our proposed method. This way, the proposed method not only combines the robustness of current methods with an improved alignment accuracy, but also drastically lowers the computational cost for computing a three-dimensional alignment (given the guiding alignment, from cubic to linear in the length of the recording or score).

4.3 Alignment Method

There are various score to performance alignment methods as reviewed in Chapter 2, however, most of them do not account for asynchronies between voices. An exception was presented by Heijink et al. (2000) but only for aligning MIDI files. Further, Niedermayer (2009b) proposed a post-processing step to refine the alignment locally on a note level. Different from them, this work aims at handling asynchronies between the melody and the accompaniment, as part of the alignment process.

To do so, it is necessary to treat the melody and the accompaniment on the score separately, so that they are not forced to align to the same temporal position, as notated by the score. Therefore this idea requires a method to align three data streams, i.e., two score voices and the audio. Interpreting the alignment as a multi-dimensional data series synchronisation problem leads to two existing methods: the Asynchronous Hidden Markov Model (AHMM) (Bengio, 2002) and the Multi-Dimensional Dynamic Time Warping (MD-DTW)(Holt et al., 2007). These methods have been applied to various problems, including audio-visual speech recognition, and in particular for bi-modal speech and gesture fusion (Wöllmer et al., 2009). In the following, the proposed method is introduced as an extension to MD-DTW.

As discussed in Chapter 2, a general DTW approach for aligning a score and an audio recording can be summarised in three simple steps. First, the score and the audio are converted to a suitable, common feature representation. Second, by comparing each element in the score feature sequence with each element in the audio sequence using a distance measure, one obtains a distance or cost matrix. Third, based on such a matrix, dynamic programming is applied to obtain a cost-minimising alignment path.

To model possible asynchronies between voices, all three steps of the procedure above need to be modified. First, the score can no longer be treated as a single data stream. Instead, the voices have to be isolated from the score and features have to be derived for each voice separately. Second, the comparison of features from all three sequences leads to a three-dimensional cost matrix (or cost tensor). Third, the dynamic programming method needs extending to three dimensions to deal with the three-dimensional cost matrix.

4.3.1 Computing Features for Individual Voices

While a musical score can often be separated into various combinations of voices, this work focuses on the melody and accompaniment parts. From a musical point of view, these voices are particularly important as asynchrony between them has been reported and analysed in musicological studies (Goebl, 2001). Also from a numerical point of view this is beneficial, as only three timelines need to be aligned, which limits the computational complexity of the alignment problem.

The melody and the accompaniment notes from the score are separated using the skyline algorithm (extracting the highest note from all simultaneous note events as the melody) (Uitdenbogerd and Zobel, 1999), which could be replaced by more complicated methods, such as the contig mapping (Chew and Wu, 2005), in future work. Once separated, the feature computation itself is similar to previous methods.

The feature sequences for the two score voices as well as the audio are computed as $X := (x_1, x_2, \ldots, x_K)$, $Y := (y_1, y_2, \ldots, y_K)$ and $Z := (z_1, z_2, \ldots, z_L)$ respectively, with $x_n, y_m, z_\ell \in \mathscr{F}$ where $\mathscr{F}$ is a space containing two types of features similar to the methods described in Chapter 2 and used in Chapter 3. However, instead of using CENS or DLNCO features, which only preserve chroma information and discard octave relationships, this work employs features of 88 dimensions, corresponding to the 88 piano pitches. The calculation is essentially same as CENS and DLNCO features, but leaves out the final step of summing over pitches in the same chroma. This change is used to improve the sensitivity regarding pitch differences, considering the fact that the melody and accompaniment voice of the score often contain simultaneous notes of the same pitch class but on different octaves. In summary, the first type of feature used in this work is an 88-dimensional log-frequency feature, whose entries encode a short-time intensity in spectral bands with centre frequencies corresponding to the fundamental frequency of the 88 keys on a grand piano. The second 88-dimensional feature type indicates possible onset positions separately for each key.

4.3.2 Three-Dimensional Dynamic Time Warping

In a standard DTW method, each element of one feature sequence is compared with one from the other sequence, which results in a cost matrix. With three feature sequences,

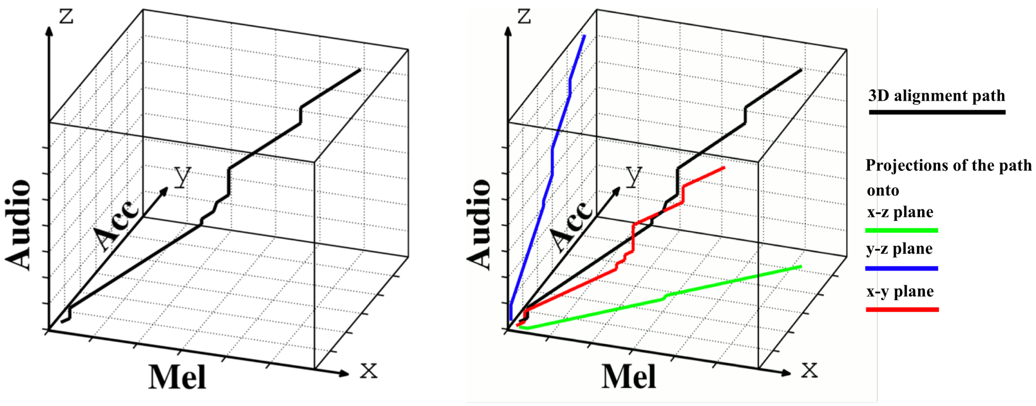

(a)

(b)

Figure 4.2: A three-dimensional cost tensor. (a) Three-dimensional alignment path of the melody (Mel), accompaniment (Acc) and audio; (b) Projections of the path (black) onto x-z (red), y-z (blue) and x-y (green) planes.

this idea is extended to a three dimensional cost tensor, see also Fig 4.2(a). More precisely, given the three feature sequences X, Y and Z, define a $(K \times K \times L)$ cost tensor C by $C(n, m, \ell) := c(x_n + y_m, z_\ell)$, where $c : \mathscr{F} \times \mathscr{F} \to \mathbb{R}_{\geq 0}$ denotes a local cost measure on $\mathscr{F}$. For $n \neq m$ we combine a melody and an accompaniment feature from different positions in the two score timelines into a single score feature, which is then compared to the audio feature. In this case, the difference $n - m$ encodes the asynchrony between the two voices. In particular, the *diagonal plane* in the cost tensor ($C(n, n, \ell)$ for $n \in [1 : N]$ and $\ell \in [1 : L]$) is essentially identical to a cost matrix between the complete score and the audio as used in classical two-dimensional DTW, where the asynchrony is not allowed between the two score voices. All entries in the cost tensor on planes parallel to the diagonal plane have the same asynchrony between the two score voices (i.e. $n - m$ is constant), compare Fig. 4.3(a).

An alignment between X, Y and Z is defined as a sequence $p = (p_1, \ldots, p_Q)$ with $p_q = (n_q, m_q, \ell_q) \in [1 : K] \times [1 : K] \times [1 : L]$ for $q \in [1 : Q]$ satisfying $p_1 = (1, 1, 1)$ and $p_Q = (K, K, L)$ as well as $p_{q+1} - p_q \in \{(1, 0, 0), (0, 1, 0), (0, 0, 1), (1, 1, 0), (1, 0, 1), (0, 1, 1), (1, 1, 1)\}$ (step size condition). An alignment through the cost tensor aligning X, Y and Z is illustrated in Fig 4.2(a).

The cost of an alignment is defined as $\sum_{q=1}^{Q} C(n_q, m_q, \ell_q)$ and an alignment having minimal cost among all possible alignments is called an *optimal alignment*. To determine such an optimal alignment, one can employ MD-DTW (Holt et al., 2007). In summary, one recursively computes a $(K \times K \times L)$-tensor D, where the entry $D(n, m, \ell)$ is the cost of an optimal alignment between $(x_1, \ldots, x_n)$, $(y_1, \ldots, y_m)$ and $(z_1, \ldots, z_\ell)$. Using dynamic programming, this tensor can be recursively computed as follows:

$$D(n,m,l) := \min \begin{cases} D(n-1,m,l) + w_1\, C(n,m,l), \\ D(n,m-1,l) + w_2\, C(n,m,l), \\ D(n,m,l-1) + w_3\, C(n,m,l), \\ D(n-1,m-1,l) + w_4\, C(n,m,l), \\ D(n-1,m,l-1) + w_5\, C(n,m,l), \\ D(n,m-1,l-1) + w_6\, C(n,m,l), \\ D(n-1,m-1,l-1) + w_7\, C(n,m,l), \end{cases}$$

for $n, m, l > 1$. Furthermore, $D(n,1,1) := \sum_{k=1}^{n} w_1\, C(k,1,1)$ for $n > 1$, $D(1,m,1) = \sum_{k=1}^{m} w_2\, C(1,k,1)$ for $m > 1$, $D(1,1,l) = \sum_{k=1}^{l} w_3\, C(1,1,k)$ for $l > 1$, and $D(1,1,1) := C(1,1,1)$. Calculations of entries on the x-y, x-z and y-z planes, i.e., $D(n,m,1)$, $D(n,1,l)$ and $D(1,m,l)$, are equivalent to the accumulated cost matrix calculation in classical two-dimensional DTW (Holt et al., 2007). The weights $(w_1, w_2, w_3, w_4, w_5, w_6, w_7) \in \mathbb{R}_+^7$ can be set to adjust the preferences for the seven step sizes. Note that a bias for any direction is removed by setting these weights to $(w_1, w_2, w_3, w_4, w_5, w_6, w_7) = (1,1,1,2,2,2,3)$. An optimal alignment is obtained by tracing the minimising argument backwards from $D(K,K,L)$ to $D(1,1,1)$. Its projections onto the x-z and y-z planes yield alignments between the melody and the audio as well as the accompaniment and the audio, respectively. The projection onto the x-y plane corresponds to an alignment between the two score voices and thus encodes the estimated local asynchrony between them; see Fig. 4.2(b).

4.3.3 Path Constraints

In principle, an asynchronous alignment could be computed using MD-DTW as described above. In practice, however, there are additional factors which render this approach infeasible. On the one hand, the computational complexity of MD-DTW is considerable. Assuming the sequences to be aligned are roughly of the same length L, the computational complexity of a three-dimensional dynamic programming algorithm is $O(L^3)$, as mentioned in Chapter 3. As the asynchrony is usually at the level of several tens of milliseconds, a high temporal resolution is required for the features used in the alignment. Therefore the value of L is typically high and the alignment becomes practically infeasible even for pieces of average length. On the other hand, splitting the score into two independent voices results in the number of notes in each voice to be lower compared to the full score. This becomes a problem, if the remaining notes do not provide enough information to be discriminative in time. For example, if a chord is repeated consecutively in the accompaniment, an asynchronous alignment might easily confuse one instance of the chord for another, resulting in a substantial alignment error. This issue is referred to as the loss-of-structure problem in the following. Note that previous approaches will not suffer from this issue if the melody is discriminative enough.

Given the above issues, the following will introduce two extensions to MD-DTW, to constrain the alignment. This strategy not only drastically lowers the computational cost but also combines the robustness of previous approaches with an increased alignment accuracy resulting from the proposed asynchronous alignment.

Asynchrony Constraints

The first constraint exploits the fact that in practice asynchronies between musical voices are not arbitrarily high (Goebl, 2001), usually smaller than 200 milliseconds. Musicians typically employ asynchronies to highlight certain elements in a piece, and if used in an extreme way, the asynchrony might result in categorical changes to the rhythm. Applying this knowledge, the amount of asynchrony between voices allowed in the alignment can be limited to a certain range. To do so, the alignment path is forced to run closely to the central diagonal plane in the cost tensor, compare Section 4.3.2.

More precisely, in order to compute the diagonal plane, features are combined without any asynchrony between them ($n = m$ as described above), and parallel planes use a non-zero but constant asynchrony $n - m$. To implement a constraint on the asynchrony, only entries on the planes where $|n-m| <= \Theta$ is satisfied are computed in C and D, where $\Theta \geq 0$ denotes the maximally allowed asynchrony. All entries not satisfying this constraint are formally set to infinity. Fig. 4.3(a) shows the diagonal plane as well as two parallel planes which satisfy the boundary case $|n - m| = \Theta$ for a given value of Θ. Other planes between

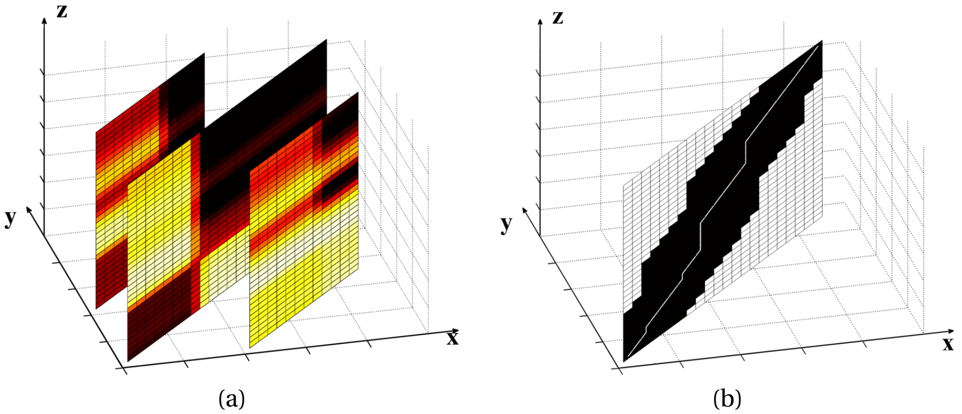

Figure 4.3: Constraining the 3D-DTW alignment. (a) Diagonal plane in the cost tensor corresponding to no asynchrony between voices, surrounded by two parallel planes corresponding to regions with constant asynchrony. (b) The alignment (white) is constrained to run in a neighbourhood (black) of a reference alignment, illustrated only on the diagonal plane.

the two boundary planes are also computed. Note that, since Θ is a fixed parameter, the number of parallel planes is fixed and the computational complexity is lowered from $O(L^3)$ to $O(L^2)$. The second constraint to be described next lowers the complexity even further.

Reference Alignment Constraints

While the main purpose of the asynchrony constraint above is to lower the computational complexity, it also yields improvement regarding the loss-of-structure issue as certain degenerate alignments are automatically eliminated. However, depending on the value of Θ, the asynchronous alignment might still be less robust than previous approaches. Additionally, the computational costs are still about $2 \cdot \Theta$ times (the number of parallel planes to be computed) higher than classical DTW. Therefore, this work introduces a second constraint, which guides the alignment using a reference alignment computed using a method based on classical DTW (Ewert et al., 2009b). More precisely, given a 2D reference alignment $\tilde{p} = (\tilde{p}_1, \ldots, \tilde{p}_R)$ with $\tilde{p}_r = (n_r, \ell_r)$, the entry (n, m, ℓ) in C and D is computed only if there is a $\tilde{p}_r$ with $\ell_r = \ell$ and $|n_r - n| < \Phi$ and $|n_r - m| < \Phi$, where $\Phi > 0$ is the size of the constraint region. This way, the reference alignment is essentially projected into the 3D cost tensor and used to define a neighbourhood in which the alignment is forced to run; see Fig 4.3(b) for an illustration. This approach resembles the general principle behind multiscale DTW, described in Chapter 2.

Overall, since Φ is fixed, the alignment now restricted to a fixed area inside the boundary set by Θ, which further reduces the computational complexity from $O(L^2)$ to $O(L)$ given the reference alignment. The method of computing the reference alignment employs a multiscale version of DTW as well, which additionally lowers the computational cost of the entire system. Furthermore, by limiting both the allowed asynchrony and the displacement from a reference alignment effectively mitigates the loss-of-structure problem, which is demonstrated by the experiments below.

4.4 Experiments

4.4.1 Data Set

The experiments were conducted with recordings of three pieces which are known to contain strong asynchronies and three pieces played without asynchrony, to illustrate the performance of our proposed method in both cases. The former three pieces are Chopin Etude op. 10/3 (first 21 measures), Chopin Prelude op. 28/15 (first 27 measures) and Chopin Nocturne op. 48/1 (first 24 measures). The other three are picked from Bach's Well-Tempered Clavier, BWV 848, BWV 849 and BWV 889. The corresponding scores (in MIDI files) were obtained from the Mutopia project[1], the KernScores website[2] and the MuseScore website[3].

Since the evaluation of the proposed method requires the onset time for each individual note as ground truth and suitable data sets are scarce, a mixed data source was used. For Chopin Etude op. 10/3, a data set was used which consists of 22 performances by skilled pianists recorded on a Bösendorfer computer-monitored piano. It includes both an audio recording as well as a corresponding MIDI version for each performance (Goebl, 2001, 1999b). For the remaining five pieces, MIDI versions of performances were downloaded from the website of the Minnesota International Piano-e-Competition[4]. These MIDI files were recorded on Yamaha Disklavier Pro pianos during annual competitions for over ten years, which capture the detailed nuances of the performances. The audio versions were generated from the performance MIDI files using Native Instruments's Vienna

[1] http://www.mutopiaproject.org

[2] http://kern.ccarh.org

[3] http://musescore.org

[4] http://www.piano-e-competition.com/

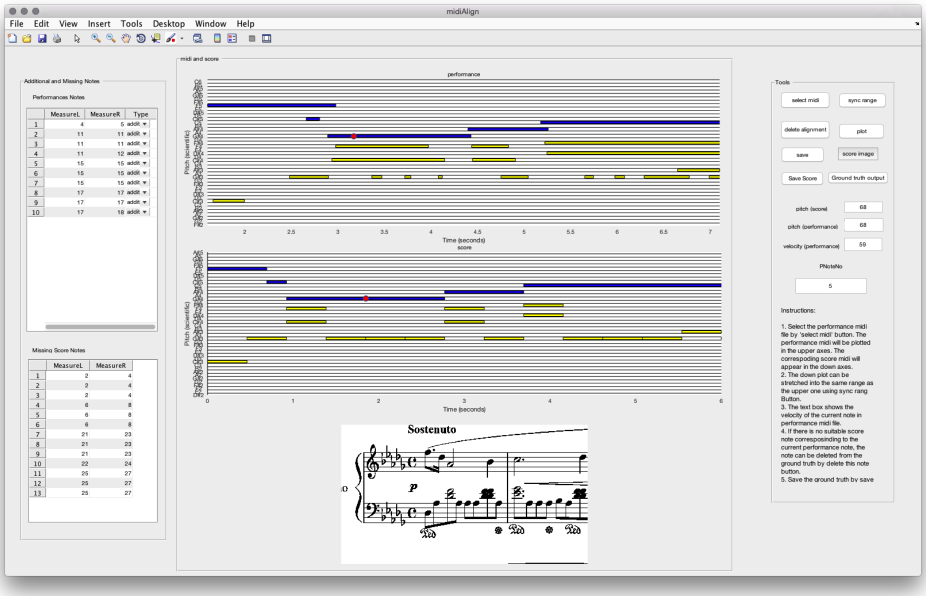

Performances Notes

	MeasureL	MeasureR	Type
1	4	5	addit ▾
2	11	11	addit ▾
3	11	11	addit ▾
4	11	12	addit ▾
5	15	15	addit ▾
6	15	15	addit ▾
7	15	15	addit ▾
8	17	17	addit ▾
9	17	17	addit ▾
10	17	18	addit ▾

Missing Score Notes

	MeasureL	MeasureR
1	2	4
2	2	4
3	2	4
4	6	8
5	6	8
6	6	8
7	21	23
8	21	23
9	21	23
10	22	24
11	25	27
12	25	27
13	25	27

pitch (score) 68
pitch (performance) 68
velocity (performance) 59
PNoteNo 5

Instructions:

1. Select the performance midi file by 'select midi' button. The performance midi will be plotted in the upper axes. The correspoding score midi will appear in the down axes.
2. The down plot can be stretched into the same range as the upper one using sync rang Button.
3. The text box shows the velocity of the current note in performance midi file.
4. If there is no suitable score note corresposinding to the current performance note, the note can be deleted from the ground truth by delete this note button.
5. Save the ground truth by save

Figure 4.4: A GUI for manually correcting the alignment between the performance MIDI and score MIDI. The performance MIDI is shown above and the score MIDI below. The GUI lists the notes which have not been matched successfully by the automatic alignment and highlights them on the MIDI graphs. By selecting corresponding notes on two MIDI graphs, one can add, modify or delete a match. The sheet score image of the selected MIDI period is also shown as a reference.

Concert Grand VST plugin comprising samples for a Boesendorfer 290 with an uncompressed size of almost 14 GB. The total number of performances for each piece is given in Table 4.1.

4.4.2 Ground Truth Generation

For each audio recording, the data set contains the corresponding performance MIDI file, which annotates when and which notes are played. Therefore the ground truth for evaluating the proposed method can be generated by aligning the performance MIDI with the score MIDI of the same piece on a note level. To do so, an automatic alignment is performed first, followed by manual correction. The automatic alignment applies the Longest Common Subsequence (LCS) algorithm to align the pitch value sequences of the performance and the score, and then refines the result according to the pitch and onset time of each note. LCS is a common matching method for symbolic sequences, described in Chapter 2. For the manual correction, a GUI tool is developed in Matlab, shown in Figure 4.4. By choosing the performance MIDI and the corresponding score MIDI, the tool firstly performs the automatic alignment. It then renders the two MIDIs as piano rolls and when a performance note is clicked, the corresponding score note match (if any) is highlighted with red circles. Also, it lists the notes which have not been matched successfully and highlights them with different colours. To perform the manual correction, one can select the corresponding notes on two piano rolls to add, modify or delete a match. If the musicXML version of the corresponding score is available and it can be rendered as image, by using the coordinate information contained in the musicXML, the GUI tool can show the score image of the selected MIDI period as a reference for manual correction. The tool currently cannot render the score image from musicXML so the rendering need to be done external application. It could be an useful function to be integrated into the tool in the future work.

4.4.3 Evaluation Measure

A ground truth alignment is generated by the procedure described in the last section for each audio recording, in order to evaluate the proposed method as follows. The alignment computed by the proposed method can be used to locate, for each note onset in the performance, the corresponding position in the score. By comparing these positions with the ground truth alignment, a note onset deviation is computed for each performance note. The error of an alignment is then the average over the deviations for all performance notes, specified in milliseconds. To indicate the influence of the proposed method in aligning each voice, the alignment error is also computed for melody notes only or accompaniment notes only.

4.4.4 Results

Evaluation results of the proposed method are compared with a synchronisation method based on classical 2D-DTW (Ewert et al., 2009b), which is also used to generate the 2D reference alignment for our 3D-DTW. In order to improve comparability, both methods employ the same types of features and cost measures, with a temporal resolution of 20ms for the features. The weights for the proposed 3D-DTW are set to $(w_1, w_2, w_3, w_4, w_5, w_6, w_7) = (1.5, 1.5, 1.5, 2.5, 2.5, 2.5, 3)$, and the weights for the 2D-DTW

	Piece	No. Rec	2D-DTW (Ewert et al., 2009b)			3D-DTW		
			Mel	Acc	OA	Mel	Acc	OA
w/ Asyn	Op. 10/3	22	16	23	21	16	18 (-22%)	17 (-19%)
	Op. 28/15	5	16	45	37	16	25 (-44%)	22 (-41%)
	Op. 48/1	4	27	64	49	25	56 (-13%)	44 (-10%)
	Average		18	31	27	17	24 (-23%)	22 (-19%)
w/o Asyn	BWV 848	3	11	14	12	11	14	12
	BWV 849	2	21	29	26	21	28	25
	BWV 889	2	11	15	13	11	17	14
	Average		14	19	16	14	19	16

Table 4.1: Experimental results for three excerpts played with strong asynchrony (upper) and three pieces without asynchrony (lower). This table shows the number of performances available and statistics of the alignment error in milliseconds for the respective pieces. Both results for the 2D-DTW (Ewert et al., 2009b) and our 3D-DTW alignment method are computed separately for the melody (Mel) and accompaniment (Acc). The error values of these two voices are averaged over the number of notes to get the overall (OA) alignment error. The change in alignment error achieved by 3D-DTW is shown in parentheses.

are set to $(w_1, w_2, w_3) = (2, 1.5, 1.5)$ [5]. The maximally allowed asynchrony between the two voices is set to 15 time frames (300 ms) and the size of the constraint region is set to 50 time frames (1 second) around the guiding path. [6]

Table 4.1 summarises the evaluation results. Compared with the classical 2D-DTW alignment method for the three pieces with strong asynchrony, the proposed method mostly improves the alignment accuracy for the accompaniment part. For op. 10/3, the overall alignment error for the accompaniment is 22% lower using 3D-DTW (23ms down to 18ms) while the error for the melody remains the same on average. The decrease in alignment error for the accompaniment is even greater for op. 28/15, by 44% (45ms down to 25ms). For op. 48/1, the 3D-DTW method reduces the alignment error for the accompaniment by 13%, and slightly for the melody. A possible explanation for the improvement being limited to the accompaniment could be that the melody is often played louder than the rest to emphasise it. This way, the melody dominates the energy distribution in the features and, not being able to differentiate between the two voices, classical DTW thus tends to focus on the dominant voice. In contrast, the two score voices are treated as inde-

[5] The weights are set to bias the diagonals. Other choices of weights were tested for the 3D-DTW and experiments showed they didn't lead to any improvement on accuracy.

[6] Larger maximally allowed asynchrony and constraint regions have been tested and experiments showed that they led to higher computational cost without any accuracy improvement.

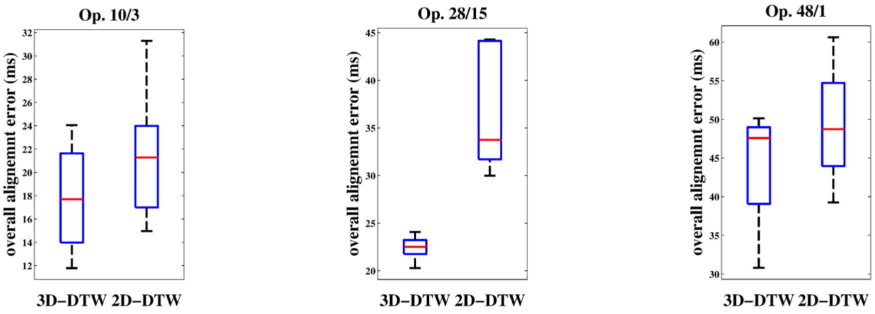

Figure 4.5: Comparison of the 2D-DTW alignment results with the proposed 3D-DTW alignment results. The boxplots illustrate the distribution of the alignment results in milliseconds for each piece separately.

pendent timelines in the proposed 3D-DTW alignment method, which reduces the local alignment error for the accompaniment. Moreover, for the three pieces without asynchrony, the average alignment error of the proposed method is the same as that of the classical 2D-DTW alignment. The average overall alignment error is 16ms for both methods, which indicates that they are relatively easy to align considering the feature resolution is 20ms.

These results indicate that the improvement in alignment accuracy provided by the proposed method depends on the characteristics of the music piece to be aligned and the amount of asynchrony played in the performances. That matched the goal of the proposed method, i.e., compensating for the asynchronies between two voices while preserving both the alignment accuracy of non-asynchronous parts and the overall alignment robustness.

The overall alignment error for the three pieces with strong asynchrony, drops from 27ms using 2D-DTW alignment to 22 ms using 3D-DTW alignment on average (decreases by 19%). This drop can also be seen from the boxplots[7] in Fig 4.5, which show the distribution of the alignment error for all score-audio pairs for the three pieces. Note that the above results were obtained by separating the melody and accompaniment notes from the score using the skyline algorithm. Compared with results obtained using a manual separation, the overall alignment error remained the same on average.

[7] Standard boxplots are used: the red bar indicates the median, the blue box gives the 25*th* and 75*th* percentiles (p_{25} and p_{75}), the black bars correspond to the smallest data point greater than $p_{25} - 1.5(p_{75} - p_{25})$ and the largest data point less than $p_{75} + 1.5(p_{75} - p_{25})$. The red crosses are called outliers.

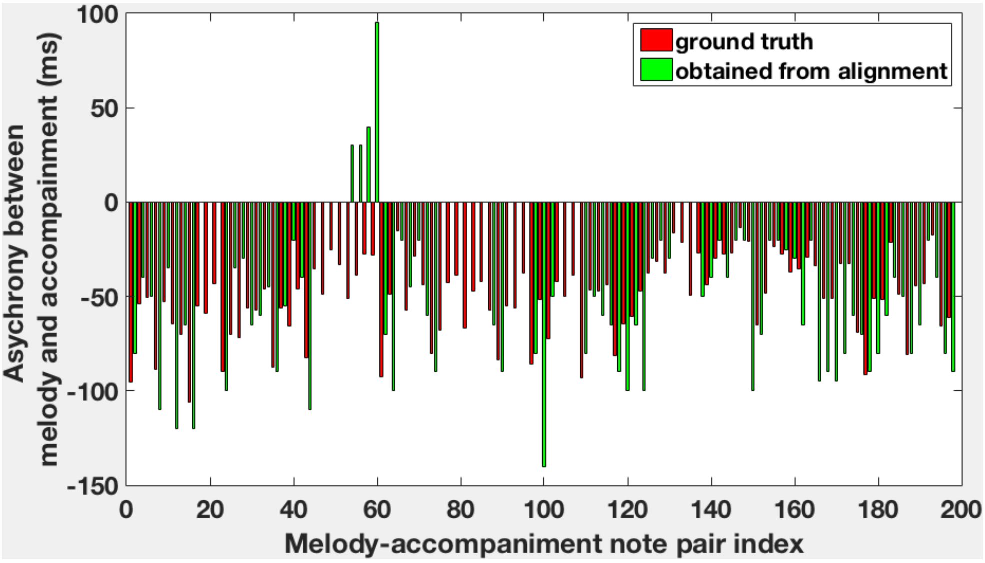

Figure 4.6: Comparison between the ground truth (red) and detected asynchronies (green) between the melody and the accompaniment for a performance of Chopin Op. 3 No. 10 (first 21 measures).

4.5 Conclusion and Future Work

This chapter proposed a score-audio alignment method to compensate for asynchronies between the melody and accompaniment. A 3D-DTW algorithm was proposed in which the two score voices are treated as independent timelines. Further, the alignment was constrained by a guiding alignment obtained via a classical 2D-DTW, providing improved robustness and reduced computational complexity. Experiments demonstrated that the proposed method can indeed improve the alignment accuracy for pieces with strong asynchrony and preserves the accuracy otherwise, compared to a previously proposed alignment method using classical DTW.

There are several possible aspects for further investigation. As a by-product, the resulting alignment can be used to indicate the positions where asynchrony occurs. Figure 4.6 shows an example of asynchronies obtained from the proposed alignment method for a performance of Chopin Op. 3 No. 10 (first 21 measures). In initial experiments, the proposed method achieved a precision of 0.44 and recall of 0.58 on average in detecting positions with strong asynchrony. In the future, the proposed method can be improved and developed as a tool to assist in the analysis of musical expression. Furthermore, the method is currently only used for the asynchrony between the melody and the accompaniment. The improvement in alignment accuracy is limited as this type of asynchrony is relatively small. However, the same idea can be applied to resolve other types of asynchrony, such as breaking chords. Last but not least, the multi-dimensional DTW could be adapted to different asynchronous data stream alignment problems, such as the asynchrony between different instruments in a musical ensemble or the asynchrony between the singing voice and the accompaniment in a karaoke setting.

CHAPTER 5

IDENTIFYING MISSING AND EXTRA NOTES IN PIANO RECORDINGS USING SCORE-INFORMED DICTIONARY LEARNING

5.1 Introduction

The previous chapter proposed a score to audio alignment method, aiming to handle the cases where musicians play with asynchrony between the melody and the accompaniment in the performance. A main application of score-audio alignment is to help extract information from the audio by exploiting the aligned score, as discussed in Chapter 2. This chapter presents such a score-informed automatic music transcription (AMT) approach to identify the missing and extra notes from the audio recording of piano performances.

The goal of AMT is to obtain a high-level symbolic representation of the notes played in a given audio recording. Despite being researched for several decades, current methods are still inadequate for many applications. To boost the accuracy of AMT, a recently presented concept (Ewert et al., 2016) is to exploit the musical score as prior knowledge for applications such as music tutoring. The aligned score is used to construct a transcription method that is tailored to the given audio recording, by applying the score-informed dictionary technique. Based on this concept, the work in this chapter identifies several systematic weaknesses of the system proposed in (Ewert et al., 2016) and presents countermeasures to improve its performance. Firstly, the dictionary of spectral templates is extended to a dictionary of variable-length spectro-temporal patterns. Secondly, the score information is integrated using soft rather than hard constraints, to better take into account that differences from the score indeed occur. Thirdly, new regularisers are introduced to guide the learning process.

This chapter is organised as follows. Section 5.2 introduces the motivation and related work. The previous work (Ewert et al., 2016) is described as a baseline method for this chapter in Section 5.3. Section 5.4 provides analysis of the baseline method and proposes several extensions accordingly. Section 5.5 reports systematic experiments to illustrate the influence of individual parameters and provides additional insights into the behaviour of the proposed methods. Finally, the conclusion is given in Section 5.6.

5.2 Motivation

Automatic music transcription (AMT) has been an active research area for several decades and is often considered to be a key technology in music signal processing (Benetos et al., 2013). Its applications range from content-based music retrieval and interactive music interfaces (Benetos et al., 2013) to musicological analysis (Bello Correa, 2003), music education (Dittmar et al., 2012) and note-based audio processing (Driedger et al., 2013). While for certain applications the accuracy of state-of-the-art methods is sufficiently high, current methods still do not reach the sophistication of a transcription made by human experts. In addition, current methods seem to have reached a plateau in performance and it has become increasingly difficult to make significant improvements (Benetos et al., 2013). Therefore, many interesting applications involving AMT technologies remain infeasible.

One way to boost the accuracy of an AMT system is to provide additional information, e.g. originating from annotations interactively made by the user during the transcription process (Kirchhoff et al., 2012), or single note recordings giving more details about the instrument in use and the recording conditions (Klapuri and Davy, 2006; Ewert and Sandler, 2016). This chapter investigates a particular type of prior knowledge available in a specific

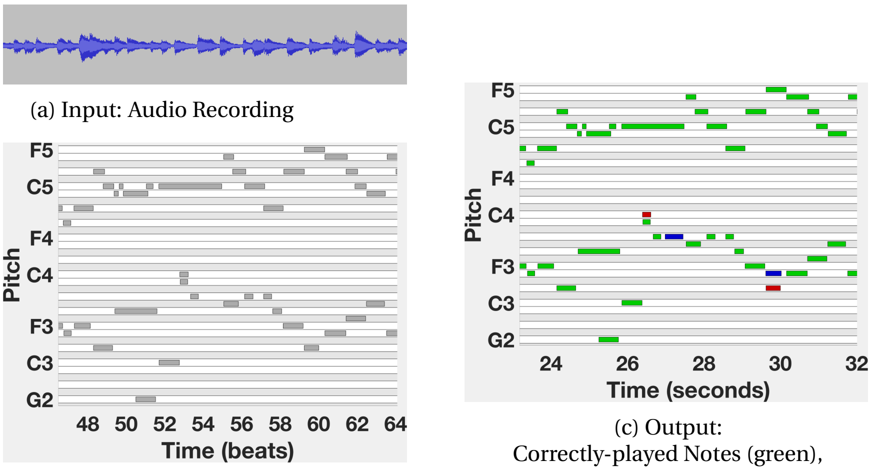

(a) Input: Audio Recording

(b) Input: Score Representation

(c) Output:
Correctly-played Notes (green),
Missing Notes (red), Extra Notes (blue)

Figure 5.1: Score-Informed Transcription: Given (a) an audio recording and (b) the corresponding score, identify (c) the correctly played score notes (green), the missing notes (red) and the extra notes (blue).

application scenario: a musical score. The scenario of a music tutoring application is explored here, in which the system evaluates a student's performance with regards to how faithfully the score was reproduced, in order to provide feedback on when and how the student deviates. Fig. 5.1 provides an example of this scenario. Given a digital encoding of the score of a piece of music (Fig. 5.1b) and an audio recording of a student playing that piece (Fig. 5.1a), the goal (Fig. 5.1c) is to identify which score notes have been played correctly (green bars), which have not been played – *missing notes* (red bars) and which notes have been played that are not found in the score – *extra notes* (blue bars) .

With a focus on music learning and tutoring, Dannenberg et al. (1990) use score following to match a student's performance (given as a MIDI file) with the score and analyse the performance based on the matching. Wang et al. (2012) introduce a system for detecting pitch activity in violin performances, such that the result can be compared with the corresponding score in order to give feedback on the student's playing technique. However, in the piano tuition scenario explored by this chapter, the proposed method needs accounting for the highly non-stationary nature of the piano sound production process and the high level of polyphony in such recordings.

Theoretically, standard AMT methods could be employed in this context by using them to generate a transcription from the audio and comparing the result with the given score.

In practice, however, the error rates of existing methods are high and thus such a comparison would often be meaningless, with many detected extra and missing notes actually being transcription errors. Moreover, using standard AMT methods in such scenarios would ignore the highly informative score. To make use of the score information, Benetos et al. (2012) first align the score to the audio and then, after synthesising the score using a wavetable method, transcribe both the real and the synthesised audio using an AMT method. To lower the number of falsely detected notes for the real recording, the method discards a detected note if the same note is also detected in the synthesised recording while no corresponding note can be found in the score. Here, the underlying assumption is that in such a situation, the combination of harmonic intervals might lead to uncertainty in the spectrum, which could cause an error in their proposed method. Furthermore, the method requires the availability of single note recordings for the instrument to be transcribed (under the same recording conditions) – a requirement not unrealistic to fulfil in this application scenario but leading to additional demands for the user. Under these additional constraints, the method lowered the number of transcription errors considerably compared to standard AMT methods.

The main usage of the score by Benetos et al. (2012) is to post-process the transcription results obtained via a standard AMT method. While this strategy leads to a certain degree of success, Ewert et al. (2016) exploit the available score information to adapt the transcription method itself to a given recording. The main idea is to obtain a system highly tuned to transcribe exactly the piece at hand under the specific acoustic conditions in the given recording. To this end, the score is used to modify two central components of an AMT system: the set of spectral patterns used to identify note objects in a time-frequency representation, and the subsequent note detection process. More precisely, similar to strategies used in score-informed source separation, introduced in Chapter 2, the method constrains the dictionary learning process in non-negative matrix factorisation (NMF) using the score information. This way, the method yields, for each pitch in the score template vectors describing the spectral energy distribution in the recording associated with notes of that pitch. After extrapolating the learned dictionary to pitches not in the score, the adapted dictionary is used to compute unconstrained activations for all pitches over time. Assuming that the number of playing mistakes is relatively low compared to the total number of notes, the score information is used to adapt the note detection process such that the match between detected notes and score notes is maximised in a certain way. By comparing the resulting final transcription to the score, the notes can be classified as either correct, missing or extra. Integrating the score information into the method itself, the method considerably improved upon the state of the art, even without the requirement to provide single note recordings as in (Benetos et al., 2012).

To the best of the author's knowledge, only the above two methods (Benetos et al., 2012; Ewert et al., 2016) have aimed at exploiting the score information to improve upon the standard AMT method in the scenario of a music tutoring application. The main contributions of this chapter are the identification of several systematic weaknesses in the signal model used by Ewert et al. (2016) and designing corresponding improvements. First, the signal representation used by Ewert et al. (2016) is based on NMF, where spectral and temporal properties are modelled independently (Smaragdis and Brown, 2003). As demonstrated by Ozerov et al. (2009) and Benetos and Dixon (2013) this decoupling of information is generally not appropriate for non-stationary sounds – for example, one typically cannot express in standard NMF that a certain spectral template for the sustain part of a note is expected a certain time after the attack. Therefore, incorporating ideas presented by Ewert and Sandler (2016), this chapter extends the concept of a dictionary of spectral templates used by Ewert et al. (2016) to a dictionary of variable-length spectro-temporal patterns to better account for the highly non-stationary behaviour of piano sounds. Similar to (Ewert and Sandler, 2016), the corresponding parameter estimation process is guided using specific regularisers instead of explicit Markov constraints (Ozerov et al., 2009; Benetos and Dixon, 2013), which circumvents various issues regarding the computational efficiency and numerical properties associated with the latter, as detailed in (Ewert and Sandler, 2016).

A second weakness of (Ewert et al., 2016) is that the score information is incorporated into the NMF dictionary learning process using hard constraints – if the aligned score specifies that a certain pitch is inactive at a given time, the learning process cannot overrule this information. As a consequence, the energy associated with extra notes must be modelled with templates associated with other pitches, which in certain situations can introduce errors into the learning process. As a countermeasure, this chapter incorporates the score information using soft constraints or regularisers into the learning process, effectively implementing rather a bias than a hard constraint. It can better account for the case of a student locally deviating from the score. As a third extension, this chapter introduces new regularisers in order to guide the learning process more explicitly, taking the typical spectro-temporal progression of piano sounds better into account (Cheng et al., 2015).

5.3 Baseline Method

This section describes the individual steps of the baseline method ((Ewert et al., 2016)). It serves both as the algorithmic framework which will be analysed and extended significantly in Section 5.4, and as a baseline for the experiments in Section 5.5. In the following, the notation and model from (Ewert et al., 2016) are adapted to prepare for the extensions to be introduced.

Step 1: Score-Audio Alignment

The first step is to align a score (given as a MIDI file) to an audio recording of a student playing that score. The alignment provides for each score note, the corresponding time position including onset and offset in the performance. By using the aligned score, the influence of tempo variations on the proposed system is reduced. The alignment method (Ewert et al., 2009b) used here is the same as the baseline method in the previous chapters, with CENS and DLNCO features. Its accuracy is sufficient for the experiments in this work despite the playing errors that are unexpected by the method (for each score note onset, the alignment deviation is 23ms on average). In particular, the next steps do not rely on an exact alignment but include generous temporal tolerances to account for possible local alignment inaccuracies. However, other alignment techniques should be employed to address cases of structural differences (Arzt et al., 2014; Müller and Appelt, 2008; Nakamura et al., 2014) or asynchronies between voices (Wang et al., 2015). This chapter, however, focuses on play-through performances with missing and extra notes, while more advanced scenarios could be explored by using suitable alignment technique in this step.

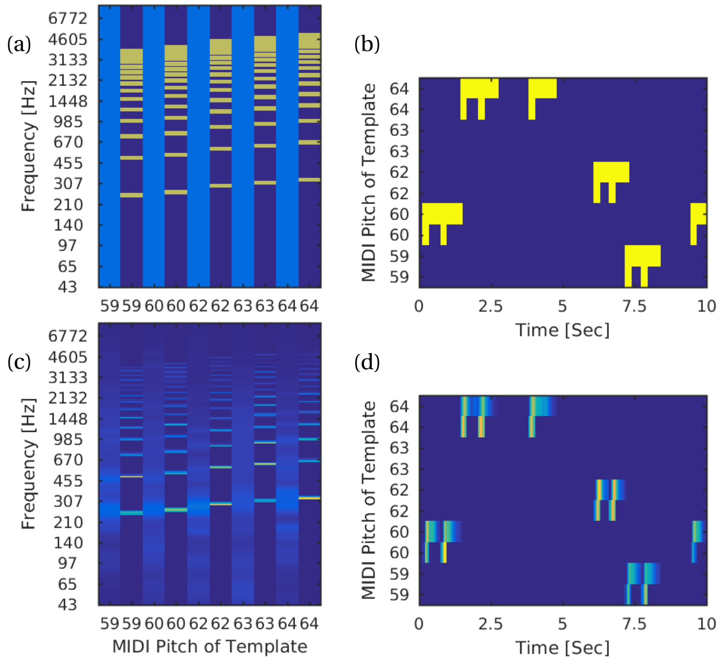

Figure 5.2: Score-Informed Dictionary Learning: Using multiplicative updates in non-negative matrix factorisation, constraints can easily be enforced by setting individual entries to zero (dark blue): (a) Templates and (b) activations after the initialisation; (c) Templates and (d) activations after the optimisation process.

Step 2: Score-Informed Adaptive Dictionary Learning

The above alignment result provides for each score note, information on the expected time position in the audio recording. With this information, this step learns how each note manifests in a time-frequency representation of the audio recording, suitably adapting techniques used in score-informed source separation. In particular, it imposes score-informed constraints on a model based on non-negative matrix factorisation (NMF) to obtain a structured, pitch-based dictionary that is adapted to the specific audio recording and can be used to model the input with high detail, as introduced in Chapter 2. The idea of learning the detailed spectral dictionary from data allows the method to make fewer general assumptions.

Let K be the number of different pitches in the model, and L the number of individual spectral template vectors associated with a single pitch. Further, define $P \in \mathbb{R}_{\geq 0}^{M\times(K\cdot L)}$ as the *spectral dictionary matrix*, where M is the number of frequency bins. Each column in P defines a *(spectral) template* vector. Accordingly, let $A \in \mathbb{R}^{(K\cdot L)\times N}$ be the activity matrix, where N is the number of time frames in the given audio recording. A tensor-like notation is used in the following to access individual elements in P and A in the sense that $P_{m,k,\ell} := P_{m,(k-1)\cdot L+\ell}$. The magnitude spectrogram $V \in \mathbb{R}^{M\times N}$ of a given audio recording is modelled by the product of P and A. As for the general NMF algorithm, the goal is to obtain P and A minimising a distance between V and PA. More precisely, P and A are derived by minimising a cost function $c(P,A)$, which is a weighted sum of a reconstruction error term $d(V||P,A)$, and regulariser terms encouraging a certain structure in the activations $c_i(A)$ and templates $\widetilde{c}_j(P)$,

$$c(P,A) = d(V||P,A) + \sum_i \zeta_i c_i(A) + \sum_j \eta_j \widetilde{c}_j(P), \tag{5.1}$$

where ζ_i and η_j are the weights of the corresponding regulariser terms.

In contrast to the extensions introduced in the next section, the baseline method does make heavy use of regularisers but incorporates the score information as hard constraints into NMF. More precisely, only two spectral templates are allocated to each pitch in the score, one for the attack and one for the sustain part, i.e. $L = 2$ and K is equal to the number of unique pitches in the score. The constraints are implemented by setting corresponding entries in P or A to zero. Due to the use of multiplicative update rules, entries set to zero will remain zero throughout the NMF learning process. This strategy can enforce a harmonic structure in templates associated with the sustain part of a specific pitch as follows: template entries between the positions of its harmonics are set to zero, as here no or little energy is expected (Ewert et al., 2014; Raczynski et al., 2007). Leaving a small non-zero neighbourhood around the expected partial positions enables learning of the exact positions of each partial. The attack templates are initialised with a uniform energy distribution to account for their broadband properties. Fig. 5.2(a) shows an example of such template initialisations.

The activations are constrained by the same strategy using the score information. If a pitch is expected to be inactive in a time segment according to the aligned score, the corresponding activation entries are set to zero, while the remaining entries are initialised with random positive values. As mentioned in the previous section, a generous tolerance of ±0.5s is used for the temporal boundaries of active pitches, in order to account for alignment inaccuracies. To account for a lack of constraints on the attack templates, the corresponding activations are only allowed in a close vicinity around expected onset positions, see Fig. 5.2(b) for an example.

After these initialisations, the commonly used Lee-Seung update rules (Lee and Seung, 2000) are employed to learn the unconstrained areas of the template matrix P and activation matrix A. Until now, the cost function $c(P, A)$ to minimise only contains a reconstruction error term in the form of a generalised Kullback-Leibler divergence:

$$d(V||P, A) = \sum_{m,n} V_{m,n} \log\left(\frac{V_{m,n}}{(PA)_{m,n}}\right) - V_{m,n} + (PA)_{m,n} \tag{5.2}$$

However, experiments showed that using only d, the attack templates sometimes capture too much of the energy associated with the sustain phase, which would interfere with the later note detection process. To discourage peaks in the attack templates, which typically correspond to partials of the sustain part, a spectral continuity regulariser is introduced to encourage smoothness in amplitude along the frequency dimension:

$$\widetilde{c}_1(P) = \sum_k \sum_m \sum_{\ell \in \mathscr{A}} (P_{m,k,\ell} - P_{m-1,k,\ell})^2 \tag{5.3}$$

where $\mathscr{A} \subset \{1, \dots, L\}$ denotes the index set of the attack templates for a pitch. It calculates one form of the total variation in the frequency direction which can be minimised to encourage the energy in the attack templates to be distributed smoothly across the entire frequency range.

Fig. 5.2(c) and (d) shows P and A after convergence. Compared with Fig. 5.2(a) and (b), the unconstrained areas have been refined to reflect the acoustical properties of the recording. Further, the attack templates show the broadband characteristics thanks to the spectral continuity regulariser, while still capturing the non-uniform, pitch dependent energy distribution typical for piano attacks.

Step 3: Dictionary Extrapolation and Residual Modelling

So far the dictionary only learned templates for pitches used in the score. Pitches outside this set cannot properly be represented, which potentially includes extra notes played by the student. Therefore this step extrapolates the learned dictionary to the full piano range, in order to model pitches not used in the score. By employing a time-frequency representation V using a logarithmic frequency scale, the extrapolation can be implemented by a simple shift operation: the template for a pitch not in the score is obtained by shifting

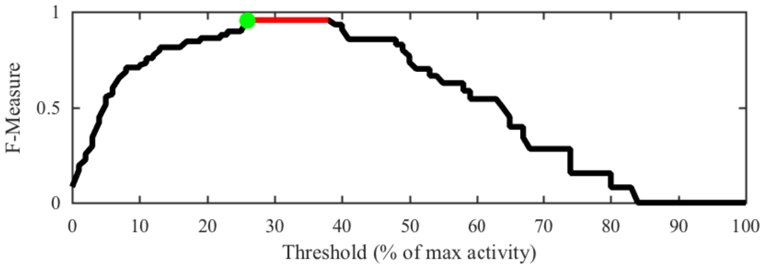

Figure 5.3: Adaptive and pitch-dependent thresholding: The threshold for each pitch is chosen as the smallest one, that can maximise the F-measure obtained by comparing the detected onsets against the aligned nominal score. The red entries show threshold candidates having maximal F-measure for a certain pitch and the green dot is the threshold chosen for this pitch.

the template of the closest pitch used in the score by the number of frequency bins corresponding to the difference between the two pitches. This complete dictionary is then fixed to compute a new and unconstrained activation matrix A for all pitches. A is initialised by adding rows for the newly extrapolated pitches and adding a small value to all entries to remove the zero constraints.

Step 4: Onset Detection Using Score-Informed Adaptive Thresholding

The result of the previous step is an activation matrix for a dictionary highly tuned to model the given input recording. This step uses the score again to adapt the decision process responsible for analysing the activation matrix and detecting onsets. A first idea would be to detect peaks in the activations associated with attack templates of individual pitches. However, while the learned attack templates are indeed pitch-dependent (compare Fig. 5.2(c)), their energy distribution is relatively flat and often leads to confusion about which templates should be active in a given frame. Therefore, this step analyses only the activity for sustain templates. To this end, define $\hat{A} \in R_{\geq 0}^{K \times N}$ via $\hat{A}_{k,n} := A_{k,2,n}$, i.e. a version of A with the activities for attack templates removed.

Next, instead of using a global threshold for all pitches as is commonly done in standard AMT methods, pitch-dependent thresholds are chosen by exploiting the score information again, to distinguish real onsets from spurious activity. In particular, as loudness perception in the human auditory system is frequency dependent and highly complex for non-sinusoidal sounds, a pianist is likely to play each key with a different intensity resulting in different energy levels. Therefore the transcription accuracy benefits directly if detection thresholds can be chosen independently. For each k that is associated with a pitch used in the score, multiple candidates are generated to find a suitable threshold. These candidates are uniformly distributed between 0 and $max_n \hat{A}_{k,n}$. Each candidate is used as a threshold on peak picking to detect onsets and an F-measure is calculated by comparing the detected onsets with the expected onset positions taken from the aligned score (using a temporal tolerance[1] of $T_1 = \pm 0.5$s). Among all candidates, the lowest threshold that maximises this F-measure is chosen, as illustrated in Fig. 5.3. Further, to improve the robustness for pitches with few notes in the score, this F-measure is calculated jointly for several neighbouring pitches. The threshold for a pitch not in the score is interpolated from those for the two closest score pitches, or extrapolated from the closest score pitch if two closest score pitch are both lower than the pitch. This procedure chooses thresholds that produce the best match between the detected onsets and the given score .

Step 5: Score-Informed Onset Classification

With the thresholds chosen in the previous step, a final transcription result is produced for the given recording. To classify the resulting onsets into *correctly played notes*, *missing notes* and *extra played notes*, the last step compares the transcription result with the given score to check for each detected onset whether there is a correspondence with the score (again using a tolerance of T_1 seconds as in the previous step). More precisely, if there is a correspondence between a detected note onset and a note in the score, then the detected note is classified as a correct note, otherwise as an extra note. On the other hand, if there is no correspondence between a score note and any detected onset, then the score note is classified as unplayed. In this case, the onset for the missing note is set using the alignment result, i.e. the onset corresponds to the expected position in the performance. Note that the correspondence is checked by a simple local search, which may lead to mistakes in the classification for cases such as repeated notes or arpeggiated chords. A more sophisticated symbolic alignment method (such as (Nakamura et al., 2014)) may help to avoid such mistakes. Fig. 5.1(c) illustrates a classification result using a different colour for each class.

[1] T_1 is mainly used to account for the alignment inaccuracies and it could be adjusted for different scenarios. For example, T_1 should be increased if the student pulls apart concurrent notes because he/she cannot yet follow the rhythm faithfully.

5.4 Analysis and Extensions

By using the score to adapt the transcription method itself to a given recording, the approach summarised in Section 5.3 considerably improves upon the state of the art (Benetos et al., 2012) in the experiments described in Section. 5.5. However, there are several conceptual weaknesses in the baseline method. This section will identify these weaknesses and design corresponding countermeasures to improve on the performance of the baseline method.

5.4.1 Example of Failure Using the Baseline Method

The baseline method achieved a relatively high level of accuracy, and so this chapter focuses on cases where it failed. The first case is an excerpt from the piece in our dataset, which led to the lowest accuracy in (Ewert et al., 2016). As illustrated in Fig. 5.4(a) and (b), the system is confused by a systematic error in the student's performance. More precisely, misreading the key signature in the score (left of Fig. 5.4(a)), the student replaces all F#3 notes with F3 notes in the performance, as illustrated on the right of Fig. 5.4(a). With no F#3 in the audio, the dictionary learning process fails to learn correct templates for the F#3, instead it learns templates corresponding to the pitch F3. However, since the dictionary interpolation step is not aware of this situation, the inaccurate F#3 templates are shifted to represent the F3 templates as well. The resulting P after dictionary interpolation is shown on the left of Fig. 5.4(b) – the template errors are visible as off-center peaks in the partials of F3 and F#3, circled in yellow. The right of Fig. 5.4(b) shows the activations A obtained using this dictionary. We can clearly see spurious activations for F#3 and missing activations for F3. Further, since the energy associated with the actually played F3 notes is not modelled well using these templates, there are even additional incorrect activations for the E3, which captures some of that residual energy. This systematic error is a worst-case scenario for the dictionary-learning method, as there is no correct data from which the omitted pitch can be learned. Similar situations also arise if a pitch is used only once (or a few times) on the score and the student makes a mistake playing this note (e.g. forgetting to play a very high or low pitched note). To account for this and related problems, several extensions are proposed in the next subsections.

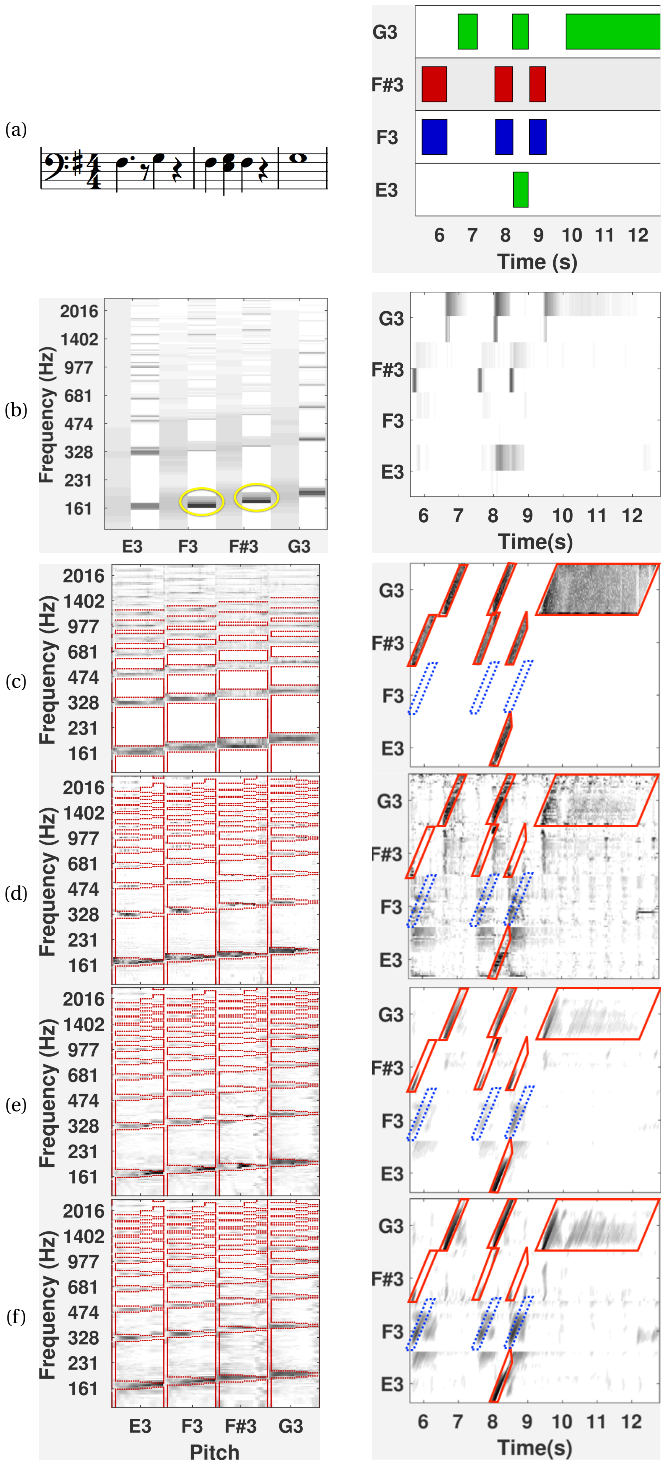

Figure 5.4: A problematic case where the method proposed in Section 5.3 failed while the proposed extensions works correctly. (a) The input score (left) and expected output (right; coloured bar: green - correct notes; red - missing notes; blue - extra notes); (b) The obtained templates (left) and activation (right) matrices by the method in (Ewert et al., 2016) (template errors are circled in yellow). For each pitch, there are two columns in the template matrix and two rows in the activation matrix; (c)-(d): The evolving idea of the proposed method (blue dotted frame on activations: extra notes), see text for details: (c) Extending spectral templates with a hard constraint (red frame on templates); (d) Softening the constraint (red frames on templates and on activations); (e) Encouraging sparsity and temporal continuity structure of the activation matrix; (f) Encouraging energy decay of the template matrix.

5.4.2 From Spectral Templates to Time-Frequency Patterns

The signal model used in Section 5.3 is NMF-based. A unifying aspect of most NMF and sparse coding methods is that time and frequency information are strictly separated. Therefore the NMF-based method proposed in the last section can neither model that a specific template for the sustain part follows an attack template after a certain amount of time, nor that the energy in a note decays in a specific way (Cheng et al., 2015). To adapt the model closer to the acoustic characteristics of piano, the first proposed extension expands the dictionary based on individual templates to a dictionary of time-frequency patterns. In particular, instead of using $L = 2$ templates, L is now set to the average note length in frames.[2] For example, in Fig. 5.4(c)-(f), the pattern length is $L = 29$. With such a drastic increase in the number of parameters, it is unclear whether the learning process will still function correctly. However, the score provides strong guidance to the learning process in the first place, which will be additionally supported by new regularisers defined below.

Similarly to the baseline method, different constraints are applied to the attack and the sustain templates. The first two templates of the extended dictionary are used for the attack, considering the attack part of a piano sound is much shorter than the sustain part. Fig. 5.4(c) shows the zero-based constraints using red frames in P and in A (the blue frames are only informational and indicate where the extra F3 notes are active). Note that the temporal constraints in A now have a diagonal structure to account for the intended spectro-temporal interpretation of each pattern: if the ℓ-th template for a pitch is active in frame n, the $(\ell+1)$-th template should be active in frame $(n+1)$ (given that the note is still active in frame $(n+1)$). The same cost function $c(P, A)$ is used as in Section 5.3, which includes a reconstruction error term $d(V||P, A)$ and a spectral continuity regulariser $\widetilde{c}_1(P)$ on the attack templates. As can be seen from Fig. 5.4(c), the template matrix after the dictionary learning step captures more details compared to the previously proposed method (b). However, due to the hard constraints, there is no activation for the actually played F3 notes. The F#3 notes that are on the score get activated with the result that the F#3 templates learn to represent the pitch F3, as shown by the energy at the bottom of the

[2] Here we try to balance the ability of the model to capture complete notes and the computational complexity. Currently, for notes which are longer than L, their length cannot be correctly modelled. If L is set to a larger value, the longer notes can be modelled with the cost of higher computational complexity. However, as this work focuses on identifying the missing and extra notes, the note length is of low importance, therefore L is set to the average note length to improve the computational efficiency.

first partial of F#3 in Fig. 5.4(c). So, while this new signal model has potential to represent more detail, it does not resolve the above problem.

5.4.3 From Hard to Soft Constraint Regions

A main reason why the dictionary learning in Section 5.4.1 fails is that the templates needed to represent the F3 cannot be activated due to the use of hard constraints (also discussed in a source separation context by Driedger et al. (2013)). Therefore, this subsection proposes another extension to change the hard constraints used in Section 5.4.1 into arbitrarily strong regularisers, which encourage zeros but allow for exceptions if necessary. More precisely, instead of using hard zero-based constraints, this extension applies terms encouraging sparsity (similar to (Virtanen, 2007)) to the score-specified constraint regions:

$$\widetilde{c}_2(P) := \sum_{m,k,\ell} P_{m,k,\ell} \cdot (1 - M^P_{m,k,\ell}) \tag{5.4}$$

$$c_1(A) := \sum_{k,\ell,n} A_{k,\ell,n} \cdot (1 - M^A_{k,\ell,n}) \tag{5.5}$$

where $M^P \in \{0,1\}^{M\times(K\cdot L)}$ and $M^A \in \{0,1\}^{(K\cdot L)\times N}$ denote with ones the unconstrained areas of P and A, respectively, shown by the red frames in Fig. 5.4(d). Further, this extension additionally tapers the constraint region on P for each partial (note the gradually narrowed shape of the red frames), which encourages harmonics to transition from being a little more broadband at the beginning to completely harmonic at the end of the note. $\widetilde{c}_2$ and c_1 are essentially (potentially strong) ℓ_1 regularisers that are selectively applied to the zero-value regions encoded in M^P and M^A, respectively.

Using these soft constraints also allows the merging of the dictionary learning and extrapolation procedures (steps 2 and 3): time-frequency patterns are learned during the dictionary learning step for all pitches. Since the pitches not found in the score typically also will not occur in the performance, it is necessary to apply additional constraints to obtain correct results. The idea here is to couple the time-frequency pattern for a pitch not used in the score with that for the closest pitch found in the score. This way, the pattern for a non-score pitch is constrained to be a shifted version of that for a score pitch. Technically, this is related to shift-invariant dictionary learning (Smaragdis et al., 2008) and more precisely to transformation-invariant NMF (Eggert et al., 2004).

As shown on the left of Fig. 5.4(d), due to these changes, templates for F#3 no longer contain energy associated with the F3 (in P) and are activated less overall (in A). However, the whole activation matrix is not very structured and contains a lot of noise, rendering onset detection quite difficult. Therefore, more regularisers are introduced next to encourage further structure in P and A.

5.4.4 Encouraging Temporal Continuity in A

As mentioned in Section 5.4.2, the temporal constraints in A have a diagonal structure to account for the intended spectro-temporal interpretation of each pattern. To further enhance diagonal structures and discourage vertical and horizontal structures as well as unnecessary fluctuations between neighbouring entries, this subsection introduces the following regulariser term, similar to (Ewert and Sandler, 2016) :

$$c_2(A) = \sum_{k,\ell,n} (A_{k,\ell+1,n+1} - A_{k,\ell,n})^2 \tag{5.6}$$

It can be seen as an anisotropic variant of the the total variation regulariser used in image processing (Chan et al., 2005) and is related to temporal smoothness terms as used in (Virtanen, 2007).

Further, another regulariser on A is introduced to encourage sparseness across all entries, in order to have fewer but stronger diagonals resulting from c_2. Note that c_1 is confined to the constrained regions.

$$c_3(A) = \sum_{k,\ell,n} A_{k,\ell,n} \tag{5.7}$$

As shown in Fig. 5.4 (e), after learning, the activation matrix becomes cleaner compared to (d) and we can see the diagonal structure of three played notes appearing for F3. Note that these three notes are not on the score so they are not able to benefit from the temporal constraints on A. In this case, the temporal continuity regulariser can help them obtain the expected diagonal structure.

However, there is still energy at the F#3 pitch, which was not played. Another problem is that, in the corresponding templates (shown on the left side of (e)), the energy does not decay with time. For example, in the first partial of E3, F3 and F#3, the energy is higher in the last several templates than in the earlier ones, which does not correspond with the true temporal evolution of piano tones.

5.4.5 Encouraging Energy Decay in the Template Matrix

The next regulariser imposes a decay structure onto the spectral templates associated with the sustain phase:

$$\widetilde{c}_3(P) = \sum_k \sum_m \sum_{\ell \in \mathscr{B}} f(P_{m,k,\ell} - P_{m,k,\ell-1}), \tag{5.8}$$

where $\mathscr{B} \subset \{1, \ldots, L\}$ denotes the index set of the sustain templates of the time-frequency pattern of one pitch. $f(\cdot)$ is a function encouraging a smooth decrease in energy while penalising sudden energy increases in the time direction. It is chosen as,

$$f(x) = (\gamma x - 1)e^{(\gamma x - 1)} \tag{5.9}$$

with $\gamma > 0$ being a non-linear parameter, see also Fig. 5.5. Using the differentiable $\widetilde{c}_3$, decreases in energy in the time direction are effectively not penalised, while increases are strongly discouraged. As shown in Fig. 5.4, after learning, individual patterns in P show energy decays in the time direction. With these more accurate patterns, the three played F3 notes are finally active in the activation matrix, while the F#3 notes (not played) are correctly no longer activated.

It should be noted that this regulariser is not intended to model all details of the decay process found in piano sounds. In particular, different partials decay at different rates and thus various decay patterns are possible. Further, the coupling between strings adds another layer of complexity to the decay pattern of a piano note, resulting in beating and other fluctuations in energy that overlay the overall energy decay (Cheng et al., 2016). Instead of modelling these details, the main purpose of this regulariser is to assist in the identification of the main effect, i.e. a strong exponential energy decay. Moreover, because the use of the dictionary of time-frequency patterns, here the decay could be modelled by the templates rather than the activations in contrast to (Cheng et al., 2016), which is easier to be implemented together with other regularisers in this work.

5.4.6 Parameter Estimation

In order to obtain P and A, the parameter estimation step needs to minimise the following cost function,

$$c(P, A) = d(V||P, A) + \zeta_1 c_1(A) + \zeta_2 c_2(A) + \zeta_3 c_3(A) + \eta_1 \widetilde{c}_1(P) + \eta_2 \widetilde{c}_2(P) + \eta_3 \widetilde{c}_3(P). \tag{5.10}$$

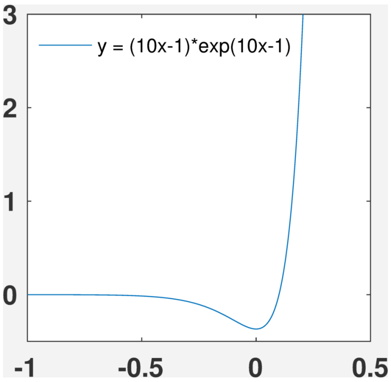

Figure 5.5: Plot of function $f(x) = (\gamma x - 1)e^{(\gamma x - 1)}$ for $\gamma = 10$.

A similar multiplicative updating strategy to (Virtanen, 2007) is applied to alternately update P and A until convergence. The gradients of terms in the cost function with respect to A are given by:

$$\nabla^A d(V||P,A) = P^\mathsf{T} 1 - P^\mathsf{T} \frac{V}{PA}, \tag{5.11}$$

$$\nabla^A c_1(A) = 1 - M_A, \tag{5.12}$$

$$[\nabla^A c_2(A)]_{k,\ell,n} = 4A_{k,\ell,n} - 2A_{k,\ell-1,n-1} - 2A_{k,\ell+1,n+1}, \tag{5.13}$$

$$\nabla^A c_3(A) = 1. \tag{5.14}$$

The gradient of the cost function is written as the difference between element-wise positive terms and negative terms:

$$[\nabla^A c(P,A)]_{k,\ell,n} = [\nabla^A c^+(P,A)]_{k,\ell,n} - [\nabla^A c^-(P,A)]_{k,\ell,n}, \tag{5.15}$$

$$[\nabla^A c^+(P,A)]_{k,\ell,n} = \sum_m P_{m,k,\ell} + \zeta_1 + 4\zeta_2 A_{k,\ell,n} + \zeta_3, \tag{5.16}$$

$$[\nabla^A c^-(P,A)]_{k,\ell,n} = \sum_m P_{m,k,\ell} \frac{V_{m,n}}{(PA)_{m,n}} + \zeta_1 (M_A)_{k,\ell,n} + 2\zeta_2 (A_{k,\ell-1,n-1} + A_{k,\ell+1,n+1}). \tag{5.17}$$

The update rule for A is given by:

$$A_{k,\ell,n} \leftarrow A_{k,\ell,n} \cdot \frac{[\nabla^A c^-(P,A)]_{k,\ell,n}}{[\nabla^A c^+(P,A)]_{k,\ell,n}}. \tag{5.18}$$

Similarly, the gradient of the cost function with regard to P can be split as:

$$\begin{aligned}[\nabla^P c^+(P,A)]_{m,k,\ell} = & \sum_n A_{k,\ell,n} + \mathscr{I}_{\mathscr{A}}(\ell) 4\eta_1 P_{m,k,\ell} + \eta_2 \\ & + \mathscr{I}_{\mathscr{B}}(\ell)\eta_3\gamma^2 \big(P_{m,k,\ell} e^{\gamma(P_{m,k,\ell} - P_{m,k,\ell-1}) - 1} + P_{m,k,\ell} e^{\gamma(P_{m,k,\ell+1} - P_{m,k,\ell}) - 1}\big)\end{aligned} \tag{5.19}$$

$$[\nabla^P c^-(P,A)]_{m,k,\ell} = \sum_n A_{k,\ell,n}\frac{V_{m,n}}{(PA)_{m,n}} + \mathscr{I}_{\mathscr{A}}(\ell)2\eta_1 P_{m+1,k,\ell} + \mathscr{I}_{\mathscr{A}}(\ell)2\eta_1 P_{m-1,k,\ell} + \eta_2(M_P)_{m,k,\ell}$$
$$+\mathscr{I}_{\mathscr{B}}(\ell)\eta_3\gamma^2\big(P_{m,k,\ell-1}e^{\gamma(P_{m,k,\ell}-P_{m,k,\ell-1})-1} + P_{m,k,\ell+1}e^{\gamma(P_{m,k,\ell+1}-P_{m,k,\ell})-1}\big) \quad (5.20)$$

where $\mathscr{I}_{\mathscr{A}}$ and $\mathscr{I}_{\mathscr{B}}$ are the indicator functions for $\mathscr{A}$ and $\mathscr{B}$, respectively. The update rule for P is given by

$$P_{m,k,\ell} \leftarrow P_{m,k,\ell} \cdot \frac{[\nabla^P c^-(P,A)]_{m,k,\ell}}{[\nabla^P c^+(P,A)]_{m,k,\ell}}. \quad (5.21)$$

As mentioned in Section 5.4.3, each non-score pitch uses the shifted version of the templates for the closest score pitch. While this is not problematic for the update of A (by actually creating a shifted copy), the update for P needs to be adapted as the shifted and unshifted versions need to be coupled, i.e. have to be updated jointly. Fortunately, the gradients given above for score and non-score pitches can easily be merged and thus be used to create a joint update, see (Eggert et al., 2004) for details.

Once the activation matrix A is obtained, the same strategy as in Section 5.3 is used for onset detection and note classification. The only difference is that, to get $\hat{A_{k,n}}$ for onset detection, all activation values associated with pitch k in frame n are summed together, i.e., $\hat{A_{k,n}} = \sum_\ell A_{k,\ell,n}$. It is because the activations resulting from the spectro-temporal dictionary are more discriminative for the attack part compared to the baseline method and it is useful to include the attack part in $\hat{A}$ as well.

5.5 Experiments

This section reports experiments conducted to investigate the influence of different extensions on the baseline method, as well as evaluate the performance of the method with and without these extensions.

5.5.1 Dataset & Evaluation Measure

5.5.1.1 Dataset

Table 5.1 shows the dataset of seven pieces used for the evaluation, which are selected from the Associated Board of the Royal Schools of Music 2011/12 syllabus for grades 1 and 2. The dataset is originally introduced by Benetos et al. (2012) and the pieces were played on a Yamaha U3 Disklavier with intentional mistakes compared to the original score. In

Table 5.1: Pieces for evaluation

ID	Composer	Title
1	Josef Haydn	Symphony No. 94: Andante (Hob I:94-02)
2	James Hook	Gavotta (Op. 81 No. 3)
3	Pauline Hall	Tarantella
4	Felix Swinstead	A Tender Flower
5	Johann Krieger	Sechs musicalische Partien: Bourrée
6	Johannes Brahms	The Sandman (WoO 31 No. 4)
7	Tim Richards (arr.)	Down by the Riverside

total, there are 1600 correctly played notes, 111 missing notes and 116 extra notes. For each piece, there is one audio recording, one MIDI file of the original score, and three MIDI files annotating the correctly played, missing and extra notes. These annotations were reviewed and corrected manually by listening to the corresponding audio recordings before the experiments described below. The corrected annotations are available online[3].

5.5.1.2 Audio Input

The audio data has a sampling rate of 44100 samples per second. It was converted to a spectrogram using a Hann window, with a window size of 4096 and 50% overlap. Using a weighted sum, the spectrogram is converted to a log-frequency scale using a resolution of 36 bins per octave.

5.5.1.3 Evaluation Measure

To evaluate a method, four performance metrics are calculated, Precision, Recall, F-Measure and Accuracy, as used in the MIREX evaluation campaign (Downie, 2008) – however, separately for each class of notes. To this end, the annotation MIDI files provide for the correctly played and extra notes the onset positions in the performance. For each missing note, the corresponding MIDI file provides an onset position indicating where that note would have been expected in the performance. By comparing the onset positions obtained by a method and those annotated in the ground truth, the performance metrics can be obtained separately for each class of notes. A temporal tolerance of $T_2 = \pm 0.2$s is used to account for the local alignment difficulties caused by playing errors.

[3] https://code.soundsoftware.ac.uk/projects/score-informed-piano-transcription-dataset

5.5.2 Influence of Individual Parameters

To indicate the influence of different terms in the cost function, six groups of experiments are conducted for the six regularisers used in the proposed method. In each group, one parameter is changed with all others fixed.

5.5.2.1 Soft Mask-Constraint Regulariser on Activation Matrix

The influence of the parameter ζ_1 is illustrated in Fig. 5.6(a). The weight controls c_1 which corresponds to a soft mask-constraint on A. The best results are obtained for $\zeta_1 = 10^{-3.5}$. The average accuracy for all three note classes declines if the activity constraint becomes too strong, i.e. if activity outside the expected positions is heavily penalised and thus extra notes cannot be modelled anymore.

5.5.2.2 Diagonal Structure Regulariser on Activation Matrix

Fig. 5.6 (b) shows a plot of the average accuracy against different values for the weight ζ_2, which is associated with the diagonal structure regulariser c_2. The average accuracy of correctly played and missing notes only changes slightly for $\zeta_2 \in [0, 10^{-1}]$. On the contrary, the average accuracy for extra notes grows considerably with ζ_2, peaking at $\zeta_2 = 10^{-1}$. The overall best results are obtained for $\zeta_2 = 10^{-1}$. These results seem to indicate that the score information alone might not be enough to guide the learning process in such a way that a physically correct diagonal structure occurs in the activations and that this regulariser is indeed needed.

5.5.2.3 Sparsity Regulariser on Activation Matrix

The influence of parameter ζ_3, which balances the sparsity regulariser on the activation matrix, is shown in Fig. 5.6 (c). The overall best results are obtained for $\zeta_3 = 0.1$. While the change of ζ_3 only leads to small fluctuations in the accuracy of identifying missing notes, it has a larger impact on identifying extra notes. A possible reason is that, when ζ_3 is too small, the activation matrix is too noisy for detecting extra notes and when ζ_3 is too large, the activations for extra notes are being heavily suppressed. In both cases, the signal-to-noise ratio for extra notes is low.

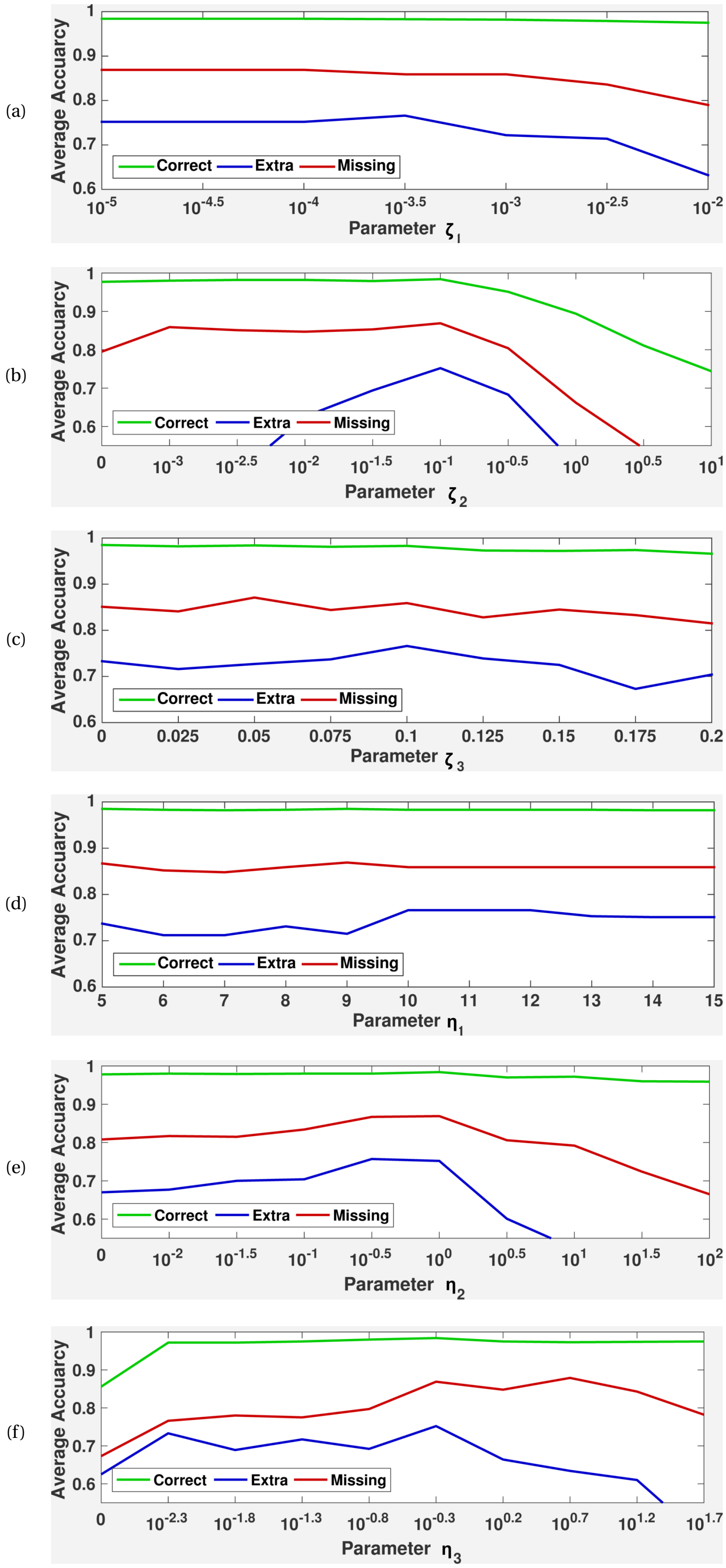

Figure 5.6: Average accuracy as a function of different parameters. (a) activation constraint ζ_1; (b) diagonal structure regulariser ζ_2; (c) activation sparsity regulariser ζ_3; (d) spectral continuity regulariser; (e) template constraint η_2; (f) decay regulariser η_3

5.5.2.4 Spectral Continuity Regulariser on Template Matrix

Fig. 5.6 (d) shows the influence of parameter η_1, which controls the spectral continuity regulariser on the template matrix. The change of η_1 has little impact on identifying correct and missing notes, while the highest accuracy of identifying extra notes is obtained for $\eta_1 = 10$.

5.5.2.5 Soft Mask-Constraint Regulariser on Template Matrix

Fig. 5.6 (e) shows the average accuracy for different values of the parameter η_2, i.e. the weight balancing the importance of the term $\widetilde{c}_2$ which implements a soft mask-constraint on P (see Section 5.4.3). The average accuracy of identifying extra and missing notes increases with η_2 and peaks at $\eta_2 = 1$, while the average accuracy for correctly played notes remains steady. If η_2 is increased beyond this point, similar to the template constraint term, the accuracy for all three note classes drops, especially for the extra and missing note classes.

5.5.2.6 Decay Structure Regulariser on Template Matrix

The influence of the parameter η_3, which balances the importance of the decay structure regulariser $\widetilde{c}_3$, is illustrated in Fig. 5.6 (f). The average accuracy for the correctly played note class remains relatively static after a short increase. The average accuracies for missing and extra notes show an upwards trend with η_3 first, followed by a decrease for the extra notes with $\eta_3 > 10^{-0.3}$ and a slight decrease for the missing notes with $\eta_3 > 10^{0.7}$. The overall best results are obtained for $\eta_3 = 10^{-0.3}$, which seems to represent a reasonable trade-off between model capacity and learning stability.

5.5.2.7 Discussion

Overall, varying the parameters has the least influence on the class of correctly played notes and the largest influence on the extra notes. This is not really surprising as the score provides strong information about the correctly played notes and thus the regularisers are not required to provide additional help. For unexpected events, such as extra notes, however, the regularisers are of much higher importance.

One surprising observation is that the influence of the mask-constraint c_1 on A is not more pronounced in the results, as it essentially carries much of the temporal information provided by the score. Indeed, using a low value for ζ_1 more noise was observed in A and yet the results do not differ much. Several aspects are important to explain this behaviour. First, even with a low value for ζ_1, the score information is still used to initialise A – which already adds a strong bias for the final result (note that, from an optimisation point of view, NMF is a bi-convex problem and as such the error surface contains various local minima). A second important aspect is the adaptive thresholding, which is part of the onset detection. While c_1 incorporates the note information as a soft constraint, the adaptive thresholding as described in Section 5.3 employs the same information in a more binary form. In particular, the adaptive method takes the noise level in A into account when choosing a threshold. Therefore, the stability of our method with respect to ζ_1 can partially be attributed to the quality of the adaptive thresholding and its noise insensitivity. For more complex pieces beyond the beginner level (i.e. intermediate levels and beyond), however, the noise level may have a stronger impact on the results – such scenarios, however, were not within the scope of this thesis. However, with additional data, this might be an interesting direction for future investigation.

With six regularisers in total, the optimisation of the joint parameter space is not trivial as parameters might influence each other. Even using only five different settings for each parameter leads to $5^6 = 15625$ different configurations in a grid search. To test each configuration on all the pieces will take around 50 seconds, which will be summed up to 9 days. However, assuming that most dependencies are already observable in pairs of parameters (i.e. in contrast to dependencies that only occur comparing two groups of parameters jointly), the search space can be decreased drastically. In particular, with six parameters there are only $\binom{6}{2} = 15$ different combinations. Testing five different values per parameter leads to 25 configurations to be tested for each combination and thus to a total of 375 configurations and corresponding evaluations on the whole dataset, which will take around 5 hours.

Overall, interaction effects were not found between most parameters, which justifies optimising them individually. However, a somewhat complex interaction was shown between the template mask-constraint parameter η_2 and the diagonal structure parameter

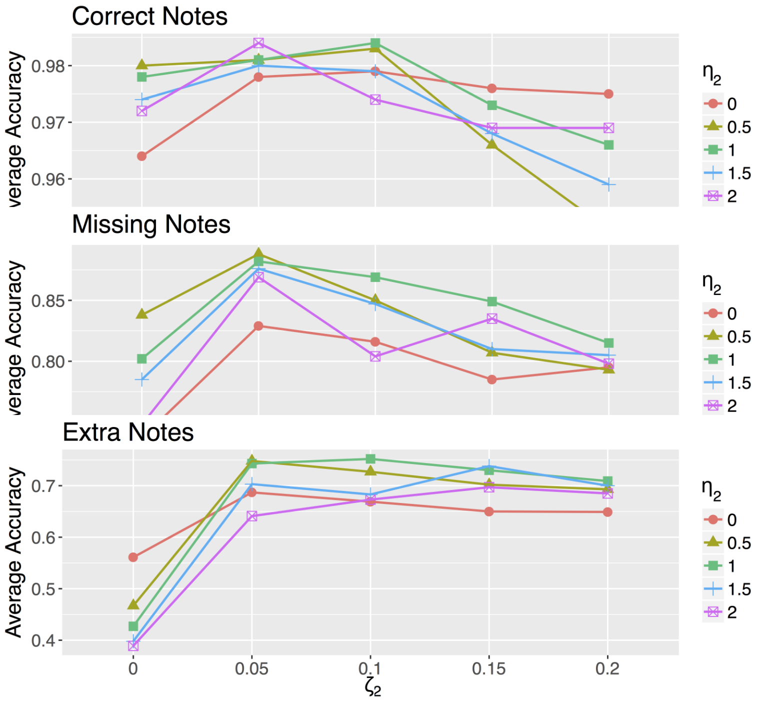

Figure 5.7: Interaction between parameters ζ_2 and η_2 as they influence identification accuracy for all three types of notes.

ζ_2. Fig. 5.7 shows various plots illustrating the performance of the proposed method for several combinations of the two parameters – plotted separately for the three note classes. If there would be no interaction, the plots would not cross. However, the interaction is observed in particular for higher values of η_2. For example, for extra notes, when the value of η_2 is high, the accuracy improves with higher values of ζ_2. When the value of η_2 is low, the opposite happens. While this interaction might just be a property of our dataset and its size, it might also be explained by the fact that a strong η_2 leads to stronger constraints on P, which might not always be appropriate. A stronger value for ζ_2 might make sure in this case that “unexplained" residual energy (resulting from enforcing incorrect constraints) is suppressed in A by other means and thus does not lead to wrong detections.

5.5.3 Comparison Between the Baseline Method and Extended Method

This subsection compares the performance of the baseline method with the extended method. The parameters for the extensions are set to a configuration found to perform

Table 5.2: Average Evaluation Results of three Methods for Correctly Played Notes(C), Extra Notes (E) and Missing Notes (M)

Method	Class	Prec.	Recall	F-Meas.	Accur.
Extended	C	0.996	0.989	0.992	0.984
	E	0.876	0.840	0.849	0.752
	M	0.895	0.980	0.932	0.869
Baseline	C	0.994	0.991	0.993	0.986
	E	0.814	0.750	0.770	0.640
	M	0.928	0.970	0.945	0.899
Benetos et al. (2012)	C	-	-	-	0.932
	E	-	-	-	0.605
	M	-	-	-	0.492

well as described above: $\zeta_1 = 10^{-3.5}, \zeta_2 = 0.1, \zeta_3 = 0.1, \eta_1 = 10, \eta_2 = 1, \eta_3 = 0.5$.

The average evaluation results of all seven pieces are shown in Table 5.2. In particular, the reported F-measure is an average over the individual F-measure values, rather than computed from the average precision and recall given in Table 5.2. Table 5.2 also includes the average accuracy of the method proposed by Benetos et al. (2012) as a reference, however, note that the evaluation for other two proposed methods uses a slightly modified ground truth as mentioned in 5.5.1.

For the correctly played notes (C), the extended method and baseline method have similar performances on all four evaluation measures. The extended method outperforms the baseline method for the extra note class (E), on all the measures. For example, the average accuracy improves by 17%, from 0.640 to 0.752. As for the missing note class (M), the extended method is slightly worse (by 2%) than the baseline method but still at a similar level, comparing 0.869 with 0.899. Note that the amounts of missing notes and extras notes are similar (see Section 5.5.1).

5.6 Conclusion

This chapter extended a score-informed transcription method to identify missing and extra notes in piano recordings. By incorporating score information into the dictionary learning process, the baseline method yields spectral patterns for each pitch closely adapted to the given recording. To better account for the specific characteristics of piano sounds and local deviations of the performance from the score, this chapter introduced several extensions to the baseline method. As demonstrated by experiments with a dataset of pieces for piano beginners, the extensions improve the accuracy in identifying extra notes over the baseline method.

One issue that could be addressed in future work is the lack of data. Informally, experiments showed that the proposed method performed differently depending on the amount and the type of deviation the performance has from the given score. It would be interesting to create a new dataset to test the proposed method across a variety of scenarios. For example, in performance analysis, the number of playing mistakes can be expected to be less compared to a music tutoring application, while deviations due to musical interpretation might increase. Further, since the alignment method in use was not designed to deal with local changes in the order of notes, such as broken or arpeggiated chords, the score constraints might provide incorrect information to the transcription process in such scenarios. Similarly, in the music tutoring application, an extremely large number of errors might occur in some cases, which might lead to the alignment getting lost and thus corrupting the transcription result. Therefore, future work could investigate strategies to adapt the score information better to different application scenarios.

Another issue for future work is the computational complexity. Since the dictionary is extended to L templates for each pitch (compared to two templates in the baseline method), the computational cost for the dictionary learning step is $L/2$ times higher. For example, for an recording of around 1 min in the experiment dataset, the computing time of the proposed method is around 1 min, comparing to 7 seconds of the baseline method. For a music tutoring system, there might be constraints on the run-time and thus it will be beneficial to investigate strategies to lower the computational cost without affecting the overall accuracy of the system.

CHAPTER 6

CONCLUSION

This thesis proposed several novel computational methods in the context of music alignment and score-informed transcription. Two music alignment methods were presented in Chapters 3 and 4, focusing on improving the robustness against local differences between the versions to be aligned. Chapter 5 presented a score-informed transcription method that applies score to performance alignment to exploit score information in the learning process of a dictionary-based transcription method. In the following, Section 6.1 summarises the main achievements of this thesis and Section 6.2 discusses some possible future directions.

6.1 Summary of Contributions

Despite the fact that the accuracy of music alignment methods has improved considerably in the last decade, the task of music alignment remains challenging, such as in the cases where there are substantial local differences between versions. This thesis proposed methods aiming to improve the alignment robustness for two scenarios. By applying an accurate and robust alignment method, this thesis also presented a score-informed transcription method.

Most state-of-the-art methods employ pairwise alignment approaches and yield high accuracy in many cases. However, they may fail when strong local differences occur between two versions. In contrast, the work presented in Chapter 3 exploits the fact that there are often multiple versions of the piece of music available, and aligning them jointly can stabilise the system with additional information of how one section might be interpreted or which acoustic conditions may arise. Two such joint alignment methods were proposed, Progressive Alignment and Profile HMM. They were both inspired by the multiple sequence alignment task in bio-informatics, but specifically adapted to take the characteristics of music signals into account. Experiments with 376 recordings from 9 classical piano pieces showed that the two proposed methods not only decrease the overall standard deviation of the alignment error, but also improve the average alignment accuracy. These results indicate that the proposed methods are particularly useful to effectively reduce large alignment errors, i.e. to increase the overall alignment robustness. The two proposed methods are conceptually different but share some algorithmic similarities. Systematic experiments were performed to further understand their behaviour. They showed that while both methods can improve the alignment robustness if a large number of versions are available, Progressive Alignment outperforms state-of-the-art pairwise alignment methods even with a small set of versions (three or more).

Chapter 4 focused on improving alignment robustness in the presence of a particular musical parameter: asychronies between musical voices. Most current alignment methods have made the simplifying assumption that simultaneous notes in the score are also played concurrently in a performance. Musicians, however, sometimes incorporate asynchronies between voices for expressive reasons. In such cases, the alignment accuracy of current methods may drop measurably on a local level. To handle such asychronies between the melody and the accompaniment, Chapter 4 presented a novel method which firstly separates a score into two voices, then jointly aligns them and the audio stream with a three-dimensional Dynamic Time Warping algorithm. To avoid a loss of accuracy caused by splitting the score information into two separate voices and to lower the computational costs, two constraints were introduced in computing the three dimensional cost matrix. The first one limits the amount of allowed asynchrony based on the fact that the asynchronies in practice are not arbitrarily high. The second constraint is based on a projection of an alignment path obtained by a standard two dimensional method to the three dimensional cost matrix. This way, the alignment path is forced to run close to the projected path, providing improved robustness and a reduced computational complexity. Experiments with three piano pieces by Chopin (with relatively strong asynchronies) and three pieces from Bach's Well-Tempered Clavier (with little asynchrony) showed that the proposed method improves the alignment accuracy for the pieces with strong asynchronies and preserves the alignment accuracy for those without.

By establishing links between different representations of the same piece of music, alignment techniques enable various applications. One of them is to improve the accuracy of automatic music transcription by exploiting the score as prior knowledge, available in certain scenarios such as music tutoring. After aligning the score to the given audio recording, the idea is to build a score-informed dictionary learning process, yielding for each pitch a spectral pattern closely adapted to the given recording. This way, a transcription method is tailored to identify the missing and extra notes from the given audio recording compared to the score. Chapter 5 presented such a score-informed transcription system which extends the state-of-the-art approach (Ewert et al., 2016) to better account for the properties of piano sounds and the possible deviations of the performance from the score. Experiments with a dataset of pieces for piano beginners showed that the proposed method considerably improves the accuracy in identifying extra notes.

6.2 Future Directions

This section suggests several possible directions to extend or apply the work described in this thesis.

Handling structural differences in joint alignment methods

The work presented in this thesis has not dealt with alignment in the case of structural differences between performances. However, preliminary experiments have been performed using the Progressive Alignment method proposed in Chapter 3 to align a set of performances, including recordings with structural differences compared to the others. Despite such structural differences, the method correctly aligned corresponding positions. If the previously aligned template contains a certain section that the new performance to be aligned skips, the method inserts the corresponding gap symbols when the performance is incorporated into the template. If the new performance contains an inserted section, then the method opens the corresponding gaps in the template. However, if the inserted section is a repeat, the method is currently unable to identify the section as such and thus cannot align the repeated section correctly. To do so, a suitable repetitive structure extraction method could be applied; see (Paulus et al., 2010) for an overview.

Annotation transfer with joint alignment of multiple performances

The joint alignment methods proposed in Chapter 3 can be applied to transfer annotations created for one performance to other versions. For instance, if one performance is annotated with beat positions, the joint alignment method can be used to map the annotations to other performances of the same piece, instead of aligning all versions to the annotated version using pairwise alignment. Aligning multiple versions simultaneously by the joint alignment method can avoid the inconsistencies between different pairwise alignments.

Handling asynchrony between different instruments

The work presented in Chapter 4 is concerned with the asynchrony between voices in piano performances. This idea, however, can be extended to deal with scenarios with asynchronies between instruments, such as in music ensembles, or asynchronies between the human voice and the accompaniment in a karaoke setting.

Improving the score MIDI to performance MIDI alignment tool

To create the ground truth for experiments in Chapter 4, a graphical user interface was developed in Matlab for manually correcting results of an automatic alignment between a score and a performance MIDI file. It can read a score in MusicXML or MIDI format. If a MusicXML version is available, the tool converts it to MIDI to perform the alignment, and exploits the coordination information contained in the MusicXML to link each score note to its corresponding score image location. This way, the tool can provide the appropriate score excerpt as a reference for manual correction of the alignment.

Currently, the tool has several weaknesses that could be addressed. Firstly, the automatic alignment based on a simple LCS method could be improved. The method could be replaced by a more sophisticated approach to reduce the amount of manual work needed. Secondly, the tool could be implemented in a more suitable programming language rather than Matlab. When dealing with long pieces of music, the current Matlab-based interface has a slow response time.

Score-informed transcription of other instruments

The score-informed transcription system in Chapter 5 is specifically for piano recordings. The idea, however, can be extended to other instruments, while taking their specific characteristics into account. For example, for transcribing string instruments, variability in the fundamental frequency could be captured by shift-invariant dictionary learning. With the score as prior information, it is possible to learn instrument-specific dictionaries because the expected time and pitch of instrumental activity is available for each instrument.

Score-informed performance analysis

The score-informed transcription system has the potential to be a basis for various performance analysis tasks, as deviations of the performance from the score can be detected. For the music tutoring application described in Chapter 5, the expected deviation is limited to missing and extra notes. However, in the case of more advanced performances, deviations might be the result of deliberate playing techniques. Such scenarios would require a more fine-grained note-level alignment.

6.3 Closing Remarks

Music alignment, one of the fundamental steps of digital music analysis, modelling and processing, has been actively researched in the last decades. Various methods have been proposed and the state-of-the-art performance has already achieved high accuracy in many cases. However, the robustness of current alignment methods may be challenged by the variation of music expression and acoustic conditions. The work of this thesis made efforts to improve robustness in two specific scenarios. The author hopes this thesis will inspires further research in the direction of building alignment methods that are robust to a wide range of scenarios.

An accurate and robust alignment can establish links between different versions of music, so as to enhance the experience of people interacting with music in real life applications. For example, Arzt et al. (2015) used automatic score following in a live concert, where multiple performances were aligned to the score in parallel to provide additional information to improve the alignment robustness (a similar idea as Chapter 3). Music alignment can also assist performance analysis; for example, manual score to performance alignment has been used in an online course about Haydn's Op.20 No.5 string quartet[1]. Meanwhile, there are quite a few commercial applications employ music alignment algorithms for concert enhancement[2] and piano learning assistance[3,4]. For piano learning assistance apps[3,4], the current use of music alignment is to provide score following functionality for practice and performance analysis based on comparison with expert pianists. For evaluating the student's performance in the aspect of reproducing the score faithfully, the piano learning assistance app (melomemo)[4] requires wearable sensors or a camera to capture the playing mistakes. The author believes the idea explored in Chapter 5, which employs music alignment to build a score-informed transcription system for identifying missing and extra notes from audio recordings has potential to benefit such music tutoring applications. However, the work in this thesis is just an early step; the author hopes it will inspire further research toward a mature system for identifying performance deviations from the score.

[1] https://lagunita.stanford.edu/courses/course-v1:HumanitiesSciences+StringQuartet1+selfpaced/info

[2] https://www.philorch.org/concert/livenote#

[3] http://tido-music.com/

[4] http://www.raintai.com/index.html

REFERENCES

J. Abeßer, K. Frieler, E. Cano, M. Pfleiderer, and W.-G. Zaddach. Score-Informed Analysis of Tuning, Intonation, Pitch Modulation, and Dynamics in Jazz Solos. *IEEE/ACM Transactions on Audio, Speech, and Language Processing*, 25(1):168–177, 2017.

A. Arzt and G. Widmer. Real-time Music Tracking using Multiple Performances as a Reference. In *Proceedings of the 16th International Society for Music Information Retrieval Conference (ISMIR)*, pages 357–363, Málaga, Spain, 2015.

A. Arzt, G. Widmer, and S. Dixon. Automatic Page Turning for Musicians via Real-Time Machine Listening. In *Proceedings of the European Conference on Artificial Intelligence (ECAI)*, pages 241–245, Patras, Greece, 2008.

A. Arzt, S. Böck, S. Flossmann, H. Frostel, M. Gasser, and G. Widmer. The Complete Classical Music Companion v0.9. In *Proceedings of the AES International Conference on Semantic Audio*, pages 133–137, London, UK, 18–20 2014.

A. Arzt, H. Frostel, T. Gadermaier, M. Gasser, M. Grachten, and G. Widmer. Artificial Intelligence in the Concertgebouw. In *Proceedings of the 24th International Joint Conference on Artificial Intelligence (IJCAI)*, pages 2424–2430, 2015.

D. Başaran, A. T. Cemgil, and E. AnarÎźm. A Probabilistic Model-Based Approach for Aligning Multiple Audio Sequences. *IEEE/ACM Transactions on Audio, Speech and Language Processing*, 23(7):1160–1171, 2015.

M. A. Bartsch and G. H. Wakefield. To Catch a Chorus: Using Chroma-based Representations for Audio Thumbnailing. In *Proceedings of the IEEE Workshop on Applications of Signal Processing to Audio and Acoustics (WASPAA)*, pages 15–18, New Paltz, NY, USA, 2001.

M. A. Bartsch and G. H. Wakefield. Audio Thumbnailing of Popular Music Using Chroma-based Representations. *IEEE Transactions on Multimedia*, 7(1):96–104, 2005.

J. P. Bello and J. Pickens. A Robust Mid-level Representation for Harmonic Content in Music Signals. In *Proceedings of the 6th International Conference on Music Information Retrieval (ISMIR)*, pages 304–311, London, UK, 2005.

J. P. Bello Correa. *Towards the Automated Analysis of Simple Polyphonic Music: A Knowledge-based Approach*. PhD thesis, University of London, 2003.

E. Benetos and S. Dixon. A Shift-Invariant Latent Variable Model for Automatic Music Transcription. *Computer Music Journal*, 36(4):81–94, 2012.

E. Benetos and S. Dixon. Multiple-Instrument Polyphonic Music Transcription using a Temporally Constrained Shift-Invariant Model. *Journal of the Acoustical Society of America*, 133(3):1727–1741, 2013.

E. Benetos, A. Klapuri, and S. Dixon. Score-Informed Transcription for Automatic Piano Tutoring. In *Proceedings of the 20th European Signal Processing Conference (EUSIPCO)*, pages 2153–2157, Bucharest, Romania, 2012.

E. Benetos, S. Dixon, D. Giannoulis, H. Kirchhoff, and A. Klapuri. Automatic Music Transcription: Challenges and Future Directions. *Journal of Intelligent Information Systems*, 41(3):407–434, 2013.

S. Bengio. An Asynchronous Hidden Markov Model for Audio-Visual Speech Recognition. In *Advances in Neural Information Processing Systems 15 (NIPS)*, pages 1213–1220, Montréal, Canada, 2002.

M. G. Bergomi. *Dynamical and Topological Tools for (Modern) Music Analysis*. PhD thesis, Université Pierre et Marie Curie (Paris 6), 2015.

N. Bertin, R. Badeau, and E. Vincent. Enforcing Harmonicity and Smoothness in Bayesian Non-negative Matrix Factorization Applied to Polyphonic Music Transcription. *IEEE Transactions on Audio, Speech, and Language Processing*, 18(3):538–549, 2010.

S. Böck and M. Schedl. Polyphonic Piano Note Transcription with Recurrent Neural Networks. In *Proceedings of the IEEE International Conference on Acoustics, Speech and Signal Processing (ICASSP)*, pages 121–124, Kyoto, Japan, 2012.

M. A. Casey, R. Veltkamp, M. Goto, M. Leman, C. Rhodes, and M. Slaney. Content-based Music Information Retrieval: Current Directions and Future Challenges. *Proceedings of the IEEE*, 96(4):668–696, 2008.

W. Chai. Semantic Segmentation and Summarization of Music: Methods Based on Tonality and Recurrent Structure. *IEEE Signal Processing Magazine*, 23(2):124–132, 2006.

T. Chan, S. Esedoglu, F. Park, and A. Yip. Recent Developments in Total Variation Image Restoration. *Mathematical Models of Computer Vision*, 17, 2005.

T.-S. Chan, T.-C. Yeh, Z.-C. Fan, H.-W. Chen, L. Su, Y.-H. Yang, and R. Jang. Vocal Activity Informed Singing Voice Separation with the iKala Dataset. In *Proceedings of the IEEE International Conference on Acoustics, Speech and Signal Processing (ICASSP)*, pages 718–722, Brisbane, Australia, 2015.

N. P. Chapman and J. Chapman. *Digital Multimedia*. John Wiley & Sons, Inc., 2000.

C.-T. Chen, J.-S. R. Jang, and W. Liou. Improved Score-Performance Alignment Algorithms on Polyphonic Music. In *Proceedings of the IEEE International Conference on Acoustics, Speech and Signal Processing (ICASSP)*, pages 1365–1369, Florence, Italy, 2014. IEEE.

T. Cheng, S. Dixon, and M. Mauch. Modelling the Decay of Piano Sounds. In *Proceedings of the IEEE International Conference on Acoustics, Speech, and Signal Processing (ICASSP)*, pages 594–598, Brisbane, Australia, 2015.

T. Cheng, M. Mauch, E. Benetos, and S. Dixon. An Attack/Decay Model for Piano Transcription. In *Proceedings of the 17th International Society for Music Information Retrieval Conference (ISMIR)*, New York City, NY, USA, 2016.

E. Chew and X. Wu. Separating Voices in Polyphonic Music: A Contig Mapping Approach. In *Computer Music Modelling and Retrieval (CMMR)*, pages 1–20, Pisa, Italy, 2005.

T. Cho, R. J. Weiss, and J. P. Bello. Exploring Common Variations in State of the Art Chord Recognition Systems. In *Proceedings of the Sound and Music Computing Conference (SMC)*, pages 1–8, Barcelona, Spain, 2010.

M. G. Christensen and A. Jakobsson. *Multi-Pitch Estimation*. Synthesis Lectures on Speech and Audio Processing, Morgan and Claypool Publishers, 2009.

E. Clarke. Expression in Performance: Generativity, Perception and serniosis. In J. Rink, editor, *The Practice of Performance: Studies in Musical Interpretation*, pages 21–54. Cambridge University Press, Cambridge, UK, 1995.

A. Cont. Realtime Audio to Score Alignment for Polyphonic Music Instruments using Sparse Non-Negative Constraints and Hierarchical HMMs. In *Proceedings of the IEEE International Conference on Acoustics, Speech and Signal Processing (ICASSP)*, volume 5, Toulouse, France, 2006.

A. Cont. A Coupled Duration-Focused Architecture for Real-Time Music-to-Score Alignment. *IEEE Transactions on Pattern Analysis and Machine Intelligence*, 32(6):974–987, 2010.

A. Cont, D. Schwarz, and N. Schnell. Training IRCAM's Score Follower. In *Proceedings of the IEEE International Conference on Acoustics, Speech and Signal Processing (ICASSP)*, Philadelphia,PA, USA, 2005.

N. Cook. *Beyond the Score: Music as Performance*. Oxford University Press, 2014.

S. J. Cox. Hidden Markov Models for Automatic Speech Recognition: Theory and Application. In C. Wheddon and R. Linggard, editors, *Speech and Language Processing*, pages 209–230. Chapman & Hall, London, UK, 1990.

R. B. Dannenberg. An On-Line Algorithm for Real-Time Accompaniment. In *Proceedings of the International Computer Music Conference (ICMC)*, pages 193–198, Paris, France, 1984.

R. B. Dannenberg and M. Goto. Music Structure Analysis from Acoustic Signals. In D. Havelock, S. Kuwano, and M. Vorländer, editors, *Handbook of Signal Processing in Acoustics*, volume 1, pages 305–331. Springer, New York City, NY, USA, 2008.

R. B. Dannenberg and N. Hu. Polyphonic audio matching for score following and intelligent audio editors. In *Proceedings of the International Computer Music Conference (ICMC)*, pages 27–34, San Francisco, USA, 2003.

R. B. Dannenberg and C. Raphael. Music Score Alignment and Computer Accompaniment. *Communications of the ACM, Special Issue: Music Information Retrieval*, 49(8): 38–43, 2006.

R. B. Dannenberg, M. Sanchez, A. Joseph, P. Capell, R. Joseph, and R. Saul. A Computer-based Multi-media Tutor for Beginning piano Students. *Journal of New Music Research*, 19(2-3):155–173, 1990.

C. Dittmar, E. Cano, J. Abeßer, and S. Grollmisch. Music Information Retrieval Meets Music Education. In *Multimodal Music Processing*, volume 3 of *Dagstuhl Follow-Ups*, pages 95–120. Schloss Dagstuhl–Leibniz-Zentrum für Informatik, 2012.

S. Dixon and G. Widmer. MATCH: A Music Alignment Tool Chest. In *Proceedings of the 6th International Conference on Music Information Retrieval (ISMIR)*, pages 492–497, London, UK, 2005.

M. Dorfer, A. Arzt, and G. Widmer. Towards Score Following in Sheet Music Images. In *In Proceedings of 17th International Society for Music Information Retrieval Conference (ISMIR)*, New York City, NY, USA, 2016a.

M. Dorfer, A. Arzt, and G. Widmer. Towards End-to-End Audio-Sheet-Music Retrieval. In *NIPS 2016 End-to-end Learning for Speech and Audio Processing Workshop*, Barcelona, Spain, 2016b.

J. S. Downie. The Music Information Retrieval Evaluation eXchange (2005–2007): A Window into Music Information Retrieval Research. *Acoustical Science and Technology*, 29 (4):247–255, 2008.

J. Driedger, H. Grohganz, T. Prätzlich, S. Ewert, and M. Müller. Score-Informed Audio Decomposition and Applications. In *Proceedings of the ACM International Conference on Multimedia (ACM-MM)*, pages 541–544, Barcelona, Spain, 2013.

Z. Duan and B. Pardo. A State Space Model for Online Polyphonic Audio-Score Alignment. In *Proceedings of the IEEE International Conference on Acoustics, Speech, and Signal Processing (ICASSP)*, pages 197–200, Prague, Czech Republic, 2011.

R. Durbin, S. R. Eddy, A. Krogh, and G. Mitchison. *Biological Sequence Analysis : Probabilistic Models of Proteins and Nucleic Acids.* Cambridge University Press, New York, USA, 1999.

A. Earis. An Algorithm to Extract Expressive Timing and Dynamics from Piano Recordings. *Musicae Scientiae*, 11(2):155–82, 2007.

J. Eggert, H. Wersing, and E. Korner. Transformation-Invariant Representation and NMF. In *Proceedings of the 2004 IEEE International Joint Conference on Neural Networks*, pages 2535–2539, Budapest, Hungary, 2004.

V. Emiya, R. Badeau, and B. David. Multipitch Estimation of Piano Sounds using a New Probabilistic Spectral Smoothness Principle. *IEEE Transactions on Audio, Speech and Language Processing*, 18(6):1643–1654, 2010.

S. Ewert and M. Müller. Estimating Note Intensities In Music Recordings. In *Proceedings of the IEEE International Conference on Acoustics, Speech, and Signal Processing (ICASSP)*, pages 385–388, Prague, Czech Republic, 2011.

S. Ewert and M. Sandler. Piano Transcription in the Studio Using an Extensible Alternating Directions Framework. *IEEE/ACM Transactions on Audio, Speech, and Language Processing*, 24(11):1983–1997, 2016.

S. Ewert, M. Müller, and R. B. Dannenberg. Towards Reliable Partial Music Alignments Using Multiple Synchronization Strategies. In *Proceedings of the International Workshop on Adaptive Multimedia Retrieval (AMR), Lecture Notes in Computer Science (LNCS)*, volume 6535, pages 35–48, Madrid, Spain, 2009a.

S. Ewert, M. Müller, and P. Grosche. High Resolution Audio Synchronization Using Chroma Onset Features. In *Proceedings of the IEEE International Conference on Acoustics, Speech, and Signal Processing (ICASSP)*, pages 1869–1872, Taipei, Taiwan, 2009b.

S. Ewert, B. Pardo, M. Müller, and M. D. Plumbley. Score-Informed Source Separation for Musical Audio Recordings: An Overview. *IEEE Signal Processing Magazine*, 31(3):116–124, 2014.

S. Ewert, M. D. Plumbley, and M. Sandler. A Dynamic Programming Variant of Non-Negative Matrix Deconvolution for the Transcription of Struck String Instruments. In *Proceedings of the IEEE International Conference on Acoustics, Speech, and Signal Processing (ICASSP)*, pages 569–573, Brisbane, Australia, 2015.

S. Ewert, S. Wang, M. Müller, and M. Sandler. Score-Informed Identification of Missing and Extra Notes in Piano Recordings. In *Proceedings of the 17th International Society for Music Information Retrieval Conference (ISMIR)*, pages 30–36, New York City, NY, USA, 2016.

D. Fabian, R. Timmers, and E. Schubert. *Expressiveness in Music Performance: Empirical Approaches across Styles and Cultures.* Oxford University Press, USA, 2014.

C. Fremerey, M. Müller, and M. Clausen. Handling Repeats and Jumps in Score-Performance Synchronization. In *Proceedings of the 11th International Conference on Music Information Retrieval (ISMIR)*, pages 243–248, Utrecht, The Netherlands, 2010.

T. Fujishima. Realtime Chord Recognition of Musical Sound: A System Using Common Lisp Music. In *Proceedings of the International Computer Music Conference (ICMC)*, pages 464–467, Beijing, China, 1999.

A. Gabrielsson. Music Performance Research at the Millennium. *Psychology of Music*, 31 (3):221–272, 2003.

W. Goebl. Numerisch-klassifikatorische Interpretationsanalyse mit dem ‘Bösendorfer Computerflügel’. Master’s thesis, Universität Wien, 1999a.

W. Goebl. The Vienna 4x22 Piano Corpus. `http://dx.doi.org/10.21939/4X22`, 1999b.

W. Goebl. Skilled Piano Performance: Melody Lead Caused by Dynamic Differentiation. In *Proceedings of the 6th International Conference on Music Perception and Cognition*, Keele, UK, 2000.

W. Goebl. Melody Lead in Piano Performance: Expressive Device or Artifact? *The Journal of the Acoustical Society of America*, 110:563–572, 2001.

W. Goebl, S. Dixon, G. De Poli, A. Friberg, R. Bresin, and G. Widmer. Sense in Expressive Music Performance: Data Acquisition, Computational Studies, and Models. In P. Polotti and D. Rocchesso, editors, *Sound to Sense-Sense to Sound: A State of the Art in Sound and Music Computing*, pages 195–242. Logos Verlag Berlin, 2008.

E. Gómez. Tonal Description of Polyphonic Audio for Music Content Processing. *INFORMS Journal on Computing*, 18(3):294–304, 2006.

M. Grachten, M. Gasser, A. Arzt, and G. Widmer. Automatic Alignment of Music Performances with Structural Differences. In *Proceedings of 14th International Society for Music Information Retrieval Conference (ISMIR)*, Curitiba, Brazil, 2013.

L. Grubb and R. B. Dannenberg. A Stochastic Method of Tracking a Vocal Performer. In *Proceedings of the International Computer Music Conference (ICMC)*, pages 301–308, Ann Arbor, MI, USA, 1997.

D. Gusfield. *Algorithms on Strings, Trees, and Sequences: Computer Science and Computational Biology*. Cambridge University Press, New York, NY, USA, 1997.

P. E. Hart, N. J. Nilsson, and B. Raphael. A Formal Basis for the Heuristic Determination of Minimum Cost Paths. *IEEE Transactions on Systems Science and Cybernetics*, 4(2): 100–107, 1968.

C. Harte and M. Sandler. Automatic Chord Identification Using a Quantised Chromagram. In *Proceedings of the 118th AES Convention*, Barcelona, Spain, 2005.

H. Heijink, P. Desain, H. Honing, and L. Windsor. Make Me a Match: An Evaluation of Different Approaches to Score-Performance Matching. *Computer Music Journal*, 24(1): 43–56, 2000.

G. Holt, M. Reinders, and E. Hendriks. Multi-Dimensional Dynamic Time Warping for Gesture Recognition. In *Advanced School for Computing and Imaging*, Delft, The Netherlands, 2007.

R. Howat. What Do We Perform? In J. Rink, editor, *The Practice of Performance: Studies in Musical Interpretation*, pages 3–20. Cambridge University Press, Cambridge, UK, 1995.

N. Hu, R. B. Dannenberg, and G. Tzanetakis. Polyphonic Audio Matching and Alignment for Music Retrieval. In *Proceedings of the IEEE Workshop on Applications of Signal Processing to Audio and Acoustics (WASPAA)*, New Paltz, NY, USA, 2003.

F. Itakura. Minimum Prediction Residual Principle Applied to Speech Recognition. *IEEE Transactions on Acoustics, Speech, and Signal Processing*, 23(1):67–72, 1975.

K. Itoyama, M. Goto, K. Komatani, T. Ogata, and H. G. Okuno. Instrument Equalizer For Query-By-Example Retrieval: Improving Sound Source Separation Based On Integrated Harmonic And Inharmonic Models. In *Proceedings of the 9th International Conference for Music Information Retrieval (ISMIR)*, pages 133–138, Philadelphia, PA, USA, 2008.

C. Joder, S. Essid, and G. Richard. A Comparative Study of Tonal Acoustic Features for a Symbolic Level Music-to-Score Alignment. In *Proceedings of the IEEE International Conference on Acoustics, Speech, and Signal Processing (ICASSP)*, Dallas, TX, USA, 2010.

C. Joder, S. Essid, and G. Richard. A Conditional Random Field Framework for Robust and Scalable Audio-to-Score Matching. *IEEE Transactions on Audio, Speech, and Language Processing*, 19(8):2385–2397, 2011.

C. Joder, S. Essid, and G. Richard. Learning Optimal Features for Polyphonic Audio-to-Score Alignment. *IEEE Transactions on Audio, Speech, and Language Processing*, 21(10): 2118–2128, 2013.

K. Katoh and D. M. Standley. MAFFT Multiple Sequence Alignment Software Version 7: Improvements in Performance and Usability. *Molecular Biology and Evolution*, 30(4): 772–780, 2013.

R. Kelz, M. Dorfer, F. Korzeniowski, S. Böck, A. Arzt, and G. Widmer. On the Potential of Simple Framewise Approaches to Piano Transcription. In *Proceedings of the 17th International Society for Music Information Retrieval Conference (ISMIR)*, New York City, NY, USA, 2016.

H. Kirchhoff, S. Dixon, and A. Klapuri. Multi-Template Shift-Variant Non-Negative Matrix Deconvolution for Semi-Automatic Music Transcription. In *Proceedings of the 13th International Society for Music Information Retrieval Conference*, pages 415–420, Porto, Portugal, 2012.

A. P. Klapuri and M. Davy, editors. *Signal Processing Methods for Music Transcription*. Springer, New York, 2006.

F. Kurth and M. Müller. Efficient Index-Based Audio Matching. *IEEE Transactions on Audio, Speech, and Language Processing*, 16(2):382–395, 2008.

D. D. Lee and H. S. Seung. Algorithms for Non-Negative Matrix Factorization. In *Advances in Neural Information Processing Systems 13 (NIPS)*, pages 556–562, Denver, CO, USA, 2000.

C. C. S. Liem and A. Hanjalic. Expressive Timing From Cross-Performance And Audio-Based Alignment Patterns: An Extended Case Study. In *Proceedings of the 12th International Society for Music Information Retrieval Conference (ISMIR)*, pages 519–524, Miami, FL, USA, 2011.

R. Macrae. *Linking Music Metadata*. PhD thesis, Queen Mary University of London, 2012.

R. Macrae and S. Dixon. Accurate Real-time Windowed Time Warping. In *Proceedings of the 11th International Society for Music Information Retrieval Conference (ISMIR)*, pages 423–428, Utrecht, The Netherlands, 2010.

A. Maezawa, K. Itoyama, Y. Kazuyoshi, and H. G. Okuno. Bayesian Audio Alignment based on a Unified Model of Music Composition and Performance. In *Proceedings of the 15th International Society for Music Information Retrieval Conference (ISMIR)*, pages 233–238, Taipei, Taiwan, 2014.

A. Maezawa, K. Itoyama, K. Yoshii, and H. G. Okuno. Unified Inter- and Intra-Recording Duration Model for Multiple Music Audio Alignment. In *Proceedings of the IEEE Workshop on Applications of Signal Processing to Audio and Acoustics (WASPAA)*, pages 1–5, New Paltz, NY, USA, 2015.

M. Marolt. A Connectionnist Approach to Automatic Transcription of Polyphonic Piano Music. *IEEE Transactions on Multimedia*, 6(3):439–449, 2004.

M. Mauch and S. Dixon. Simultaneous Estimation of Chords and Musical Context from Audio. *IEEE Transactions on Audio, Speech, and Language Processing*, 18(6):1280–1289, 2010.

R. Miotto, N. Montecchio, and N. Orio. Statistical Music Modeling Aimed at Identification and Alignment. In Z. W. Raś and A. A. Wieczorkowska, editors, *Advances in Music Information Retrieval*, volume 274 of *Studies in Computational Intelligence*, pages 187–212. Springer, 2010.

N. Montecchio and A. Cont. A Unified Approach to Real Time Audio-to-Score and Audio-to-Audio Alignment using Sequential Montecarlo Inference Techniques. In *Proceedings of the IEEE International Conference on Acoustics, Speech and Signal Processing (ICASSP)*, pages 193–196, Prague, Czech Republic, 2011a.

N. Montecchio and A. Cont. Accelerating the Mixing Phase in Studio Recording Productions by Automatic Audio Alignment. In *Proceedings of the 12th International Society for Music Information Retrieval Conference (ISMIR)*, Miami, FL, United States, 2011b.

M. Müller. *Information Retrieval for Music and Motion.* Springer Verlag, 2007.

M. Müller and D. Appelt. Path-Constrained Partial Music Synchronization. In *Proceedings of the International Conference on Acoustics, Speech and Signal Processing (ICASSP)*, pages 65–68, Las Vegas, NV, USA, 2008.

M. Müller and S. Ewert. Towards Timbre-Invariant Audio Features for Harmony-Based Music. *IEEE Transactions on Audio, Speech, and Language Processing*, 18(3):649–662, 2010.

M. Müller and T. Röder. Motion Templates for Automatic Classification and Retrieval of Motion Capture Data. In *Proceedings of the ACM SIGGRAPH/Eurographics Symposium on Computer Animation (SCA)*, pages 137–146, Vienna, Austria, 2006.

M. Müller, F. Kurth, and M. Clausen. Audio Matching via Chroma-Based Statistical Features. In *Proceedings of the 6th International Conference on Music Information Retrieval (ISMIR)*, pages 288–295, London, UK, 2005.

M. Müller, H. Mattes, and F. Kurth. An Efficient Multiscale Approach to Audio Synchronization. In *Proceedings of the 7th International Conference on Music Information Retrieval (ISMIR)*, pages 192–197, Victoria, Canada, 2006.

M. Müller, F. Kurth, D. Damm, C. Fremerey, and M. Clausen. Lyrics-based Audio Retrieval and Multimodal Navigation in Music Collections. In *Proceedings of the 11th European Conference on Digital Libraries (ECDL)*, pages 112–123, Budapest, Hungary, 2007.

M. Müller, V. Konz, A. Scharfstein, S. Ewert, and M. Clausen. Towards Automated Extraction of Tempo Parameters from Expressive Music Recordings. In *Proceedings of the 10th International Society for Music Information Retrieval Conference (ISMIR)*, pages 69–74, Kobe, Japan, 2009.

M. Müller, M. Clausen, V. Konz, S. Ewert, and C. Fremerey. A Multimodal Way of Experiencing and Exploring Music. *Interdisciplinary Science Reviews (ISR)*, 35(2):138–153, 2010.

E. Nakamura, T. Nakamura, Y. Saito, N. Ono, and S. Sagayama. Outer-Product Hidden Markov Model and Polyphonic MIDI Score Following. *Journal of New Music Research*, 43(2):183–201, 2014.

J. Nam, J. Ngiam, H. Lee, and M. Slaney. A Classification-Based Polyphonic Piano Transcription Approach Using Learned Feature Representations. In *Proceedings of the 12th International Society for Music Information Retrieval Conference*, pages 175–180, Miami, FL, USA, 2011.

S. B. Needleman and C. D. Wunsch. A General Method Applicable to the Search for Similarities in the Amino Acid Sequence of Two Proteins. *Journal of Molecular Biology*, 48 (3):443–453, 1970.

R. Nichols. *Debussy Remembered*. Amadeus Press, 1992.

B. Niedermayer. Towards Audio To Score Alignment In The Symbolic Domain. In *Proceedings of the Sound and Music Computing Conference (SMC)*, pages 77–82, Porto, Portugal, 2009a.

B. Niedermayer. Improving Accuracy of Polyphonic Music-to-Score Alignment. In *Proceedings of the 10th International Society for Music Information Retrieval Conference (ISMIR)*, pages 585–590, Kobe, Japan, 2009b.

B. Niedermayer and G. Widmer. A Multi-pass Algorithm for Accurate Audio-to-Score Alignment. In *Proceedings of the 11th International Conference on Music Information Retrieval (ISMIR)*, pages 417–422, Utrecht, The Netherlands, 2010.

N. Orio and F. Déchelle. Score Following Using Spectral Analysis and Hidden Markov Models. In *Proceedings of the International Computer Music Conference (ICMC)*, pages 125–129, Havana, Cuba, 2001.

N. Orio and D. Schwarz. Alignment of Monophonic and Polyphonic Music to a Score. In *Proceedings of the International Computer Music Conference (ICMC)*, pages 155–158, Havana, Cuba, 2001.

A. Ozerov, C. Févotte, and M. Charbit. Factorial Scaled Hidden Markov Model for Polyphonic Audio Representation and Source Separation. In *Proceedings of the IEEE Workshop on Applications of Signal Processing to Audio and Acoustics (WASPAA)*, pages 121–124, New Paltz, NY, USA, 2009.

A. Ozerov, E. Vincent, and F. Bimbot. A General Flexible Framework for the Handling of Prior Information in Audio Source Separation. *IEEE Transactions on Audio, Speech, and Language Processing*, 20(4):1118–1133, 2012.

F. S.-M. Pais, P. de Cássia Ruy, G. Oliveira, and R. S. Coimbra. Assessing the Efficiency of Multiple Sequence Alignment Programs. *Algorithms for Molecular Biology*, 9(1):1–8, 2014.

B. Pardo and W. Birmingham. Modeling Form for On-line Following of Musical Performances. In *Proceedings of the National Conference on Artificial Intelligence (AAAI)*, Pittsburgh, PA, USA, 2005.

J. Paulus, M. Müller, and A. P. Klapuri. Audio-based Music Structure Analysis. In *Proceedings of the 11th International Conference on Music Information Retrieval (ISMIR)*, pages 625–636, Utrecht, The Netherlands, 2010.

G. Peeters. Chroma-based Estimation of Musical Key from Audio-Signal Analysis. In *Proceedings of the 7th International Conference on Music Information Retrieval (ISMIR)*, pages 115–120, Victoria, Canada, 2006.

G. E. Poliner and D. P. W. Ellis. A Discriminative Model for Polyphonic Piano Transcription. *EURASIP Journal on Advances in Signal Processing*, 2007(1), 2007.

T. Prätzlich, J. Driedger, and M. Müller. Memory-Restricted Multiscale Dynamic Time Warping. In *Proceedings of the IEEE International Conference on Acoustics, Speech, and Signal Processing (ICASSP)*, pages 569–573, Shanghai, China, 2016.

L. Rabiner and B.-H. Juang. *Fundamentals of Speech Recognition*. Prentice Hall, 1993.

L. R. Rabiner. A Tutorial on Hidden Markov Models and Selected Applications in Speech Recognition. *Proceedings of the IEEE*, 77(2):257–286, 1989.

S. A. Raczynski, N. Ono, and S. Sagayama. Multipitch Analysis with Harmonic Nonnegative Matrix Approximation. In *Proceedings of the 8th International Conference on Music Information Retrieval (ISMIR)*, pages 381–386, Vienna, Austria, 2007.

C. Raffel and D. P. W. Ellis. Large-Scale Content-Based Matching of MIDI and Audio Files. In *Proceedings of the 16th International Society for Music Information Retrieval Conference (ISMIR)*, Málaga, Spain, 2015.

C. Raphael. Automatic Segmentation of Acoustic Musical Signals Using Hidden Markov Models. *IEEE Transactions on Pattern Analysis and Machine Intelligence*, 21:360–370, 1998.

C. Raphael. A Hybrid Graphical Model for Aligning Polyphonic Audio with Musical Scores. In *Proceedings of the 5th International Conference on Music Information Retrieval (ISMIR)*, pages 387–394, Barcelona, Spain, 2004.

S. Rho and E. Hwang. FMF: Query Adaptive Melody Retrieval System. *Journal of Systems and Software*, 79(1):43–56, 2006.

C. Roads. *The Computer Music Tutorial.* The MIT Press, 1996.

A. Roebel, J. Pons, M. Liuni, and M. Lagrangey. On Automatic Drum Transcription using Non-Negative Matrix Deconvolution and Itakura Saito Divergence. In *Proceedings of the IEEE International Conference on Acoustics, Speech and Signal Processing (ICASSP)*, pages 414–418, Brisbane, Australia, 2015.

C. Rother, T. Minka, A. Blake, and V. Kolmogorov. Cosegmentation of Image Pairs by Histogram Matching – Incorporating a Global Constraint into MRFs. In *IEEE Conference on Computer Vision and Pattern Recognition (CVPR)*, pages 993–1000, New York City, NY, USA, 2006. IEEE.

H. Sakoe and S. Chiba. Dynamic Programming Algorithm Optimization for Spoken Word Recognition. *IEEE Transactions on Acoustics, Speech, and Signal Processing*, 26(1):43–49, 1978.

S. Salvador and P. Chan. FastDTW: Toward Accurate Dynamic Time Warping in Linear Time and Space. In *Proceedings of the KDD Workshop on Mining Temporal and Sequential Data*, Seattle, WA, USA, 2004.

C. S. Sapp. Comparative Analysis of Multiple Musical Performances. In *Proceedings of the 8th International Conference on Music Information Retrieval (ISMIR)*, pages 497–500, Vienna, Austria, 2007.

E. Scheirer. Using Musical Knowledge to Extract Expressive Performance Information from Audio Recordings. In *International Joint Conferences on Artificial Intelligence (IJCAI) – Workshop on Computational Auditory Scene Analysis*, pages 153–160, Montréal, Canada, 1995.

C. Seashore. *Psychology of Music.* Dover Books on Music. Dover Publications, 1938.

J. Serrà and E. Gómez. Audio Cover Song Identification Based on Tonal Sequence Alignment. In *Proceedings of the IEEE International Conference on Acoustics, Speech, and Signal Processing (ICASSP)*, pages 61–64, Las Vegas, NV, USA, 2008.

J. Serrà, E. Gómez, P. Herrera, and X. Serra. Chroma binary similarity and local alignment applied to cover song identification. *IEEE Transactions on Audio, Speech and Language Processing*, 16:1138–1151, 2008.

A. Sheh and D. P. W. Ellis. Chord Segmentation and Recognition Using EM-Trained Hidden Markov Models. In *Proceedings of the 4th International Conference on Music Information Retrieval (ISMIR)*, pages 185–191, Baltimore, MD, USA, 2003.

R. N. Shepard. Circularity in Judgments of Relative Pitch. *Journal of the Acoustic Society of America*, 36(12):2346–2353, 1964.

F. Sievers, A. Wilm, D. Dineen, T. J. Gibson, K. Karplus, W. Li, R. Lopez, H. McWilliam, M. Remmert, J. Söding, J. D. Thompson, and D. G. Higgins. Fast, Scalable Generation of High-Quality Protein Multiple Sequence Alignments using Clustal Omega. *Molecular Systems Biology*, 7(1), 2011.

S. Sigtia, E. Benetos, and S. Dixon. An End-to-End Neural Network for Polyphonic Music Transcription. *IEEE/ACM Transactions on Audio, Speech, and Language Processing*, 24 (5):927–939, 2015.

P. Smaragdis. Non-Negative Matrix Factor Deconvolution; Extraction of Multiple Sound Sources from Monophonic Inputs. In *Proceedings of the 5th International Conference on Independent Component Analysis and Blind Signal Separation*, pages 494–499, Granada, Spain, 2004.

P. Smaragdis and J. C. Brown. Non-Negative Matrix Factorization for Polyphonic Music Transcription. In *Proceedings of the IEEE Workshop on Applications of Signal Processing to Audio and Acoustics (WASPAA)*, pages 177–180, New Paltz, NY, USA, 2003.

P. Smaragdis, B. Raj, and M. Shashanka. Sparse and Shift-Invariant Fature Extraction from Non-Negative Data. In *Proceedings of the IEEE International Conference on Acoustics, Speech, and Signal Processing (ICASSP)*, pages 2069–2072, Las Vegas, NV, USA, 2008.

T. F. Smith and M. S. Waterman. Identification of Common Molecular Subsequences. *Journal of Molecular Biology*, 147:195–197, 1981.

M. Stamp. A Revealing Introduction to Hidden Markov Models. Department of Computer Science, San Jose State University, 2004.

D. H. Thomas and R. P. Smiraglia. Beyond the Score. *Notes*, 54(3):649–666, 1998.

J. D. Thompson, P. Koehl, R. Ripp, and O. Poch. BAliBASE 3.0: Latest Developments of the Multiple Sequence Alignment Benchmark. *Proteins: Structure, Function, and Bioinformatics*, 61(1):127–136, 2005.

R. J. Turetsky and D. P. W. Ellis. Ground-Truth Transcriptions of Real Music from Force-Aligned MIDI Syntheses. In *Proceedings of the 4th International Conference on Music Information Retrieval (ISMIR)*, pages 135–141, Baltimore, MD, USA, 2003.

A. Uitdenbogerd and J. Zobel. Melodic Matching Techniques for Large Music Databases. In *Proceedings of the 7th ACM International Conference on Multimedia*, pages 57–66, Orlando, FL, USA, 1999.

B. Vercoe. The Synthetic Performer in the Context of Live Performance. In *Proceedings of the International Computer Music Conference (ICMC)*, pages 199–200, Paris, France, 1984.

E. Vincent, N. Bertin, and R. Badeau. Adaptive Harmonic Spectral Decomposition for Multiple Pitch Estimation. *IEEE Transactions on Audio, Speech, and Language Processing*, 18(3):528–537, 2010.

T. Virtanen. Monaural Sound Source Separation by Nonnegative Matrix Factorization with Temporal Continuity and Sparseness Criteria. *IEEE Transactions on Audio, Speech and Language Processing*, 15(3):1066–1074, 2007.

T. Virtanen, J. F. Gemmeke, B. Raj, and P. Smaragdis. Compositional Models for Audio Processing: Uncovering the Structure of Sound Mixtures. *IEEE Signal Processing Magazine*, 32(2):125–144, 2015.

G. H. Wakefield. Mathematical Representation of Joint Time-Chroma Distributions. In *Proceedings of the SPIE International Symposium on Optical Science, Engineering, and Instrumentation*, pages 637–645, Denver, CO, USA, 1999.

J.-H. Wang, S.-A. Wang, W.-C. Chen, K.-N. Chang, and H.-Y. Chen. Real-Time Pitch Training System for Violin Learners. In *Proceedings of the IEEE International Conference on Multimedia and Expo Workshops (ICMEW)*, pages 163–168, Melbourne, Australia, 2012.

S. Wang, S. Ewert, and S. Dixon. Robust Joint Alignment of Multiple Versions of a Piece of Music. In *Proceedings of the 15th International Society for Music Information Retrieval Conference (ISMIR)*, pages 83–88, Taipei, Taiwan, 2014.

S. Wang, S. Ewert, and S. Dixon. Compensating for Asynchronies between Musical Voices in Score-Performance Alignment. In *Proceedings of the IEEE International Conference on Acoustics, Speech, and Signal Processing (ICASSP)*, pages 589–593, Brisbane, Australia, 2015.

S. Wang, S. Ewert, and S. Dixon. Robust and Efficient Joint Alignment of Multiple Musical Performances. *IEEE/ACM Transactions on Audio, Speech, and Language Processing*, 24 (11):2132–2145, 2016.

S. Wang, S. Ewert, and S. Dixon. Identifying Missing and Extra Notes in Piano Recordings Using Score-Informed Dictionary Learning. *IEEE/ACM Transactions on Audio, Speech, and Language Processing*, (Advance Online Publication), 2017.

G. Widmer, S. Dixon, W. Goebl, E. Pampalk, and A. Tobudic. In Search of the Horowitz Factor. *AI Magazine*, 24(3):111–130, 2003.

M. Wöllmer, M. Al-Hames, F. Eyben, B. Schuller, and G. Rigoll. A Multidimensional Dynamic Time Warping Algorithm for Efficient Multimodal Fusion of Asynchronous Data Streams. *Neurocomputing*, 73:366–380, 2009.

J. Woodruff, B. Pardo, and R. B. Dannenberg. Remixing Stereo Music with Score-Informed Source Separation. In *Proceedings of the 7th International Conference on Music Information Retrieval (ISMIR)*, pages 314–319, Victoria, Canada, 2006.

C. Yeh, A. Roebel, and X. Rodet. Multiple Fundamental Frequency Estimation and Polyphony Inference of Polyphonic Music Signals. *IEEE Transactions on Audio, Speech, and Language Processing*, 18(6):1116–1126, 2010.

K. Yoshii and M. Goto. A Nonparametric Bayesian Multipitch Analyzer based on Infinite Latent Harmonic Allocation. *IEEE Transactions on Audio, Speech, and Language Processing*, 20(3):717–730, 2012.